THE STUDY OF MHC CLASS IB MOLECULES AND MHC CLASS IB-RESTRICTED CD8+ T CELL RESPONSES

by

Lili Chen

A dissertation submitted to the faculty of
The University of Utah
in partial fulfillment of the requirements for the degree of

Doctor of Philosophy

in

Microbiology and Immunology

Department of Pathology

The University of Utah

December 2012

ProQuest LLC.
789 East Eisenhower Parkway
P.O. Box 1346
Ann Arbor, MI 48106 - 1346

The University of Utah Graduate School

STATEMENT OF DISSERTATION APPROVAL

The dissertation of **Lili Chen**

has been approved by the following supervisory committee members:

Peter E. Jensen	, Chair	**7/18/2012** Date Approved
Robert S. Fujinami	, Member	**7/18/2012** Date Approved
Gerald Spangrude	, Member	**7/18/2012** Date Approved
June L. Round	, Member	**7/18/2012** Date Approved
Matthew A. Williams	, Member	**7/18/2012** Date Approved

and by **Peter E. Jensen** , Chair of the Department of **Pathology**

and by Charles A. Wight, Dean of The Graduate School.

ABSTRACT

Major histocompatibility complex (MHC) class Ib molecules share similar structure with the classical MHC class Ia molecules, but they generally have low expression levels and limited tissue distributions. Nevertheless, there are many different class Ib molecules and the well-studied ones have various specific functions. Many Ib molecules remain to be studied.

Increasing evidence shows that MHC class Ib molecules can restrict CD8+ T cell responses during infections, just as the classical MHC class Ia molecules do. In this thesis, classical MHC class I deficient mice were employed to study the MHC class Ib restricted anti-lymphocytic choriomeningitis virus (LCMV) responses. The mice were able to generate CD8+ T cell dependent immune response to the acute viral infection and partially control the infection in the early phase. IFNγ and granzyme B were produced *in vivo* by the CD8+ T cells. The response was restricted by MHC class Ib molecules as indicated by *in vitro* restimulation assays. However, the mounted responses were not strong enough to fully control the viral infection such that the infection becomes chronic in these mice and antigen-specific CD8+ T cells gradually lost their ability to produce cytokines and survive.

One MHC class Ib molecule, H2-T11, was selected to test an approach for studying MHC class Ib systematically. H2-T11 has high similarity to the Qa-1^b encoding gene, H2-T23. Reverse-transcriptional PCR and quantitative-PCR showed that it was

expressed at relatively high levels in mouse spleen, thymus, and intestine. The transduced hybrid T11 molecule containing an antibody-recognizable H2-D^b α3 domain could be detected on both $TAP^{+/+}$ Hela and $TAP^{-/-}$ T2 cell surfaces. The hybrid T11 expressing cells were not able to present insulin to the 6C5 T cell hybridoma, while the hybrid T23 expressing cells did. While T23 required Qdm peptide for its *in vitro* folding, T11 could fold in the absence of Qdm peptides. However, in the presence of Qdm, the folding efficiency was higher. Multiple peptides were eluted from the hybrid T11 and T23 expressing Hela cells. Qdm was found in both T11 and T23 peptide pools, but it was much more frequently found from T23 pool. Fewer peptides were eluted from T11 than T23. The T11-Qdm tetramers could not recognize NK or NKT cells, but the T23-Qdm tetramers could. Together, these studies indicated that T11 might be a functional paralog to H2-T23, but it does not appear to share the specific functions of T23.

To the Chen, Ren, and Zhang families, and especially Liang

CONTENTS

LIST OF FIGURES

Figure Page

LIST OF TABLES

ACKNOWLEDGEMENTS

First of all, I'd like to express my great thanks to my advisor, Dr. Peter Jensen, for his continuous and patient support of my Ph.D. study and research. His enthusiasm for science always motivates me; his broad-area knowledge is always a better source than textbooks; his clear guidance always leads me out when I get lost during research. Without his help, I wouldn't have been able to finish the thesis work. I would also like to thank Dr. Xiao He. He is always there and ready to help with any questions and problems. He is a great teacher, leading me to the area of molecular biology and immunology. He was indispensable for me to finish the Ph.D. study. I also gratefully thank my thesis committee members, Matthew Williams, Robert Fujinami, Gerald Spangrude, June Round and Raymond Daynes, for their helpful discussions and advice on my research.

I wish to thank all the former and current members of Jensen lab, for their discussions, collaborations and creation of a friendly lab environment. I am grateful to the support of all administrative staff, Allison Boyer, Kimberly Antry, Barbara Saffel et. al. Their help made my life as a graduate student much easier.

I wish to thank my family for their unconditional love and support. My parents are always there for me emotionally at any time. My words are not sufficient to express my thanks to them. I thank my husband, Liang, for his understanding of a graduate

student-wife. His love is the most important support for me to get through the years in a foreign country.

CHAPTER 1

INTRODUCTION

The major histocompatibility complex (MHC) was first described in the 1940s during organ transplantation research. It is a ~4Mb gene region containing a set of genes encoding proteins with antigen presentation function. This gene region has been found in all investigated vertebrates, such as mouse, chicken, frog and bony fish (1, 2). Human MHC molecules are also called human leukocyte antigens (HLA), and they are located on the short arm of chromosome 6. In the well-studied experimental animal, house mouse, the MHC is located on chromosome 17, and names usually start with "I" or "H2" due to historical reasons. The MHC region encodes three types of MHC genes, MHC class I, II and "III". The MHC class I and II encode proteins belonging to the immunoglobulin-like protein family. They are capable of binding antigens, usually short peptides, in their binding groove and present these antigens to T cells. The MHC class III region encodes various proteins that do not have antigen presentation functions but are generally related to immune response.

The various MHC genes were generated by gene duplication during evolution. They can be classified as "old," "middle-aged," and "young" MHCs (3). The old ones were generated long ago, and their original function retained. The middle-aged genes gathered multiple mutations after the original duplication. Some of them become very polymorphic and usually have multiple allels. They may co-evolute with the pathogens

under selection pressures to retain their abilities to bind specific peptides derived from pathogens (4, 5). Some of the mutations may be harmful and these genes are thought to become pseudogenes. The "young" MHCs are the ones duplicated recently; the new generated genes may still have the same functions as the parent gene, because there are not enough mutations accumulated to lead to a functional change.

The function of MHC molecules is closely related to T cells. T cells are derived from the hematopoietic stem cells in the bone marrow. After the differentiation of common lymphoid progenitor cells to T cell progenitors in the bone marrow, immature T cells migrate to the thymus for further development. The successful maturation of T cells requires their contact with MHC class I or II molecules expressed on thymus epithelial cells and dendritic cells. After positive selection and negative selection processes, the T cells with proper affinity for self-MHC are selected in the thymus and migrate to the peripheral. In the peripheral, the T cells will survail the environment for antigens through interactions between TCR and MHC. MHC deficient mice have significantly decreased T cell output from the thymus and have much fewer T cells in their peripheral than the wild type animal (6-10). In the peripheral, mature T cells require contact with MHC for their survival and activation (11, 12).

MHC class II

MHC class II molecules are expressed in professional antigen presenting cells (APCs), such as dendritic cells, macrophages, and B cells. MHC class II expression is controlled by a master transcription factor CIITA. In CIITA deficient hosts, the MHC class II molecules are not expressed (13). Class II molecules are composed of two equal-

weighted α and β chains. The α1 and β1 domains form the peptide-binding groove, which has a β-sheet bottom and two α-helix walls. The groove is an open tunnel and can accommodate peptides of 10 to 30 amino acids long or even longer (14). Usually, these peptides are generated from exogenous proteins that are internalized in the cells by endocytosis or phagocytosis. The internalized proteins are trapped inside the phagosomes or endosomes. The class II molecules are assembled in the endoplasmic reticulum (ER) and stabilized by the invariant chain (Ii) that occupies the class II peptide-binding groove. The assembled MHC class II is secreted through the Golgi complex to the MHC class II compartment (MIIC) (15, 16). The phagosome/endosome containing the exogenous proteins will fuse with MIIC. The exogenous proteins are degraded to small peptides by the proteases and peptidases in the MIIC. Invariant chain is also cleaved and a short peptide, CLIP, is left inside the MHC class II binding groove. Then the CLIP is replaced by an exogenous peptide with the help of a nonclassical MHC class II molecule, DM (17, 18). The MHC class II with the exogenous peptide is further transported to the cell membrane surface, where the peptide is presented by MHC class II to T cell receptors (TCR) on CD4+ T cells. The MHC class II and TCR interaction is required for the selection of CD4+ T cells in the thymus, and the interaction initiates the downstream TCR signaling to activate CD4+ T cells in the periphery. Besides exogenous proteins, intracellular proteins, including self-proteins and pathogen proteins, can also be processed through the MHC class II pathway through autophagy (19-21).

MHC class I

MHC class I molecules are expressed on almost all nucleated cells. They are composed of a heavy chain and a smaller β-2-microglobulin (β2m) subunit. The heavy chain α1 and α2 domains form the peptide-binding groove similar to the one of MHC class II except that class I groove has closed ends. In most instances, only short peptides 8 to 10 amino acids in length can fit into the MHC class I binding groove. The class I molecules are synthesized by ribosomes on the rough ER. The MHC class I peptides are usually generated from cytoplasmic proteins, such as proteins of intracellular microbes or mis-folded self-proteins. These proteins are degraded by the proteasome to peptides and further trimmed by proteases and peptidases in the cytosol. The short peptides are transported into the ER through the transporter associated with antigen processing (TAP), which is a heterodimer formed by TAP-1 and TAP-2 proteins. As a member of ATP-binding cassette family, TAP consumes ATP to transport peptides from cytosol into ER (22). Inside the ER, the peptides are further trimmed by endoplasmic reticulum aminopeptidase associated with antigen processing (ERAAP), and loaded onto the MHC class I molecules with the help of Tapsin and ERp57 (23). The assembled MHC class I molecules are transported through the Golgi complex to the cell surface and the peptides are presented to TCRs on CD8+ T cells. The classical mouse MHC class I molecules include H2-D, H2-K and H2-L. MHC class I deficient mice are generally CD8+ T cell deficient due to the lack of MHC class I selection in the thymus. In the C57BL/6 mice, which are of the b haplotype, the L gene is not expressed because of a large deletion in the L gene. Thus, the $K^{b-/-}D^{b-/-}$ mice on the B6 background are MHC class I deficient and have very few CD8+ T cells.

The class I MHC is subdivided to two groups: classical MHC class I (MHC class Ia) and nonclassical MHC class I (MHC class Ib). The Ia molecules are ubiquitously expressed at high levels and they are very polymorphic. Ia molecules are very well studied and all the basic characterization of MHC class I is based on Ia. The nonclassical MHC class I molecules share similar structure to the classical ones. Most Ib molecules are encoded at the telomeric end of the MHC region. They are less polymorphic compared to the Ia molecules. Ib molecules usually have limited tissue distribution and their expression levels on the cell surface are lower than Ia. The mouse telomeric end of MHC is separated to three regions: H2-Q region, H2-T region and H2-M region. Each region encodes multiple MHC class Ib genes. Some Ib molecules are encoded outside MHC, such as CD1 and MR1. They also fold with β2m to form an MHC structure. Despite the low expression level and constrained expression in tissues, MHC class Ib molecules have some interesting functions. More and more studies in both human and mouse have shown that Ib molecules participate in the host anti-pathogen immune response and tumor surveillance (24-32).

CD1

CD1 molecules are encoded outside MHC region, and they are conserved in mammals (33). Humans express six forms of CD1, CD1a-CD1e. CD1d is the only form expressed in mice. CD1d molecules in mice, as well as CD1a-CD1d molecules in human, bind lipid antigens as opposed to peptide antigens. CD1 ligands include glycolipids, lipopeptides, and even inorganic compounds with alkyl tails. These ligands all have an alkyl component that can fit into the hydrophobic ligand-binding groove of CD1. Crystal

structures show that the CD1 groove is narrower and deeper than the peptide binding groove of classical MHC class I molecules (34). CD1d molecules select a special group of T cells, named natural killer T cells (NKT), which express both TCRs and the natural killer cell receptor, NK1.1 (35, 36). The majority of NKT cells exclusively utilize TCR Vα14-Jα18 in mice and Vα24-Jα18 in humans as their α chain and have a limited usage of specific TCR β chains. NKT cells can respond to pathogen infections rapidly and robustly by producing large amount of IFNγ cytokine, and granzyme B/perforin cytotoxic factors. The TCRs on NKT cells recognize the lipid antigens presented by CD1d molecules. Although CD1 molecules have a similar structure to MHC class Ia, they use different pathways for antigen presentation. CD1 molecules are synthesized inside the ER, and bind to self lipid, they are transported to the cell surface through the Golgi complex; surface CD1 then can be endocytosed back to endocytic compartments; after that they are sorted to the compartments containing foreign lipid antigens, where the self -lipid can be replaced with a foreign one; the new complex is secreted back to the cell surface, where the foreign lipid antigen is presented by CD1 to NKT cells (37). Unlike the protein antigens, almost all the lipid antigens with large alkyl chains are hydrophobic, that raises the question of how the lipid antigens are delivered to the antigen presenting cells. It was discovered that the apolipoproteins, which are the lipid transporters in the serum and transport lipids between liver and other tissues and organs for metabolism, can deliver lipid antigen cargo to antigen presenting cells. APCs can secrete ApoE to capture the nearby lipid antigens, and ApoE can be endocytosed through a specific receptor to cytosolic compartments, where the lipid is unloaded and transferred to CD1 molecules (38).

H2-M3

H2-M3 is encoded in the M region of mouse MHC complex. It preferentially binds N-formylated peptides from bacterial or mitochondrial proteins. Although H2-M3 can bind normal peptides, the affinity is ~1000-fold lower than the binding affinity of N-formylated peptides; H2-M3 restricted CTLs kills N-formylated peptide pulsed target cells better than nonformylated peptide pulsed ones (39, 40). H2-M3 was not detectable constitutively on the cell surface, and it appears to remain inside the cell until the proper N-formylated ligand is provided, after which H2-M3 is transported to the cell surface (41). H2-M3 was first found to participate in immune responses against *Listeria monocytogenes* by presenting Listeria peptides to CD8+ T cells (42-44). $K^{b-/-}D^{b-/-}$ mice were reported to control *L. monocytogene* infection as well as wild type mice, but H2-M3 didn't seem to be critical for the defense; other MHC class Ib might also contribute to the anti-Listeria response, as demonstrated in $K^{b-/-}D^{b-/-}$H2-$M3^{-/-}$ mice (30, 45, 46). H2-M3 restricted CD8+ T cells respond to primary intracellular bacterial infection rapidly, indicating that they may bridge the innate and adaptive immune responses, but they seem to lack memory (47-49). Specific CD8+ T cells are selected by H2-M3 in the thymus and selection requires N-formylated peptides (50). It was shown that these CD8+ T cells could be selected by either thymic epithelial cells or the bone marrow-derived hematopoietic cells. The cells selected by H2-M3 on thymic epithelial cells had normal CD8+ T cell properties in reaction to pathogenic antigens. The cells selected by H2-M3 on hematopoietic cells could react faster than other CD8+ T cells, and they did not form protective memory responses (51). Besides Listeria, H2-M3 restricted anti-*Mycobacteria*

tuberculosis CD8+ T cell response could also be elicited by immunizing the mice with dendritic cells pulsed with Mycobacteria N-formylated peptides (52).

Qa-2

Qa-2 is encoded by four different genes in the Q region, H2-Q6/8 and H2-Q7/9. Q6 and Q8 are highly conserved; and Q9 and Q7 are similar to each other (53-55). They are probably new divided genes that have not evolved enough to be distinct from each other. The surface expression of Qa-2 is TAP dependent (56). Qa-2 is ubiquitously expressed on nucleated cells; these molecules are also expressed in some special locations where classical MHC class I is not expressed, such as embryo, placenta, hair follicle, etc. (57). Qa-2 is special in that unlike other MHC class I molecules, which have transmembrane tails, Qa-2 is fixed on the cell surface by GPI linkers; Qa-2 molecules can also be found in the extracellular matrix as a soluble protein (58). Qa-2 molecules are relatively polymorphic. They can bind various peptides that share a peptide sequence motif. The peptides are usually of 8 to 10 amino acids long like the classical MHC class I ligands. Position 7 (P7) and position 9 (P9) are important anchor positions, and P7 usually is His, whereas P9 prefers Leu, Ile and Phe (59, 60). The crystal structure shows that Qa-2 has a relatively shallower binding groove than classical MHC class I (57). Qa-2 might participate in the development of CD8αα+ TCRαβ+ intestinal epithelial lymphocytes (IELs) as the number of IELs was reported to be very low in the Qa-2 deficient mice BALB/cAnN, but BALB/cAnN mice with Q9 transgene have significantly increased IEL cell number (61). Qa-2 was found to be a key factor in controlling polyoma virus infection in MHC class Ia deficient mice (62). A subset of CD8+ T cells was

observed to be specifically reactive to H2-Q9 with a peptide from the polyoma virus VP2 capsid protein. The H2-Q9 restricted VP2 specific CTLs expand for about 3 months post infection and they are maintained at high level during chronic PyV infection (63). Qa-2 was also reported to be involved in the control of tumor cells (64).

TLA

Thymic leukemia antigen (TLA) is encoded by H2-T18^{d}, T3^{b}, T3^{d}, Tla^{a}-1, Tla^{a}-2 and Tla^{a}-3 genes (65). It is exclusively expressed in thymus, intestine and T cell lymphoma cells (65). It does not require TAP for cell surface expression and the engagement with peptides is also not required for stable folding and expression (66-68). In contrast to MHC class Ia, which interacts with CD8αβ+ T cells, TLA tetramer can specifically recognize a group of cells expressing CD8αα, especially intestinal intraepithelial lymphocytes (IEL) (69). The crystal structure shows that due to the conformational change, the TLA peptide binding groove is closed, preventing peptide binding. More interestingly, TLA does not interact with TCR, but directly interacts with the CD8αα homodimer with high affinity through the TLA α3 domain (70, 71). The interaction between TLA and CD8αα regulates the IEL function such that TLA$^{-/-}$ mice showed severe colitis in TLA$^{-/-}$TCRα$^{-/-}$ mice, although TLA$^{-/-}$ mice of wild type background have normal numbers of IEL and do not develop colitis spontaneously (72). Recent research suggests that TLA can also regulate CD4+ T cell function in the intestine to promote the IL-17 production, and this interaction can protect mice from *Citrobacter rodentium* infection (73).

MR1

Like TLA, MR1 is also abundant in the intestine, though MR1 is expressed ubiquitously in many tissues. MR1 was first discovered in humans, and later was found in rat and mouse (74-76). It is conserved in many mammals (77), and it is not polymorphic (78). The α1 and α2 domains, which usually form the peptide-binding groove, are very close in amino acid sequence to the domains of classical MHC class I (74). Just like the classical MHC class I, MR1 also associates with β2m to form a stable structure (79). Although MR1 seems to have antigen-presenting function (80), no MR1 ligand has been found. The most important discovery about MR1 is that it can select mucosal-associated invariant T cells (MAIT). MAIT cells are abundant in the gut lamia propria; they might be selected in the thymus in small numbers and expand in peripheral to reach a large population in the intestine (81). The development of MAIT requires MR1 molecules expressed on B cells (82). The successful generation of MAIT is also dependent on commensal bacteria, which indicates that the MR1 bound ligand may originate from the commensal bacteria (82). Like the NKT cells selected by CD1 molecules, MAIT cells also have limited TCR α chain usage, such that human MAIT exclusively express Vα7.2-Jα33, and mouse MAIT express Vα19-Jα33. The human MAIT cells are either CD4-CD8- or CD8αα+, but unlike the TLA interacting CD8αα, MAIT CD8αα does not bind MR1 molecules (83). The study of Vα19i transgenic mice show that MAIT cells can produce IL-4, IL-5, IL-10 and IFNγ shortly after TCR signaling, indicating they may be more innate-like (84); Vα19i T cells were also reported to be involved in the suppression of experimental autoimmune encephalomyelitis (EAE) that $MR1^{-/-}$ mice had exacerbated EAE (85). Although MR1 is an MHC class I molecule, the MR1 expression on the cell

surface and MAIT cell activation was found to be independent on MHC class I antigen-processing machinery, such as the proteasome, TAP, tapsin, and calreticulin; instead, invariant chain (Ii) and DM, which are critical components for MHC class II antigen processing, were reported to be important for MR1 expression and MAIT cell activation (86). MR1 is conserved in mammals, and MAIT cells selected by MR1 are also conserved to the extent that human and mouse MAIT can cross-react with MR1 from each other and also MR1 molecules from other mammals (81).

Qa-1^b

Qa-1 is another MHC class I gene encoded in the mouse H2-T region. There are four different haplotypes of Qa-1 (a, b, c and d); a and b haplotypes are encoded in the majority of the mouse strains, and the b haplotype is more prevalent (87). Qa-1^b in mouse and its human homolog HLA-E are the most well-studied MHC class Ib molecules. Qa-1^b is encoded by the mouse H2-T23 gene. It is ubiquitously expressed in a TAP independent manner, but its expression level is relatively low compared to classical MHC molecules. Qa-1^b /HLA-E have a specific peptide ligand, which is named as Qa-1 determinant modifier (Qdm) (88, 89). Qdm is a nonomer peptide derived from the signal sequence of other MHC class I molecules, such as HLA-A2, H2-D and H2-L; amino acids at position 2 and 9 of the nonomer are important for Qdm binding to the Qa-1^b molecule (90). Although Qa-1^b cell surface expression is independent of TAP, TAP is required for the presentation of Qdm (91, 92). It is possible that Qdm is cleaved and left outside the ER when the class I molecules are synthesized by the ribosomes on rough ER (92).

Qdm is presented by Qa-1^b /HLA-E to CD94/NKG2 receptors on NK cells, NKT cells and some activated T cells (93-96). CD94/NKG2 is a receptor family expressed on NK cells, and CD94 is covalently linked to NKG2 by disulfide bonds (97). The family includes CD94/NKG2A, CD94/NKG2C and CD94/NKG2E, and all three can interact with Qa-1^b /Qdm. The cytoplasmic end of NKG2A contains immuno-receptor associated tyrosine-based inhibitory motif (ITIM) that upon interaction with Qa-1^b /Qdm, CD94/NKG2A will initiate inhibitory signals to downstream pathways which leads to the inhibition of NK cell function. NKG2C and NKG2E have short cytoplasmic tails that do not contain ITIM, but the two receptors are noncovalently associated with DAP12, which has an immuno-receptor associated tyrosine-based activation motif (ITAM) (98). The interaction between Qa-1^b /Qdm and CD94/NKG2C or CD94/NKG2E may induce NK cell activation signals (99). The NK cell status is dependent on the balance of activation and inhibitory signals. Although NKG2A, NKG2C and NKG2E are expressed by about half of the total natural killer cells, NKG2A has a much higher expression level than NKG2C and NKG2E, thus the Qa-1^b /Qdm interaction with NK cells usually leads to the inhibition of NK cell function (98).

Because MHC class Ia molecules express Qdm in their leader sequence, when viral infection of cells or cell tumorization lead to reduced MHC class Ia expression, the Qdm peptide will also be reduced, such that the Qa-1^b /Qdm interaction with NK cells will be interrupted. This may lead to the activation of NK cells to kill the viral infected cells or tumor cells (100). Although Qdm is the dominant peptide that Qa-1^b /HLA-E bind, they do have the ability to bind various peptides other than Qdm (101, 102). Qdm appears to have an ideal sequence motif for binding to Qa-1^b /HLA-E, yet the binding

complex still has a very fast dissociation rate, requiring constant formation of new complexes to maintain cell surface expression and inhibit NK cell activation (103). Besides binding Qdm, Qa-1^b is also involved in anti-bacterial responses. CD8+ T cells from *Listeria monocytogene* infected mice were able to kill *L. monocytogene* infected target cells and the restriction element was Qa-1^b (104). Qa-1^b was also recognized by a group of CTLs in anti-*Salmonella typhimurium* responses in mice (105), and a group of HLA-E restricted CTLs were also found within the PBMC population of cells of individuals who have been vaccinated with Salmonella vaccine Ty21a (106). The Salmonella peptide bound to Qa-1^b was encoded in the bacterial chaperone, GroEL. The GroEL specific CD8+ T cells restricted by Qa-1^b also cross-reacted with a peptide from mammalian hsp60 protein (25). The hsp60 peptide GMKFDRGYI is the dominant peptide bound to Qa-1^b when Qdm is absent (107). Qa-1^b was also found to be essential for the control of mouse poxvirus infection, such that H2-$T23^{-/-}$ mice had a much higher ectromelia virus titer than wild type mice after infection (108). Interestingly, it was found that Qa-1^b could also present insulin to activate a subset of CD8+ T cells and those T cells were naturally selected in mouse thymus by Qa-1^b (109, 110). A recent study also indicated that Qa-1^b can restrict CTL responses against antigen-processing deficient cells, and that the peptides presented by Qa-1 on the $TAP^{-/-}$ cells might be different from those from $TAP^{+/+}$ cells (111). Qa-1^b on a population of activated CD4+ T cells has also been reported to bind peptides originating from the TCR Vβ8 chain and to present these peptides to regulatory CD8+ T cells; the regulatory CD8+ T cells can inhibit CD4+ T cells (112-114).

References

1. Wang C, Perera TV, Ford HL, Dascher CC. 2003. Characterization of a divergent nonclassical MHC class I gene in sharks. *Immunogenetics* 55: 57-61

2. Kumánovics A, Takada T, Lindahl KF. 2003. Genomic organization of the mammalian MHC. *Annu Rev Immunol* 21: 629-57

3. Rodgers JR, Cook RG. 2005. MHC class Ib molecules bridge innate and acquired immunity. *Nat Rev Immunol* 5: 459-71

4. Apanius V, Penn D, Slev PR, Ruff LR, Potts WK. 1997. The nature of selection on the major histocompatibility complex. *Crit Rev Immunol* 17: 179-224

5. Jeffery KJ, Bangham CR. 2000. Do infectious diseases drive MHC diversity? *Microbes Infect* 2: 1335-41

6. Cosgrove D, Gray D, Dierich A, Kaufman J, Lemeur M, Benoist C, Mathis D. 1991. Mice lacking MHC class II molecules. *Cell* 66: 1051-66

7. Grusby MJ, Johnson RS, Papaioannou VE, Glimcher LH. 1991. Depletion of CD4+ T cells in major histocompatibility complex class II-deficient mice. *Science* 253: 1417-20

8. Zijlstra M, Bix M, Simister NE, Loring JM, Raulet DH, Jaenisch R. 1990. Beta 2-microglobulin deficient mice lack CD4-8+ cytolytic T cells. *Nature* 344: 742-6

9. Koller BH, Marrack P, Kappler JW, Smithies O. 1990. Normal development of mice deficient in beta 2M, MHC class I proteins, and CD8+ T cells. *Science* 248: 1227-30

10. Grusby MJ, Auchincloss H, Lee R, Johnson RS, Spencer JP, Zijlstra M, Jaenisch R, Papaioannou VE, Glimcher LH. 1993. Mice lacking major histocompatibility complex class I and class II molecules. *Proc Natl Acad Sci USA* 90: 3913-7

11. Takada K, Jameson SC. 2009. Naive T cell homeostasis: from awareness of space to a sense of place. *Nat Rev Immunol* 9: 823-32

12. Zhang N, Bevan MJ. 2011. CD8(+) T cells: foot soldiers of the immune system. *Immunity* 35: 161-8

13. Mach B, Steimle V, Martinez-Soria E, Reith W. 1996. Regulation of MHC class II genes: lessons from a disease. *Annu Rev Immunol* 14: 301-31

14. Trombetta ES, Mellman I. 2005. Cell biology of antigen processing in vitro and in vivo. *Annu Rev Immunol* 23: 975-1028

15. Nijman HW, Kleijmeer MJ, Ossevoort MA, Oorschot VM, Vierboom MP, van de Keur M, Kenemans P, Kast WM, Geuze HJ, Melief CJ. 1995. Antigen capture and major histocompatibility class II compartments of freshly isolated and cultured human blood dendritic cells. *J Exp Med* 182: 163-74

16. Watts C. 1997. Capture and processing of exogenous antigens for presentation on MHC molecules. *Annu Rev Immunol* 15: 821-50

17. Schulze MS, Wucherpfennig KW. 2012. The mechanism of HLA-DM induced peptide exchange in the MHC class II antigen presentation pathway. *Curr Opin Immunol* 24: 105-11

18. Brocke P, Garbi N, Momburg F, Hammerling GJ. 2002. HLA-DM, HLA-DO and tapasin: functional similarities and differences. *Curr Opin Immunol* 14: 22-9

19. Paludan C, Schmid D, Landthaler M, Vockerodt M, Kube D, Tuschl T, Munz C. 2005. Endogenous MHC class II processing of a viral nuclear antigen after autophagy. *Science* 307: 593-6

20. Strawbridge AB, Blum JS. 2007. Autophagy in MHC class II antigen processing. *Curr Opin Immunol* 19: 87-92

21. Munz C. 2010. Antigen processing via autophagy--not only for MHC class II presentation anymore? *Curr Opin Immunol* 22: 89-93

22. Procko E, Gaudet R. 2009. Antigen processing and presentation: TAPping into ABC transporters. *Curr Opin Immunol* 21: 84-91

23. Chapman DC, Williams DB. 2010. ER quality control in the biogenesis of MHC class I molecules. *Semin Cell Dev Biol* 21: 512-9

24. Lewinsohn DM, Briden AL, Reed SG, Grabstein KH, Alderson MR. 2000. Mycobacterium tuberculosis-reactive CD8+ T lymphocytes: the relative contribution of classical versus nonclassical HLA restriction. *J Immunol* 165: 925-30

25. Lo WF, Woods AS, DeCloux A, Cotter R, Metcalf ES, Soloski MJ. 2000. Molecular mimicry mediated by MHC class Ib molecules after infection with gram-negative pathogens. *Nat Med* 6: 215-8

26. Moody DB, Ulrichs T, Muhlecker W, Young DC, Gurcha SS, Grant E, Rosat JP, Brenner MB, Costello CE, Besra GS, Porcelli SA. 2000. CD1c-mediated T-cell

recognition of isoprenoid glycolipids in Mycobacterium tuberculosis infection. *Nature* 404: 884-8

27. Moody DB, Guy MR, Grant E, Cheng TY, Brenner MB, Besra GS, Porcelli SA. 2000. CD1b-mediated T cell recognition of a glycolipid antigen generated from mycobacterial lipid and host carbohydrate during infection. *J Exp Med* 192: 965-76

28. Chun T, Serbina NV, Nolt D, Wang B, Chiu NM, Flynn JL, Wang CR. 2001. Induction of M3-restricted cytotoxic T lymphocyte responses by N-formylated peptides derived from Mycobacterium tuberculosis. *J Exp Med* 193: 1213-20

29. Chiang EY, Stroynowski I. 2004. A nonclassical MHC class I molecule restricts CTL-mediated rejection of a syngeneic melanoma tumor. *J Immunol* 173: 4394-401

30. Cho H, Choi HJ, Xu H, Felio K, Wang CR. 2011. Nonconventional CD8+ T cell responses to Listeria infection in mice lacking MHC class Ia and H2-M3. *J Immunol* 186: 489-98

31. Hofstetter AR, Sullivan LC, Lukacher AE, Brooks AG. 2010. Diverse roles of non-diverse molecules: MHC class Ib molecules in host defense and control of autoimmunity. *Curr Opin Immunol* 23: 104-10

32. Lança T, Correia DV, Moita CF, Raquel H, Neves-Costa A, Ferreira C, Ramalho JS, Barata JT, Moita LF, Gomes AQ, Silva-Santos B. 2010. The MHC class Ib protein ULBP1 is a non-redundant determinant of leukemia/ lymphoma susceptibility to {gamma}{delta} T-cell cytotoxicity. *Blood* 115: 2407-11

33. Kulski JK, Dunn DS, Gaudieri S, Shiina T, Inoko H. 2001. Genomic and phylogenetic analysis of the human CD1 and HLA class I multicopy genes. *J Mol Evol* 53: 642-50

34. Silk JD, Salio M, Brown J, Jones EY, Cerundolo V. 2008. Structural and functional aspects of lipid binding by CD1 molecules. *Annu Rev Cell Dev Biol* 24: 369-95

35. Chen YH, Chiu NM, Mandal M, Wang N, Wang C-R. 1997. Impaired NK1+ T cell development and early IL-4 production in CD1-deficient mice. *Immunity* 6: 459-67

36. Godfrey DI, MacDonald HR, Kronenberg M, Smyth MJ, Van Kaer L. 2004. NKT cells: what's in a name? *Nat Rev Immunol* 4: 231-7

37. Barral DC, Brenner MB. 2007. CD1 antigen presentation: how it works. *Nat Rev Immunol* 7: 929-41

38. van den Elzen P, Garg S, Leon L, Brigl M, Leadbetter EA, Gumperz JE, Dascher CC, Cheng TY, Sacks FM, Illarionov PA, Besra GS, Kent SC, Moody DB, Brenner MB. 2005. Apolipoprotein-mediated pathways of lipid antigen presentation. *Nature* 437: 906-10

39. Byers DE, Fischer Lindahl K. 1998. H2-M3 presents a nonformylated viral epitope to CTLs generated in vitro. *J Immunol* 161: 90-6

40. Princiotta MF, Lenz LL, Bevan MJ, Staerz UD. 1998. H2-M3 restricted presentation of a Listeria-derived leader peptide. *J Exp Med* 187: 1711-9

41. Chiu NM, Chun T, Fay M, Mandal M, Wang C-R. 1999. The majority of H2-M3 is retained intracellularly in a peptide-receptive state and traffics to the cell surface in the presence of N-formylated peptides. *J Exp Med* 190: 423-34

42. Pamer EG, Wang C-R, Flaherty L, Lindahl KF, Bevan MJ. 1992. H-2M3 presents a Listeria monocytogenes peptide to cytotoxic T lymphocytes. *Cell* 70: 215-23

43. Gulden PH, Fischer P, Sherman NE, Wang W, Engelhard VH, Shabanowitz J, Hunt DF, Pamer EG. 1996. A Listeria monocytogenes pentapeptide is presented to cytolytic T lymphocytes by the H2-M3 MHC class Ib molecule. *Immunity* 5: 73-9

44. Lenz LL, Dere B, Bevan MJ. 1996. Identification of an H2-M3-restricted Listeria epitope: implications for antigen presentation by M3. *Immunity* 5: 63-72

45. Seaman MS, Pérarnau B, Lindahl KF, Lemonnier FA, Forman J. 1999. Response to Listeria monocytogenes in mice lacking MHC class Ia molecules. *J Immunol* 162: 5429-36

46. D'Orazio SEF, Shaw CA, Starnbach MN. 2006. H2-M3-restricted CD8+ T cells are not required for MHC class Ib-restricted immunity against Listeria monocytogenes. *J Exp Med* 203: 383-91

47. Kerksiek KM, Busch DH, Pilip IM, Allen SE, Pamer EG. 1999. H2-M3-restricted T cells in bacterial infection: rapid primary but diminished memory responses. *J Exp Med* 190: 195-204

48. Hamilton SE, Porter BB, Messingham KA, Badovinac VP, Harty JT. 2004. MHC class Ia-restricted memory T cells inhibit expansion of a nonprotective MHC class Ib (H2-M3)-restricted memory response. *Nat Immunol* 5: 159-68

49. Xu H, Chun T, Choi H-J, Wang B, Wang C-R. 2006. Impaired response to Listeria in H2-M3-deficient mice reveals a nonredundant role of MHC class Ib-specific T cells in host defense. *J Exp Med* 203: 449-59

50. Chiu NM, Wang B, Kerksiek KM, Kurlander R, Pamer EG, Wang C-R. 1999. The selection of M3-restricted T cells is dependent on M3 expression and presentation of N-formylated peptides in the thymus. *J Exp Med* 190: 1869-78

51. Cho H, Bediako Y, Xu H, Choi H-J, Wang C-R. 2011. Positive selecting cell type determines the phenotype of MHC class Ib-restricted CD8+ T cells. *Proc Natl Acad Sci USA*: 1-6

52. Doi T, Yamada H, Yajima T, Wajjwalku W, Hara T, Yoshikai Y. 2007. H2-M3-restricted CD8+ T cells induced by peptide-pulsed dendritic cells confer protection against Mycobacterium tuberculosis. *J Immunol* 178: 3806-13

53. Devlin JJ, Weiss EH, Paulson M, Flavell RA. 1985. Duplicated gene pairs and alleles of class I genes in the Qa2 region of the murine major histocompatibility complex: a comparison. *EMBO J* 4: 3203-7

54. Stroynowski I, Tabaczewski P. 1996. Multiple products of class Ib Qa-2 genes which ones are functional? *Res Immunol* 147: 290-301

55. Wu L, Feng H, Warner CM. 1999. Identification of two major histocompatibility complex class Ib genes, Q7 and Q9, as the Ped gene in the mouse. *Biol Reprod* 60: 1114-9

56. Tabaczewski P, Shirwan H, Lewis K, Stroynowski I. 1994. Alternative splicing of class Ib major histocompatibility complex transcripts in vivo leads to the expression of soluble Qa-2 molecules in murine blood. *Proc Natl Acad Sci USA* 91: 1883-7

57. He X, Tabaczewski P, Ho J, Stroynowski I, Garcia KC. 2001. Promiscuous antigen presentation by the nonclassical MHC Ib Qa-2 is enabled by a shallow, hydrophobic groove and self-stabilized peptide conformation. *Structure* 9: 1213-24

58. Stroynowski I, Soloski M, Low MG, Hood L. 1987. A single gene encodes soluble and membrane-bound forms of the major histocompatibility Qa-2 antigen: anchoring of the product by a phospholipid tail. *Cell* 50: 759-68

59. Rotzschke O, Falk K, Stevanovic S, Grahovac B, Soloski MJ, Jung G, Rammensee HG. 1993. Qa-2 molecules are peptide receptors of higher stringency than ordinary class I molecules. *Nature* 361: 642-4

60. Tabaczewski P, Chiang E, Henson M, Stroynowski I. 1997. Alternative peptide binding motifs of Qa-2 class Ib molecules define rules for binding of self and nonself peptides. *J Immunol* 159: 2771-81

61. Das G, Gould DS, Augustine MM, Fragoso G, Sciutto E, Stroynowski I, Van Kaer L, Schust DJ, Ploegh HL, Janeway CA, Scitto E. 2000. Qa-2-dependent selection of CD8alpha/alpha T cell receptor alpha/beta(+) cells in murine intestinal intraepithelial lymphocytes. *J Exp Med* 192: 1521-8

62. Swanson PA, Pack CD, Hadley A, Wang C-R, Stroynowski I, Jensen PE, Lukacher AE. 2008. An MHC class Ib-restricted CD8 T cell response confers antiviral immunity. *J Exp Med* 205: 1647-57

63. Swanson PA, Hofstetter AR, Wilson JJ, Lukacher AE. 2009. Cutting edge: Shift in antigen dependence by an antiviral MHC class Ib-restricted CD8 T cell response during persistent viral infection. *J Immunol* 182: 5198-202

64. Gomes AQ, Correia DV, Silva-Santos B. 2007. Nonclassical major histocompatibility complex proteins as determinants of tumour immunosurveillance. *EMBO Rep* 8: 1024-30

65. Obata Y, Satta Y, Moriwaki K, Shiroishi T, Hasegawa H, Takahashi T, Takahata N. 1994. Structure, function, and evolution of mouse TL genes, nonclassical class I genes of the major histocompatibility complex. *Proc Natl Acad Sci USA* 91: 6589-93

66. Rodgers JR, Mehta V, Cook RG. 1995. Surface expression of beta 2-microglobulin-associated thymus-leukemia antigen is independent of TAP2. *Eur J Immunol* 25: 1001-7

67. Holcombe HR, Castaño AR, Cheroutre H, Teitell M, Maher JK, Peterson PA, Kronenberg M. 1995. Nonclassical behavior of the thymus leukemia antigen: peptide transporter-independent expression of a nonclassical class I molecule. *J Exp Med* 181: 1433-43

68. Weber DA, Attinger A, Kemball CC, Wigal JL, Pohl J, Xiong Y, Reinherz EL, Cheroutre H, Kronenberg M, Jensen PE. 2002. Peptide-independent folding and CD8 alpha alpha binding by the nonclassical class I molecule, thymic leukemia antigen. *J Immunol* 169: 5708-14

69. Leishman AJ, Naidenko OV, Attinger A, Koning F, Lena CJ, Xiong Y, Chang HC, Reinherz E, Kronenberg M, Cheroutre H. 2001. T cell responses modulated through interaction between CD8alphaalpha and the nonclassical MHC class I molecule, TL. *Science* 294: 1936-9

70. Liu Y, Xiong Y, Naidenko OV, Liu JH, Zhang R, Joachimiak A, Kronenberg M, Cheroutre H, Reinherz EL, Wang JH. 2003. The crystal structure of a TL/CD8alphaalpha complex at 2.1 A resolution: implications for modulation of T cell activation and memory. *Immunity* 18: 205-15

71. Attinger A, Devine L, Wang-Zhu Y, Martin D, Wang JH, Reinherz EL, Kronenberg M, Cheroutre H, Kavathas P. 2005. Molecular basis for the high affinity interaction between the thymic leukemia antigen and the CD8alphaalpha molecule. *J Immunol* 174: 3501-7

72. Olivares-Villagómez D, Mendez-Fernandez YV, Parekh VV, Lalani S, Vincent TL, Cheroutre H, Van Kaer L. 2008. Thymus leukemia antigen controls intraepithelial lymphocyte function and inflammatory bowel disease. *Proc Natl Acad Sci USA* 105: 17931-6

73. Olivares-Villagómez D, Algood HMS, Singh K, Parekh VV, Ryan KE, Piazuelo MB, Wilson KT, Van Kaer L. 2011. Intestinal Epithelial Cells Modulate CD4 T Cell Responses via the Thymus Leukemia Antigen. *J Immunol 187: 4051-60*

74. Hashimoto K, Hirai M, Kurosawa Y. 1995. A gene outside the human MHC related to classical HLA class I genes. *Science* 269: 693-5

75. Walter L, Gunther E. 1998. Isolation and molecular characterization of the rat MR1 homologue, a non-MHC-linked class I-related gene. *Immunogenetics* 47: 477-82

76. Yamaguchi H, Hirai M, Kurosawa Y, Hashimoto K. 1997. A highly conserved major histocompatibility complex class I-related gene in mammals. *Biochem Biophys Res Commun* 238: 697-702

77. Riegert P, Wanner V, Bahram S. 1998. Genomics, isoforms, expression, and phylogeny of the MHC class I-related MR1 gene. *J Immunol* 161: 4066-77

78. Parra-Cuadrado JF, Navarro P, Mirones I, Setien F, Oteo M, Martinez-Naves E. 2000. A study on the polymorphism of human MHC class I-related MR1 gene and identification of an MR1-like pseudogene. *Tissue antigens* 56: 170-2

79. Yamaguchi H, Hashimoto K. 2002. Association of MR1 protein, an MHC class I-related molecule, with beta(2)-microglobulin. *Biochem Biophys Res Commun* 290: 722-9

80. Huang S, Gilfillan S, Cella M, Miley MJ, Lantz O, Lybarger L, Fremont DH, Hansen TH. 2005. Evidence for MR1 antigen presentation to mucosal-associated invariant T cells. *Journal Biol Chem* 280: 21183-93

81. Huang S, Martin E, Kim S, Yu L, Soudais C, Fremont DH, Lantz O, Hansen TH. 2009. MR1 antigen presentation to mucosal-associated invariant T cells was highly conserved in evolution. *Proc Natl Acad Sci USA* 106: 8290-5

82. Treiner E, Duban L, Bahram S, Radosavljevic M, Wanner V, Tilloy F, Affaticati P, Gilfillan S, Lantz O. 2003. Selection of evolutionarily conserved mucosal-associated invariant T cells by MR1. *Nature* 422: 164-9

83. Treiner E, Duban L, Moura IC, Hansen TH, Gilfillan S, Lantz O. 2005. Mucosal-associated invariant T (MAIT) cells: an evolutionarily conserved T cell subset. *Microbes Infect* 7: 552-9

84. Kawachi I, Maldonado J, Strader C, Gilfillan S. 2006. MR1-restricted V alpha 19i mucosal-associated invariant T cells are innate T cells in the gut lamina propria that provide a rapid and diverse cytokine response. *J Immunol* 176: 1618-27

85. Croxford JL, Miyake S, Huang Y-Y, Shimamura M, Yamamura T. 2006. Invariant V(alpha)19i T cells regulate autoimmune inflammation. *Nat Immunol* 7: 987-94

86. Huang S, Gilfillan S, Kim S, Thompson B, Wang X, Sant AJ, Fremont DH, Lantz O, Hansen TH. 2008. MR1 uses an endocytic pathway to activate mucosal-associated invariant T cells. *J Exp Med* 205: 1201-11

87. Jensen PE, Sullivan BA, Reed-Loisel LM, Weber DA. 2004. Qa-1, a nonclassical class I histocompatibility molecule with roles in innate and adaptive immunity. *Immunol Res* 29: 81-92

88. Aldrich CJ, Rodgers JR, Rich RR. 1988. Regulation of Qa-1 expression and determinant modification by an H-2D-linked gene, Qdm. *Immunogenetics* 28: 334-44

89. Aldrich CJ, DeCloux A, Woods AS, Cotter R, Soloski MJ, Forman J. 1994. Identification of a Tap-dependent leader peptide recognized by alloreactive T cells specific for a class Ib antigen. *Cell* 79: 649-58

90. Kurepa Z, Forman J. 1997. Peptide binding to the class Ib molecule, Qa-1b. *J Immunol* 158: 3244-51

91. Bai A, Broen J, Forman J. 1998. The pathway for processing leader-derived peptides that regulate the maturation and expression of Qa-1b. *Immunity* 9: 413-21

92. Bai A, Aldrich CJ, Forman J. 2000. Factors controlling the trafficking and processing of a leader-derived peptide presented by Qa-1. *J Immunol* 165: 7025-34

93. Braud VM, Allan DS, O'Callaghan CA, Soderstrom K, D'Andrea A, Ogg GS, Lazetic S, Young NT, Bell JI, Phillips JH, Lanier LL, McMichael AJ. 1998. HLA-E binds to natural killer cell receptors CD94/NKG2A, B and C. *Nature* 391: 795-9

94. Vance RE, Kraft JR, Altman JD, Jensen PE, Raulet DH. 1998. Mouse CD94/NKG2A is a natural killer cell receptor for the nonclassical major histocompatibility complex (MHC) class I molecule Qa-1(b). *J Exp Med* 188: 1841-8

95. Salcedo M, Bousso P, Ljunggren HG, Kourilsky P, Abastado JP. 1998. The Qa-1b molecule binds to a large subpopulation of murine NK cells. *Eur J Immunol* 28: 4356-61

96. McMahon CW, Zajac AJ, Jamieson AM, Corral L, Hammer GE, Ahmed R, Raulet DH. 2002. Viral and bacterial infections induce expression of multiple NK cell receptors in responding CD8(+) T cells. *J Immunol* 169: 1444-52

97. Lazetic S, Chang C, Houchins JP, Lanier LL, Phillips JH. 1996. Human natural killer cell receptors involved in MHC class I recognition are disulfide-linked heterodimers of CD94 and NKG2 subunits. *J Immunol* 157: 4741-5

98. Lanier LL. 2008. Up on the tightrope: natural killer cell activation and inhibition. *Nat Immunol* 9: 495-502

99. Vance RE, Jamieson AM, Raulet DH. 1999. Recognition of the class Ib molecule Qa-1(b) by putative activating receptors CD94/NKG2C and CD94/NKG2E on mouse natural killer cells. *J Exp Med* 190: 1801-12

100. Vivier E, Tomasello E, Baratin M, Walzer T, Ugolini S. 2008. Functions of natural killer cells. *Nat Immunol* 9: 503-10

101. Kraft JR, Vance RE, Pohl J, Martin AM, Raulet DH, Jensen PE. 2000. Analysis of Qa-1(b) peptide binding specificity and the capacity of CD94/NKG2A to discriminate between Qa-1-peptide complexes. *J Exp Med* 192: 613-24

102. Stevens J, Joly E, Trowsdale J, Butcher GW. 2001. Peptide binding characteristics of the nonclassical class Ib MHC molecule HLA-E assessed by a recombinant random peptide approach. *BMC Immunol* 2: 5

103. Kambayashi T, Kraft-Leavy JR, Dauner JG, Sullivan BA, Laur O, Jensen PE. 2004. The nonclassical MHC class I molecule Qa-1 forms unstable peptide complexes. *J Immunol* 172: 1661-9

104. Bouwer HG, Seaman MS, Forman J, Hinrichs DJ. 1997. MHC class Ib-restricted cells contribute to antilisterial immunity: evidence for Qa-1b as a key restricting element for Listeria-specific CTLs. *J Immunol* 159: 2795-801

105. Lo WF, Ong H, Metcalf ES, Soloski MJ. 1999. T cell responses to Gram-negative intracellular bacterial pathogens: a role for CD8+ T cells in immunity to Salmonella infection and the involvement of MHC class Ib molecules. *J Immunol* 162: 5398-406

106. Salerno-Gonçalves R, Fernandez-Viña M, Lewinsohn DM, Sztein MB. 2004. Identification of a human HLA-E-restricted CD8+ T cell subset in volunteers immunized with Salmonella enterica serovar Typhi strain Ty21a typhoid vaccine. *J Immunol* 173: 5852-62

107. Davies A, Kalb S, Liang B, Aldrich CJ, Lemonnier FA, Jiang H, Cotter R, Soloski MJ. 2003. A peptide from heat shock protein 60 is the dominant peptide bound to Qa-1 in the absence of the MHC class Ia leader sequence peptide Qdm. *J Immunol* 170: 5027-33

108. Fang M, Orr MT, Spee P, Egebjerg T, Lanier LL, Sigal LJ. 2011. CD94 Is Essential for NK Cell-Mediated Resistance to a Lethal Viral Disease. *Immunity*

109. Tompkins SM, Kraft JR, Dao CT, Soloski MJ, Jensen PE. 1998. Transporters associated with antigen processing (TAP)-independent presentation of soluble insulin to alpha/beta T cells by the class Ib gene product, Qa-1(b). *J Exp Med* 188: 961-71

110. Sullivan BA, Kraj P, Weber DA, Ignatowicz L, Jensen PE. 2002. Positive selection of a Qa-1-restricted T cell receptor with specificity for insulin. *Immunity* 17: 95-105

111. Oliveira CC, van Veelen PA, Querido B, de Ru A, Sluijter M, Laban S, van der Burg SH, Offringa R, van Hall T. 2010. The nonpolymorphic MHC Qa-1b mediates CD8+ T cell surveillance of antigen-processing defects. *J Exp Med* 207: 207-21, S1-2

112. Jiang H, Ware R, Stall A, Flaherty L, Chess L, Pernis B. 1995. Murine CD8+ T cells that specifically delete autologous CD4+ T cells expressing V beta 8 TCR: a role of the Qa-1 molecule. *Immunity* 2: 185-94

113. Jiang H, Kashleva H, Xu LX, Forman J, Flaherty L, Pernis B, Braunstein NS, Chess L. 1998. T cell vaccination induces T cell receptor Vbeta-specific Qa-1-restricted regulatory CD8(+) T cells. *Proc Natl Acad Sci USA* 95: 4533-7

114. Lu L, Werneck MBF, Cantor H. 2006. The immunoregulatory effects of Qa-1. *Immunol Rev* 212: 51-9

CHAPTER 2

MHC CLASS IB RESTRICTED ANTI-LCMV T CELL RESPONSES

Abstract

MHC class Ib molecules have low expression level and limited tissue distribution, nevertheless, some CD8+ T cells are restricted by MHC class Ib. Class Ib restricted CD8+ T cells were reported to participate in immune responses against bacterial infections. There have been limited studies on the role MHC class Ib restricted T cells in anti-viral responses. In this study, $K^{b-/-}D^{b-/-}$ and $K^{b-/-}D^{b-/-}CIITA^{-/-}$ mice, which only express the MHC class Ib molecules but not the class Ia molecules, were used to study the MHC class Ib restricted anti-LCMV response. LCMV was partially but not completely cleared during the early phase of the acute infection in the $K^{b-/-}D^{b-/-}CIITA^{-/-}$ mice, while the virus infection was not controlled in the $K^{b-/-}D^{b-/-}\beta2m^{-/-}$ mice. Clearance was dependent on CD8+ T cells. CD8+ T cells responded by expansion, producing IFNγ and granzyme B. *In vitro* assays demonstrated that the CD8+ T cell responses were restricted by MHC class Ib molecules. The CD8+ T cells in wild type mice expanded and contracted to a constant level, and memory responses were detected by *in vitro* assays. The CD8+ T cell number in the $K^{b-/-}D^{b-/-}CIITA^{-/-}$ mice continued to drop and the CD8+ T cells lost the ability to produce IFNγ while the infection became chronic.

Introduction

CD8+ T cells play critical roles in the host immune response to infections. They are selected by MHC class I molecules in the thymus. CD8+ T cells in the periphery expand upon infection to increase their numbers in a few days. The effector CD8+ T cells interact with antigens presented by MHC class I molecules through the TCR, and respond by producing large amounts of IFNγ and TNFα, and perforin/granzyme B cytotoxic factors. After the expansion, which lasts for about 1 week, majority of the CD8+ T cells die by apoptosis leaving ~5% of the cells alive and becoming long-live memory cells (1, 2). These principles were determined from the studies of CD8+ T cells restricted by classical MHC class I molecules, and little is known about the CD8+ T cells restricted by nonclassical MHC class I. The nonclassical MHC class I restricted CD8+ cells naturally occur in animals and they represent a small percentage of the total CD8+ T cell population (3). The numerically dominant conventional CD8+ T cells may compete with the Ib-restricted CD8+ T cells for niche, cytokines and other factors that are important for CD8+ T cells survival (4, 5). In $K^{b-/-}D^{b-/-}$ mice, which do not express MHC class Ia and thus do not have Ia-restricted T cells, the CD8+ T cells are much fewer than in wild type mice, but these CD8+ T cells are restricted by MHC class Ib molecules in theory (6). In naïve $K^{b-/-}D^{b-/-}CIITA^{-/-}$ mice, which do not express either MHC class Ia or MHC class II, CD8+ T cells were significantly expanded compared to the ones in $K^{b-/-}D^{b-/-}$ mice (7, 8). The increased CD8+ T cells in $K^{b-/-}D^{b-/-}CIITA^{-/-}$ mice were observed to arise from homeostatic expansion. CD8+ T cells in both $K^{b-/-}D^{b-/-}$ and $K^{b-/-}D^{b-/-}CIITA^{-/-}$ mice express high level of CD44, CD122 and Ly6C, and behave like memory cells (8). Class Ib

restricted CD8+ T cells were reported to participate in host anti-bacteria responses (9-16). Their role during virus infection was rarely studied (17, 18).

LCMV belongs to Arenovirus family. It is an ambisense RNA virus containing two genomic RNAs. The RNA genome encodes four proteins: glycoprotein (GP), nucleoprotein (NP), the RNA polymerase (L protein) and a protein required for the virus budding (Z protein) (19). LCMV is widely used in studies of anti-viral immune responses. The dominant peptide specificities in the CD8+ T cell response in C57BL/6 mice are NP396 (FQPQNGQFI), which binds H2-D^b, and GP33 (KAVYNFATM), which is a ligand for both H2-D^b and H2-K^b. The K^b/D^b restricted CD8+ T cells response against NP396 and GP33 accounts for half of the CTL response during LCMV acute infection (20, 21). There are many different strains of LCMV isolated after the first discovery of the virus. Armstrong and clone 13 are both common laboratory strains. There are only two amino acids difference between LCMV-Arm and LCMV-CL13, but LCMV-Arm causes an acute infection in their natural rodent host, while LCMV-CL13 causes protracted or chronic infections that require several months for the host to clear the virus (22-24).

Although MHC class Ia restricted CD8+ T cell response are critical for control of pathogen, more and more studies show that MHC class Ib molecules also play an important role in the host defense against microbial infections. For example, H2-M3 restricted anti-Listeria CD8+ T cells (9, 10, 25, 26). Qa-1^b restricted CD8+ T cells were found in Salmonella infected hosts (12, 13). In addition, H2-Q9, which encodes Qa-2, was found to be an important restriction element of CD8+ T cell response to the polyoma virus infection (17, 27). These findings lead to the question of whether MHC class Ib is

involved in other anti-viral responses, whether it is generally true that MHC class Ib participates in host anti-viral responses, how do Ib molecules participate in the response, and how important their participation is.

In this study, we used LCMV-Arm virus as a model pathogen to investigate the participation of MHC class Ib restricted CD8+ T cells in the host anti-viral response.

Materials and methods

Mice

C57BL/6, CIITA$^{-/-}$, β2M$^{-/-}$, and B6.K1(Qa-2$^{-/-}$) mice were obtained from Jackson Laboratory. The CIITA$^{-/-}$ mice were backcrossed with C57BL/6 mice for 7 generations (Jackson Lab). K$^{b-/-}$D$^{b-/-}$ mice were backcrossed to C57BL/6 mice for 10 generations and were obtained from Taconic Farm (6). K$^{b-/-}$D$^{b-/-}$CIITA$^{-/-}$ mice and K$^{b-/-}$D$^{b-/-}$β2M$^{-/-}$ mice were generated by crossing K$^{b-/-}$D$^{b-/-}$ mice with either CIITA$^{-/-}$ mice or β2M$^{-/-}$ mice (8). B6.129S6-H2-T23^{tm1Cant}/J mice, which are Qa-1$^{-/-}$, were a gift from Dr. Harvey Cantor (Harvard). CD1d$^{-/-}$ mice were a gift from Dr. Luc Van Kaer (Vanderbilt University). H2-M3$^{-/-}$ mice were a gift from Dr. Chyung-Ru Wang (Northwestern University). Mice 8-12 weeks old were used in the experiments. Both male and female mice were used in the LCMV clearance studies; the mice were sex-matched in all the other experiments. Mice were housed in a specific pathogen-free facility at the University of Utah and were handled according to the IACUC policies.

Cell lines

Vero cells and BHK-21 cells were cultured in DMEM media supplemented with 10% fetal bovine serum, 100 U/ml penicillin, 100 μg/ml streptomycin and 292 μg/ml L-glutamine (Invitrogen). Mouse primary cells were cultured in RPMI-1640 media

supplemented with 10% fetal bovine serum, 100 U/ml penicillin, 100 μg/ml streptomycin, 292 μg/ml L-glutamine, 100 μM nonessential amino acids, 1 mM sodium pyruvate, and 55 μM 2-mercaptoethanol (Invitrogen). All the cells are maintained in humidified 37°C, 5% CO_2 incubator.

Virus and infection

LCMV-Armstrong virus was a gift from Dr. Matthew Williams (University of Utah). Virus was maintained in BHK-21 cells, and the titer was obtained by Vero cell plaque assay (28). Briefly, $6x10^5$/well Vero cells were seeded in 6-well plate (Corning Costar) 1 day before the plaque assay, so that they would form confluent monolayers; virus stock were 10-fold serially diluted in DMEM media, and 200 μl of the diluted virus was added on top of the Vero cell monolayer; the plate was incubated for 1 hour before the addition of 0.5% agarose in 199 media (Invitrogen); 4 days later, 0.5% agarose in 199 media containing neutral red was added to the plate, and the plaque number was counted the following day. The infection of mice was achieved by intraperitoneal inoculation with LCMV-Armstrong virus in a dose of $2x10^5$ PFU/mouse in 200 μl of sterile PBS. At certain time points after the infection, mouse tissues were harvested for the desired experiments. Tissues collected for plaque assay were weighed and homogenized in DMEM media, followed by 10-fold serial dilutions and incubation with Vero cell monolayers to determine virus titers as described (28).

Antibodies and flow cytometry

Mouse-specific TCRβ (H57-597), CD4 (GK1.5, RM4-5), CD8α (53-6.7), IFNγ (XMG1.2), Granzyme B (16G6) monoclonal antibodies, and TCR Vβ panel antibodies conjugated with FITC, PE, PerCP, APC, PerCP-Cy5.5, PE-Cy5, PE-Cy7, pacific blue or

Alexafluor488 fluorophore were purchased from BD Bioscience or eBiosience. Suspended single cells were stained with antibodies for detecting surface proteins in 4°C for 20 min. If necessary, intracellular staining was done after surface staining by the BD Cytofix/Cytoperm Fixation/Permeabilization Solution Kit according to the manufacture's instructions. Cells were fixed by 1% paraformaldehyde in PBS after the staining. The fluorescence was detected by FACS Canto II machine (BD Bioscicence) and the data were analyzed by Flowjo software (Tree Star).

The MR1 blocking antibody (26.5) used in *in vitro* stimulation assay was a gift from Dr. Ted Hansen (Washington University School of Medicine).

CD8+ T cell depletion

Mice were intraperitoneally injected with 300 μg CD8 monoclonal antibody (2.43) in PBS at day -3, -2, -1 before the LCMV infection, and at day 6 after the LCMV infection. The depletion efficiency was ≥95% based on analysis by flow cytometry.

In vitro restimulation assay

Peritoneal macrophages or bone marrow-derived macrophages were used as antigen presenting cells in the assay. To harvest the peritoneal macrophages, mice were i.p. injected with 100 μg concanavalin A (ConA) in 200 μl PBS; 3 days after the injection, peritoneal exudates were harvested and $4x10^5$ cells were plated in one well of the 96-well plate; 2 hours after incubation, nonadherent cells were washed away and the remaining macrophage cells were either mock-treated with culture media or infected with LCMV-Armstrong (MOI=5) for 1 day. Bone marrow cells were harvested from the femur and tibia and cultured in RPMI-1640 media containing 30% L929 supernatant for 6 days; the nonadherent cells were removed and the remaining adherent cells, which were >99%

F4/80+, were harvested and re-plated in $1x10^5$/well in a 96-well plate as antigen presenting cells; the cells were either mock-treated with culture media or infected with LCMV-Arm (MOI=5) for 1 day before the addition of responding cells. Spleens from LCMV infected mice were harvested at day 8 after the LCMV infection. Single splenocyte suspensions were made, and CD8+ T cells were enriched using a CD8a+ T cell isolation kit (Miltenyi Biotec), and if necessary, further purified by staining with CD8 antibody (53-6.7), followed by FACS sorting to obtain high purified CD8+ T cells,. $1x10^5$ enriched CD8+ T cells were added as responding cells to the prepared antigen presenting macrophages. The MR1 blocking antibody was added to the antigen presenting macrophages at 5 μg/ml 1 hour before the addition of the responding cells. The cells were co-cultured for 20 hours, 10μg/ml Brefeldin A was added to the cells for additional 4 hours, and the cells were harvested for analysis of IFNγ containing cells by flow cytometry.

Results

Partial clearance of LCMV-Arm virus in the MHC class Ia deficient mice

CD8 but not CD4 are required for clearance of LCMV, although CD4 is required to form CTL memory (29, 30). MHC class II knockout mice can clear the virus as well as the wild type mice, but β2-microglobulin is required for the virus clearance (29, 30). To investigate the importance of MHC class Ib restricted CD8+ T cells for LCMV clearance, $K^{b-/-}D^{b-/-}CIITA^{-/-}$ mice, which do not express MHC class II and MHC class Ia, were infected with the LCMV-Arm, with wild type mice and $K^{b-/-}D^{b-/-}\beta2m^{-/-}$ mice as controls. All the three types of mice have high virus titer in the spleen at day 3. At day 8, the virus was not detectable in the B6 mice, and the titer was consistently lower in the $K^{b-/-}D^{b-/-}$

CIITA$^{-/-}$ mice compared to in the K$^{b-/-}$D$^{b-/-}$β2m$^{-/-}$ mice (Figure 2.1). This suggested that MHC class Ib restricted T cells contribute to virus clearance.

CD8+ T cells are critical for the partial virus control in the K$^{b-/-}$D$^{b-/-}$ mice

CD8+ T cells are important for control LCMV; in the CD8$^{-/-}$ mice, the infection becomes persistent (31). The K$^{b-/-}$D$^{b-/-}$CIITA$^{-/-}$ mice have low amounts of CD8+ T cells compared to the wild type mice, and in theory, these CD8+ T cells are restricted by MHC class Ib molecules since the mice are deficient in MHC class Ia. To investigate the role of CD8+ T cells in the K$^{b-/-}$D$^{b-/-}$CIITA$^{-/-}$ mice during LCMV-Arm infection, the mice were inoculated with CD8α antibody (clone 2.43) before and after LCMV-Arm infection. Flow cytometry showed that over 95% of the CD8+ T cells in the mice were depleted by the antibody treatment (data not shown). With CD8+ T cells depleted, the virus titer in the

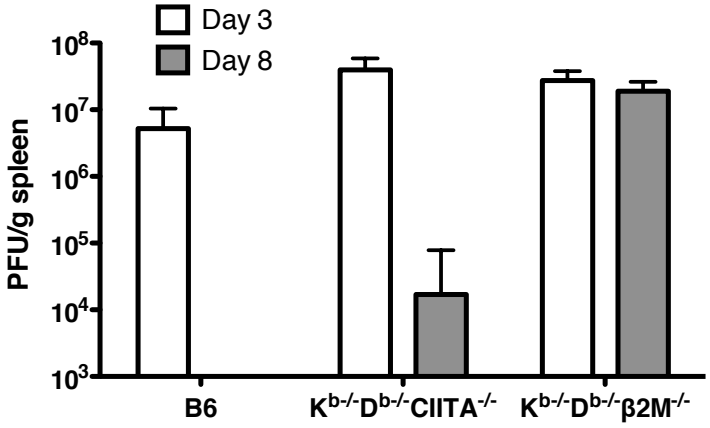

Figure 2.1 Partial control of LCMV infection in K$^{b-/-}$D$^{b-/-}$CIITA$^{-/-}$ mice. B6, K$^{b-/-}$D$^{b-/-}$CIITA$^{-/-}$, K$^{b-/-}$D$^{b-/-}$β2M$^{-/-}$ mice were injected i.p. with 2x10^5 PFU/mouse LCMV-Armstrong. Day 3 and day 8 postinfection, virus titers in spleen tissues were measured by plaque assay. Three to four mice were included in each group; the data represent one of two independent experiments.

$K^{b-/-}D^{b-/-}CIITA^{-/-}$ mice at day 8 after infection was significantly increased to a level as high as in the $K^{b-/-}D^{b-/-}\beta2m^{-/-}$ mice (Figure 2.2). The virus was also abundant in the CD8+ T cell depleted B6 mice spleen, liver, lung and kidney. This proved that CD8+ T cells in the $K^{b-/-}D^{b-/-}CIITA^{-/-}$ mice are critical for the observed partial control of LCMV-Arm infection.

CD8+ T cell expansion during LCMV-Arm infection

Virus specific CD8+ T cells undergo vigorous expansion upon acute LCMV infection and the cell percentage and number peaks at 1 week postinfection (32). In both the wild type mice and $K^{b-/-}D^{b-/-}CIITA^{-/-}$ mice, CD8+ T cells expanded after the LCMV-Arm infection (Figure 2.3A). The percentage and number of CD8+ T cells reaches maximum at day 8 in the B6 mice, while the CD8+ T cells continue to expand from day 8 to at least day 12 in the $K^{b-/-}D^{b-/-}CIITA^{-/-}$ mice, but $K^{b-/-}D^{b-/-}CIITA^{-/-}$ CD8+ T cell numbers were much lower in number than in the wild type mice (Figure 2.3B). The CD8+ T cells in naive $K^{b-/-}D^{b-/-}CIITA^{-/-}$ mice had a diverse TCR repertoire as shown by Vβ staining (Figure 2.3C). The expanded CD8+ T cells also had a diverse Vβ repertoire and the Vβ usage was skewed such that the percentage of Vβ8, Vβ10, and Vβ13 positive cells was considerably higher than in the uninfected mice. There were very few CD4+ T cells in the $K^{b-/-}D^{b-/-}CIITA^{-/-}$ mice due to the deficiency of MHC class II transactivator CIITA, and a considerable percentage of CD4+ T cells in the $K^{b-/-}D^{b-/-}CIITA^{-/-}$ mice were CD1d restricted NK1.1+ NKT cells (data not shown). The CD4+ cell number decreased after the infection (Figure 2.3D), probably representing the apoptotic depletion of NKT cells after acute viral infections (33, 34). The CD8+ T cells were selectively expanded in the $K^{b-/-}D^{b-/-}CIITA^{-/-}$ mice after LCMV-Arm infection.

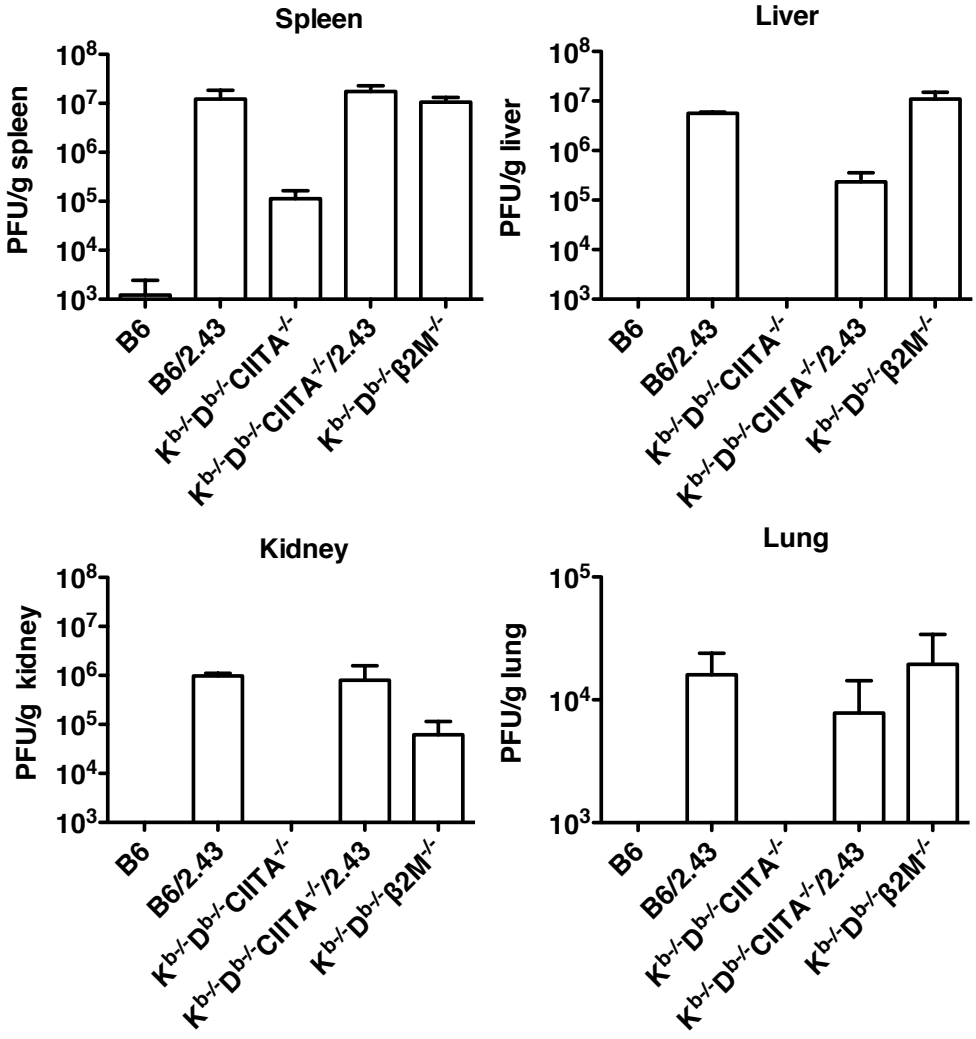

Figure 2.2 Control of LCMV-Arm infection in B6 and $K^{b-/-}D^{b-/-}CIITA^{-/-}$ mice is dependent on CD8+ cells. B6, $K^{b-/-}D^{b-/-}CIITA^{-/-}$, and $K^{b-/-}D^{b-/-}\beta2M^{-/-}$ mice were either mock treated or i.p. inoculated with CD8-specific antibody (clone 2.43) at day -3, -2, -1 and day 6 of LCMV-Arm infection to deplete the CD8+ T cells. Spleen, liver, kidney, and lung tissues were harvested for plaque assay at day 8 post-LCMV-Arm infection.

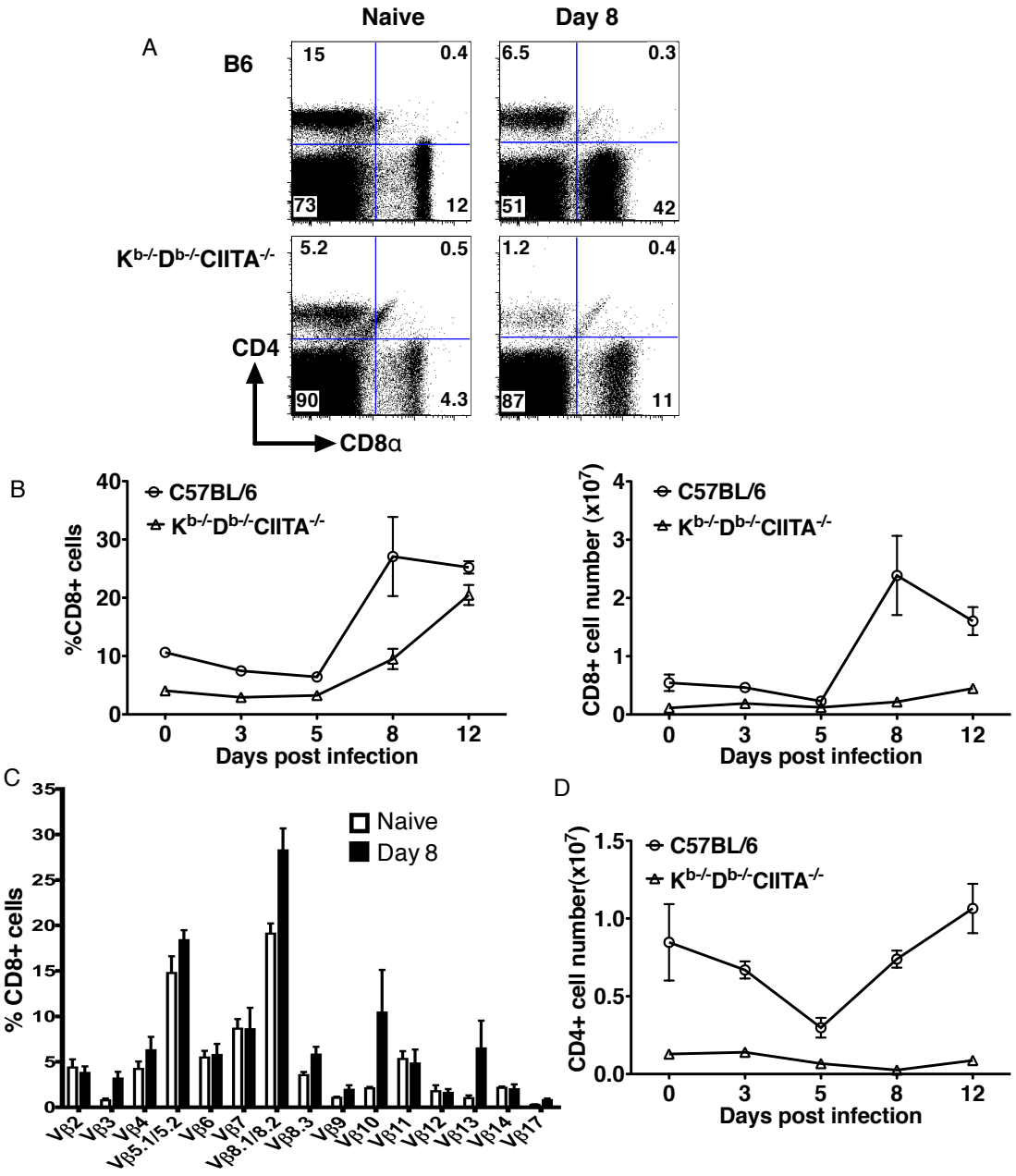

Figure 2.3 CD8+ T cells in $K^{b-/-}D^{b-/-}CIITA^{-/-}$ mice undergo expansion after LCMV infection. B6 and $K^{b-/-}D^{b-/-}CIITA^{-/-}$ mice were inoculated i.p. with $2x10^5$ PFU/mouse LCMV-Armstrong. At day 3, 5, 8, 12 postinfection, splenocytes were harvested for flow cytometry analysis and enumeration. (A) Representative flow cytometry of CD4+ and CD8+ cells in spleens from naïve and day 8 LMCV infected mice. (B) The percentage and absolute number of CD8+ cells in LCMV-Arm infected mice at different days postinfection were analyzed. (C) TCR Vβ usage in splenic CD8+ T cells from naïve and 8 day LCMV infected $K^{b-/-}D^{b-/-}CIITA^{-/-}$ mice was determined by flow cytometry. (D) The absolute number of CD4+ cells in the LCMV-Arm infected mice spleen at different days post infection as determined by flow cytometry. These results are representative of at least two independent experiments.

CD8+ T cells effector phenotype

CD8+ T cells in the $K^{b-/-}D^{b-/-}CIITA^{-/-}$ mice undergo homeostatic expansion and acquire activation phenotypes in the naïve mice, such that the cells express high levels of CD44, CD122, Ly6C and low levels of β7 integrin (8). This makes it impossible to study the infection induced CD8+ T cell activation using these markers. The effector phenotypes of CD8+ T cells were investigated by examining the presence of Granzyme B and IFNγ. Wild type and $K^{b-/-}D^{b-/-}CIITA^{-/-}$ CD8+ T cells did not produce Granzyme B in the naïve state and increased Granzyme B production was observed after LCMV infection. At day 5 and day 8 after the infection, about 50% of the CD8+ T cells became Granzyme B+, indicating that CD8+ T cells in both B6 and $K^{b-/-}D^{b-/-}CIITA^{-/-}$ mice were activated to clear the virus infection (Figure 2.4A). Noticeably, the mean fluorescence of the $K^{b-/-}D^{b-/-}CIITA^{-/-}$ mice CD8+ T cells were higher than that of the B6 cells at day 3, 8 and 12 (Figure 2.4B). IFNγ production was examined by direct *ex vivo* staining splenocytes from the infected mice. Both B6 and $K^{b-/-}D^{b-/-}CIITA^{-/-}$ CD8+ cells increase IFNγ production after the infection (Figure 2.5A). The percentage of IFNγ+CD8+ cells peaked at day 5 and the number reached peak at day 8 in the wild type mice. The percentage and number of IFNγ+CD8+ cells peaked at day 8 and remained high at day 12 after infection in the $K^{b-/-}D^{b-/-}CIITA^{-/-}$ mice. Although naive $K^{b-/-}D^{b-/-}CIITA^{-/-}$ mice had much fewer CD8+ T cells than naïve wild type mice, there were higher percentage and number of IFNγ+CD8+ cells in the LCMV-infected $K^{b-/-}D^{b-/-}CIITA^{-/-}$ mice than in the infected B6 mice (Figure 2.5B). The results indicated that MHC class Ib restricted CD8+ T cells could respond vigorously to the virus infection by producing granzyme B factors and IFNγ cytokines.

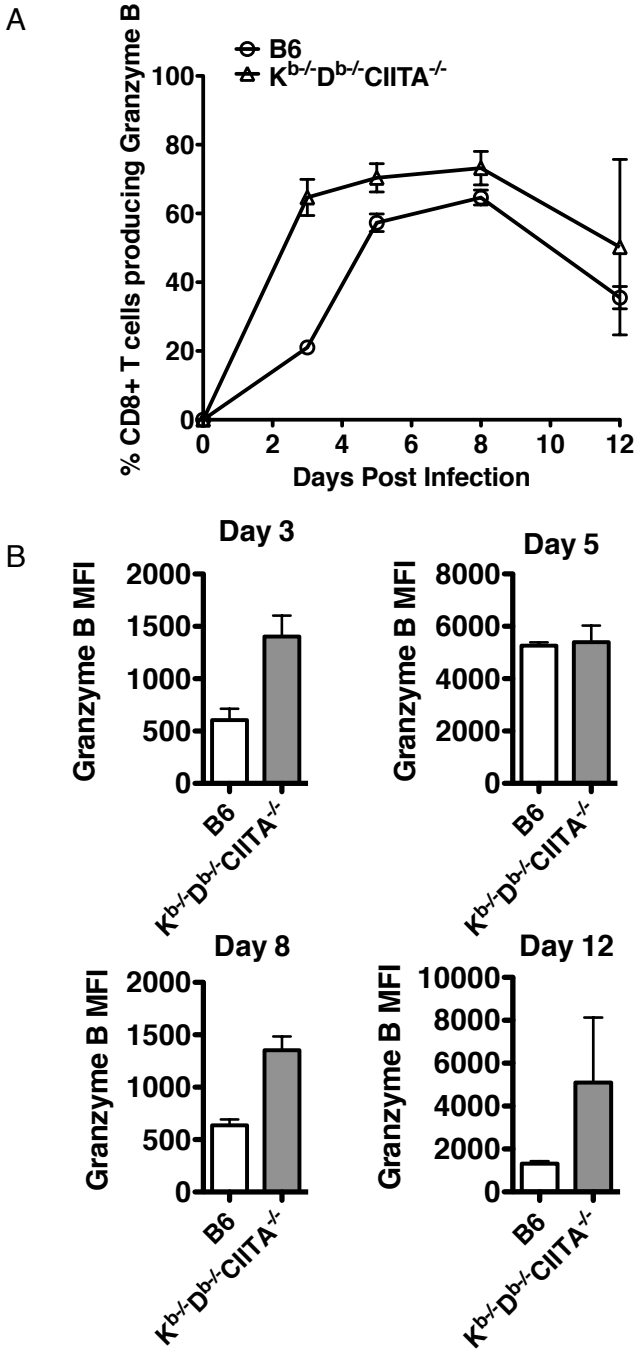

Figure 2.4 Early and robust LCMV-specific granzyme B production by CD8 T cells during LCMV infection in $K^{b-/-}D^{b-/-}CIITA^{-/-}$ mice. Splenocytes from LCMV-infected B6, and $K^{b-/-}D^{b-/-}CIITA^{-/-}$ mice were stained on the surface for CD8α and TCRβ, then intracellularly for granzyme B and analyzed by flow cytometry. (A) The percentage of granzyme B producing-$CD8\alpha^{+}TCR\beta^{+}$ splenocytes from B6 and $K^{b-/-}D^{b-/-}CIITA^{-/-}$ mice at day 3, 5, 8 and 12 post LCMV-Arm infection. (B) The mean fluorescence intensity (MFI) of granzyme B expression on the CD8α+TCRβ+ cells at day 3, 5, 8 and 12 postinfection.

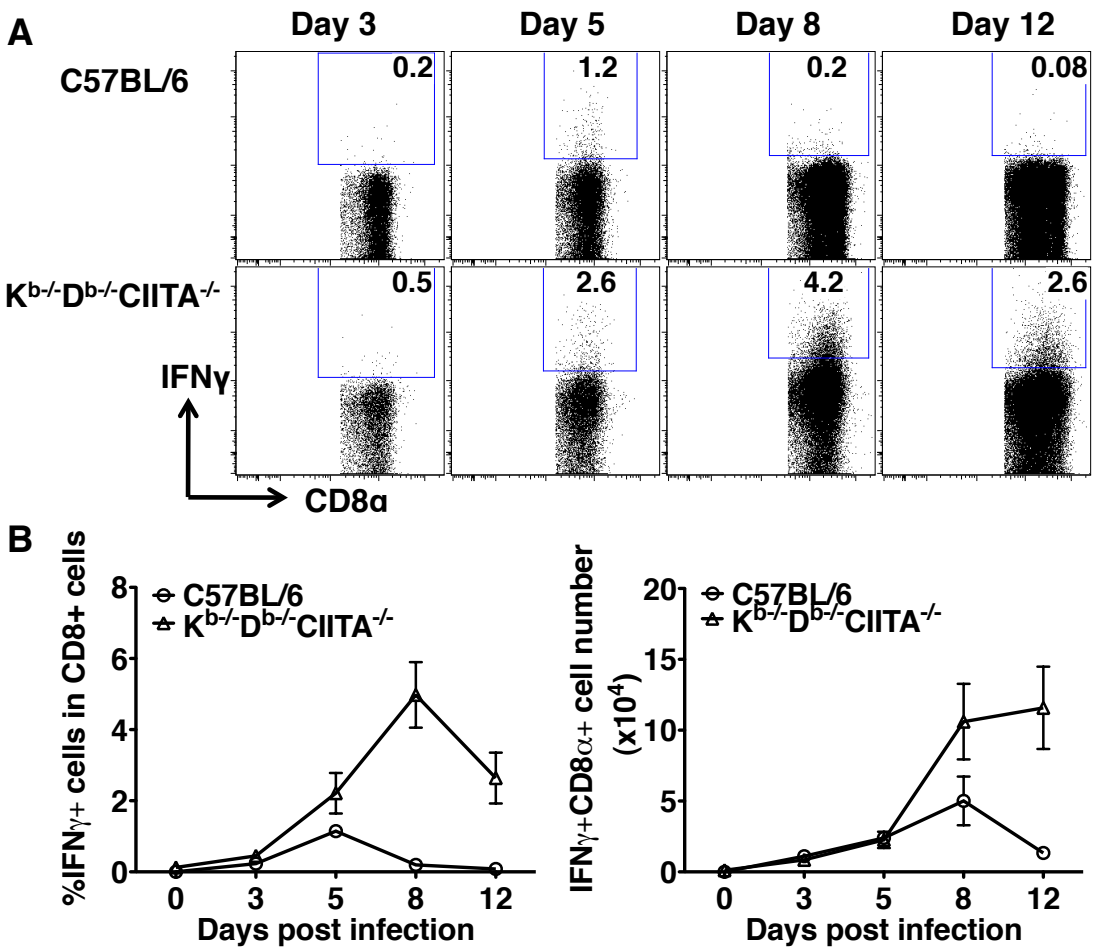

Figure 2.5 Substantial *ex vivo* IFNγ production by CD8+ cells from LCMV-infected mice. (A) B6 and $K^{b-/-}D^{b-/-}CIITA^{-/-}$ mice were infected with 2 x 10^5 PFUs LCMV-Armstrong and, at days 3, 5, 8, and 12, spleens were harvested and analyzed for surface CD8α and intracellular IFNγ by flow cytometry. (B) The percentage and total number of IFNγ producing CD8α+ spleen lymphocytes was determined for B6, and $K^{b-/-}D^{b-/-}CIITA^{-/-}$ mice at various time points postinfection.

MHC class Ib restricted anti-viral CD8+ T cell response

Although $K^{b-/-}D^{b-/-}CIITA^{-/-}$ CD8+ T cell produced IFNγ and granzyme B *in vivo* after LCMV-Arm infection, it was not known whether the response was specifically induced by the MHC/Antigen/TCR interactions. Memory phase CD8+ T cells might be activated nonspecifically to produce IFNγ and granzyme B by IL-15 cytokine without TCR signaling (35). The naïve $K^{b-/-}D^{b-/-}CIITA^{-/-}$ CD8+ T cells show memory phenotypes. To exclude the possibility that CD8+ T cells in the infected $K^{b-/-}D^{b-/-}CIITA^{-/-}$ mice were activated by some bystander mechanism, *in vitro* culture assays were established. The initial experiments showed that B6 CD8+ T cells produced IFNγ detectable by ELISA and flow cytometry when they are co-cultured with LCMV infected macrophages for 6 hours, but the $K^{b-/-}D^{b-/-}CIITA^{-/-}$ CD8+ cells did not produce IFNγ after 6 hours of co-culture with the virus infected macrophages (data not shown). After carefully examining multiple experiment parameters, it was found that only when the coculture time was elongated, could the $K^{b-/-}D^{b-/-}CIITA^{-/-}$ CD8+ T cells produce IFNγ cytokines. The primed CD8+ T cells were restimulated with the virus-infected macrophages for 24 hours and the IFNγ production was examined by intracellular staining (Figure 2.6A). Primed B6 CD8+ T cells could respond to the virus infected B6 macrophages, but not the uninfected macrophages or the infected $K^{b-/-}D^{b-/-}CIITA^{-/-}$ and $K^{b-/-}D^{b-/-}\beta2m^{-/-}$ macrophages, suggesting that majority of the CD8+ T cells from the B6 mice were restricted by the classical MHC class I molecules. The $K^{b-/-}D^{b-/-}CIITA^{-/-}$ CD8+ T cells could respond to both LCMV infected B6 and $K^{b-/-}D^{b-/-}CIITA^{-/-}$ macrophages but not $K^{b-/-}D^{b-/-}\beta2m^{-/-}$ macrophages, suggesting that the CD8+ T cells are restricted by β2m-bearing MHC class Ib molecules that were expressed on B6 and $K^{b-/-}D^{b-/-}CIITA^{-/-}$ APCs

but not on $K^{b-/-}D^{b-/-}\beta2m^{-/-}$ APCs. The LCMV infection activated a population of Ag-specific, β2m-dependent CD8+ T cells in the mice that lack the expression of MHC class Ia and MHC class II.

To further study which MHC class Ib molecule restricted CD8+ T cell anti-LCMV response in the $K^{b-/-}D^{b-/-}CIITA^{-/-}$ mice, bone-marrow derived macrophages from single MHC class Ib knockout mice and MHC class Ib blocking antibodies were used in the *in vitro* restimulation assay. Qa-$1^{b-/-}$, B6.K1(Qa-$2^{-/-}$), H2-$M3^{-/-}$, $CD1^{d-/-}$ macrophages were used and anti-MR1 blocking antibody (clone 26.5) was used in the assay (Figure 2.6B and Figure 2.6C). Although $K^{b-/-}D^{b-/-}CIITA^{-/-}$ CD8+ T cells responded weaker when re-stimulated by Qa-$2^{-/-}$ macrophages, no full-reduced IFNγ response was detected. This indicated that the MHC class Ib restricted anti-LCMV CD8+ T cell response might be restricted by multiple elements or by some yet to-be defined unknown MHC class Ib molecule.

$K^{b-/-}D^{b-/-}$ mice response to the LCMV-Arm infection

$K^{b-/-}D^{b-/-}CIITA^{-/-}$ mice do not have normal CD4+ T cells, this raises the possibility that CD8+ T cell response in the $K^{b-/-}D^{b-/-}CIITA^{-/-}$ mice were not fully competent due to the lack of CD4 + T cell help. $K^{b-/-}D^{b-/-}$ mice, which do have CD4+ T cells, were also infected with the LCMV-Arm virus to examine the CD8+ T cell responses in the presence of helper T cells. $K^{b-/-}D^{b-/-}$ CD8+ T cells expanded upon LCMV infection in a similar manner to the cells in $K^{b-/-}D^{b-/-}CIITA^{-/-}$ mice, that the percentage of CD8+ increased after the infection but the total CD8+ T cell number remained at low level

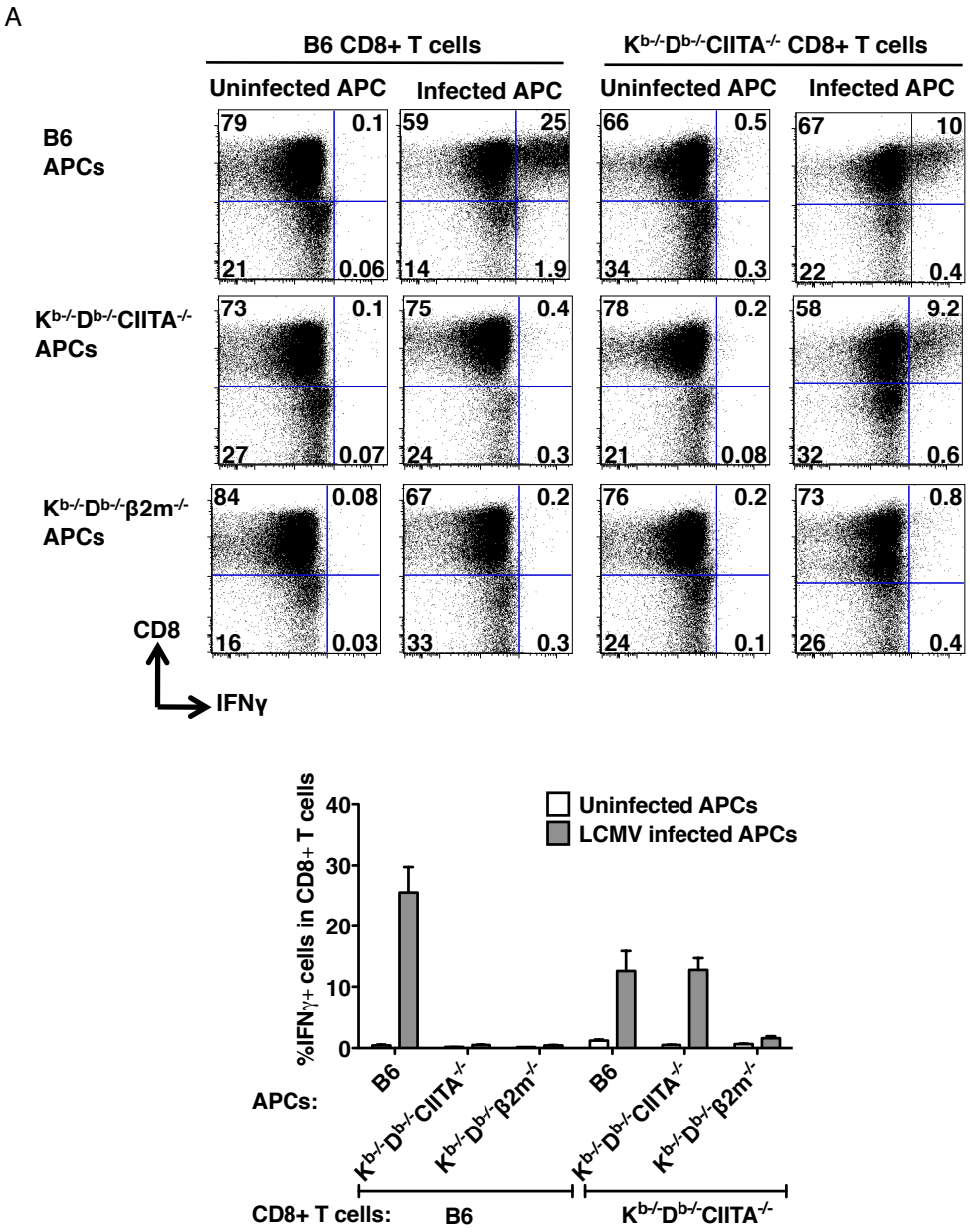

Figure 2.6 MHC class Ib-restricted CD8+ T cells from LCMV-infected $K^{b-/-}D^{b-/-}CIITA^{-/-}$ mice. (A) Peritoneal macrophages were harvested from ConA inoculated B6, $K^{b-/-}D^{b-/-}CIITA^{-/-}$, or $K^{b-/-}D^{b-/-}\beta2M^{-/-}$ mice as a source of antigen presenting cells (APCs). APCs were either uninfected or infected with LCMV-Arm for 1 day. At day 8 post LCMV-infection, splenocytes were harvested from B6 or $K^{b-/-}D^{b-/-}CIITA^{-/-}$ mice and CD8+ T cells were enriched and co-cultured with APC for 1 day, followed by analysis of IFNγ production by flow cytometry. Left: Representative flow cytometry plots showing the production of IFNγ by cultured CD8+ T cells. Right: The percentage of IFNγ+ CD8+ T cells. T cells were obtained from 3 mice for each group. The data represent one of three independent experiments.

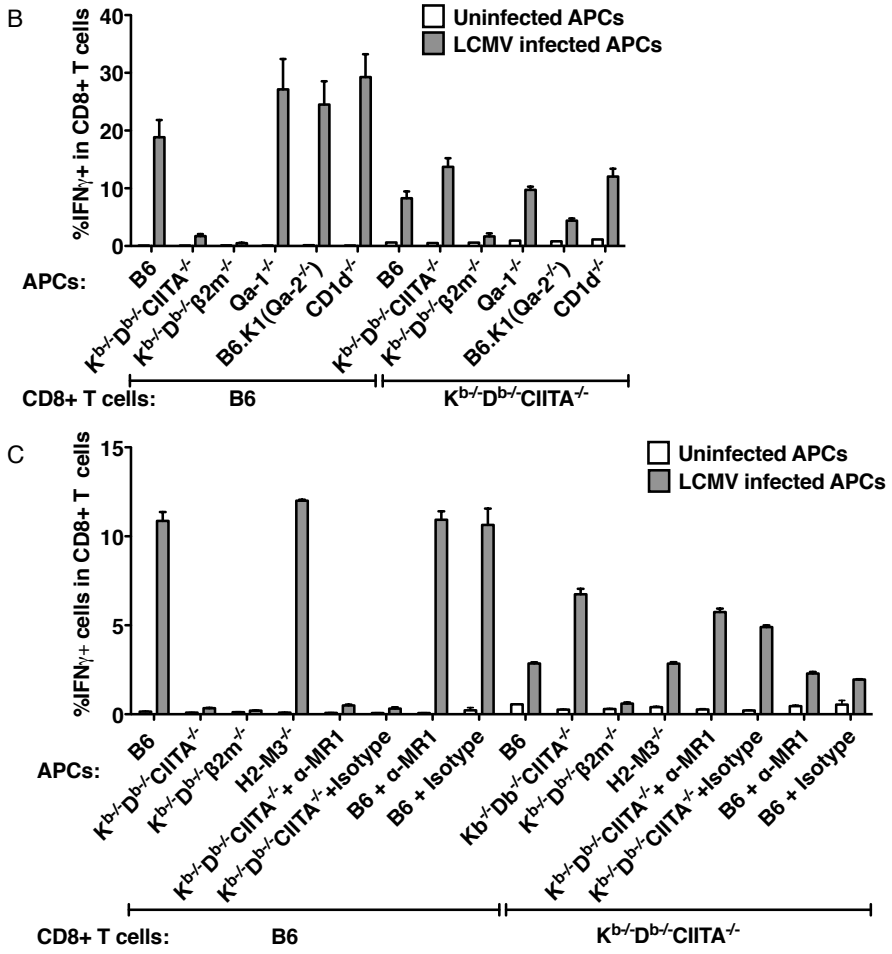

Figure 2.6 continued (B) B6, $K^{b-/-}D^{b-/-}CIITA^{-/-}$, $K^{b-/-}D^{b-/-}\beta2m^{-/-}$, Qa-$1^{-/-}$, B6.K1($Qa2^{-/-}$), and $CD1d^{-/-}$ bone marrow-derived macrophages were used as APCs. CD8+ T cells enriched from day 8 infected mice were co-cultured with the LCMV uninfected or infected APCs for 1 day, and the production of IFNγ was measure by flow cytometry. (C) B6, $K^{b-/-}D^{b-/-}CIITA^{-/-}$, $K^{b-/-}D^{b-/-}\beta2m^{-/-}$, and $H2\text{-}M3^{-/-}$ bone marrow-derived macrophages were used as APCs. MR1 blocking antibody was added as indicated to the B6 or the $K^{b-/-}D^{b-/-}CIITA^{-/-}$ APCs in 5μg/ml to block the MR1 molecule. CD8+ T cells enriched from day 8 infected mice were co-cultured with the LCMV uninfected or infected APCs for 1 day, and the production of IFNγ was measure by flow cytometry.

during the infection (Figure 2.7A). Although the CD8+ T cell number was low, large numbers of the cells produced IFNγ after the infection and the percentage of IFNγ+ CD8+ T cells was higher than B6 mice at all measured time points. The IFNγ+ CD8+ T cell number in the $K^{b-/-}D^{b-/-}$ mice was comparable to that in the B6 mice at the first week post infection, and the number remained high to at least day 12 postinfection (Figure 2.7B). The CD8+ T cells from day 8 infected $K^{b-/-}D^{b-/-}$ mouse responded to syngeneic LCMV infected macrophages, but not to $K^{b-/-}D^{b-/-}\beta2m^{-/-}$ macrophages, proving the CD8+ T cell response was MHC class Ib restricted (Figure 2.7C).

Chronic viral infection in the Class Ia deficient mice

LCMV-Arm infection usually induces acute infection in the wild type mice and the virus is cleared after about 1 week (23). In the early LCMV infection phase, $K^{b-/-}D^{b-/-}CIITA^{-/-}$ mice partially cleared the virus as shown by the lower virus titer at day 8 post infection, but the virus was not completely gone. To study whether the virus was fully cleared in the $K^{b-/-}D^{b-/-}CIITA^{-/-}$ mice, long-term infection experiment was performed. The result showed that the virus was completely cleared in the B6 mice at early phase of the infection. The virus titer was low at day 8 and 13 postinfection in the $K^{b-/-}D^{b-/-}CIITA^{-/-}$ mice, but the virus titer was high at day 37 and 82 postinfection (Figure 2.8A). The wild type CD8+ T cells expanded at the beginning of the infection and contracted to normal level after 2 months. The CD8+ T cells in the $K^{b-/-}D^{b-/-}CIITA^{-/-}$ mice also expands at the beginning, but the percentage and number decreased continuously; at day 82 post infection, the CD8+ T cell percentage and number were much lower than normal level (Figure 2.8B). A high percentage of $K^{b-/-}D^{b-/-}CIITA^{-/-}$ CD8+ T cells produced IFNγ

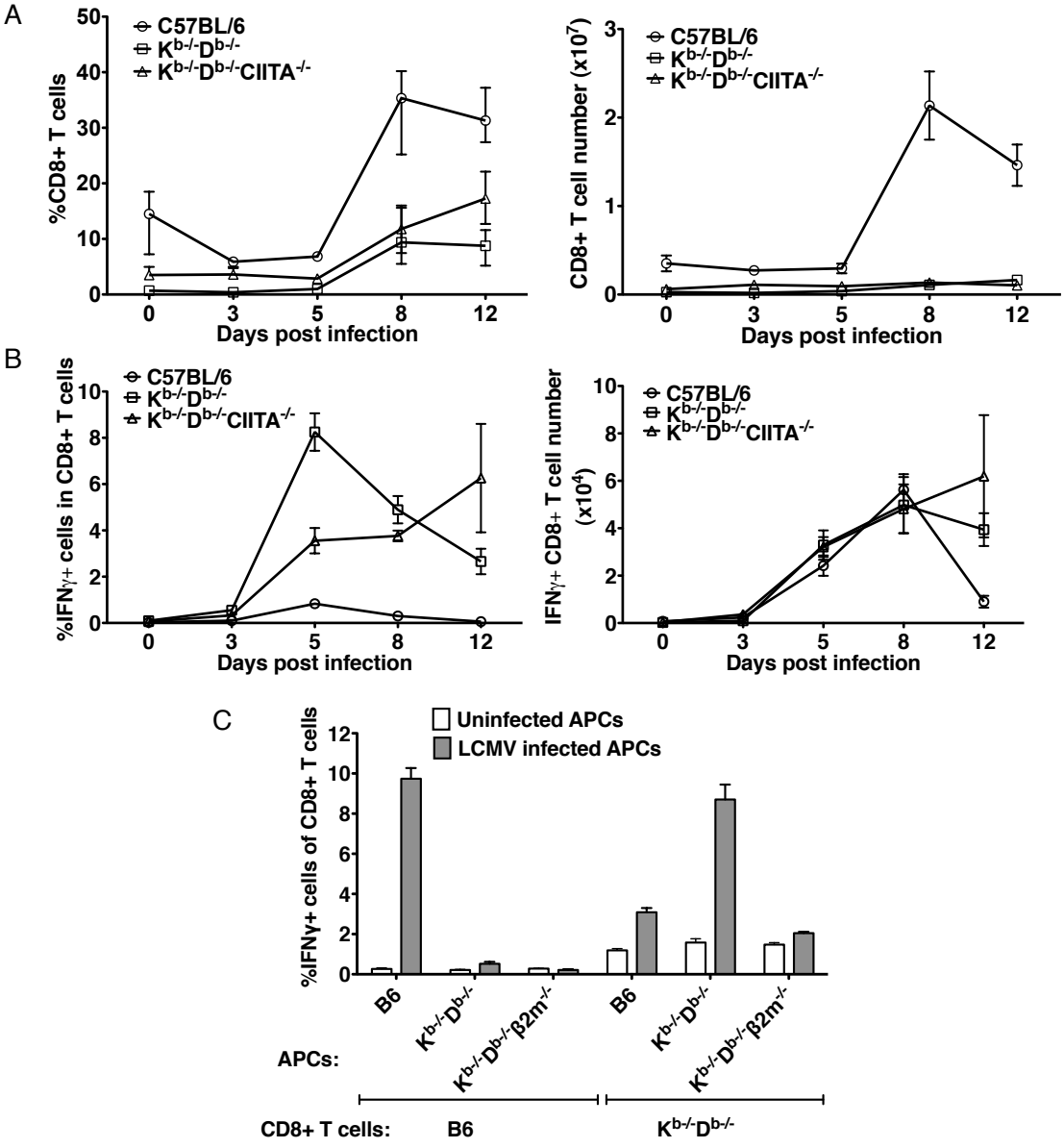

Figure 2.7 Class Ib-restricted T cells are induced in LCMV-Arm infected $K^{b-/-}D^{b-/-}$ mice. (A) B6 and $K^{b-/-}D^{b-/-}$ CD8+ T cells from day 8 infected mice were restimulated with B6, $K^{b-/-}D^{b-/-}$ or $K^{b-/-}D^{b-/-}$ $\beta2m^{-/-}$ bone marrow-derived macrophages which were uninfected or infected with LCMV. (B) The percentage and number of spleen CD8+ T cells in naïve and day 3, 5, 8, 12 LCMV-Arm infected B6, $K^{b-/-}D^{b-/-}$ and $K^{b-/-}D^{b-/-}CIITA^{-/-}$ mice. (C) The IFNγ+ CD8+ T cell percentage and number in the naïve, day 3, 5, 8, 12 LCMV-Arm infected B6, $K^{b-/-}D^{b-/-}$ and $K^{b-/-}D^{b-/-}CIITA^{-/-}$ mice spleen. The data represent one of two independent experiments.

during the observed time frame (Figure 2.8C). These results indicated that the low-numbered CD8+ T cells in the $K^{b-/-}D^{b-/-}CIITA^{-/-}$ were activated to control the infection, but the virus replication may over-counter the CD8+ T cell number, that the CD8+ T cell could not fully clear the virus infection and the infection becomes chronic (36). As the infection went on, large numbers of the $K^{b-/-}D^{b-/-}CIITA^{-/-}$ CD8+ T cells die from activation-induced cell death and even the remaining live CD8+ T cells become exhausted that in the *in vitro* assay, the CD8+ T cells could not respond to LCMV-infected syngeneic macrophages any more (Figure 2.8D).

Discussion

In this project, MHC class Ia deficient mice were studied for their immune responses against viral infections. The $K^{b-/-}D^{b-/-}$ mice on C57BL/6 background do not express MHC class Ia molecules, thus do not have MHC class Ia restricted CD8+ T cells. The MHC class Ib restricted CD8+ T cells represent a small faction of CD8+ T cells in the wild type mice and it is difficult to study their immune functions in the wild type mice. The $K^{b-/-}D^{b-/-}$ mice have much fewer CD8+ T cells compared to the wild type animal, but majority of the CD8+ T cells should be restricted by MHC class Ib, providing a potential good model for studying the MHC class Ib restricted CD8+ T cell responses (6). The $K^{b-/-}D^{b-/-}$ mice were crossed to $CIITA^{-/-}$ mice to generate mice that are deficient in both MHC class Ia and MHC class II. The mice have very few CD4+ T cells and CD8+ T cells in the peripheral, but the CD8+ T cell number was significantly increased compared to $K^{b-/-}D^{b-/-}$ mice, which was caused by the homeostatic expansion (8). The T cells in the $K^{b-/-}D^{b-/-}CIITA^{-/-}$ mice also show activated phenotype. Both $K^{b-/-}D^{b-/-}$ and

Figure 2.8 Long-term infection. Groups of B6 and $K^{b-/-}D^{b-/-}CIITA^{-/-}$ mice were infected with $2x10^5$ PFU LCMV-Arm. At day 3, 8, 13, 37, 82 postinfection, a minimum of three mice of each strain were characterized to determine the virus titer in the spleen tissue, and the CD8+ T cell expansion and INFγ production were determined. (A) Virus in spleen was measured by plaque assay. (B) The kinetics of spleen CD8+ T cell expansion and contraction. (C) The kinetics of *ex vivo* IFNγ production by CD8+ T cells. (D) *In vitro* restimulation of CD8+ T cells from day 49 infected mice. The CD8+ T cells from day 49 infected mice were co-cultured with infected or uninfected B6, $K^{b-/-}D^{b-/-}CIITA^{-/-}$, $K^{b-/-}D^{b-/-}\beta2m^{-/-}$bone marrow-derived macrophages for 1 day, and the IFNγ production was measured by flow cytometry.

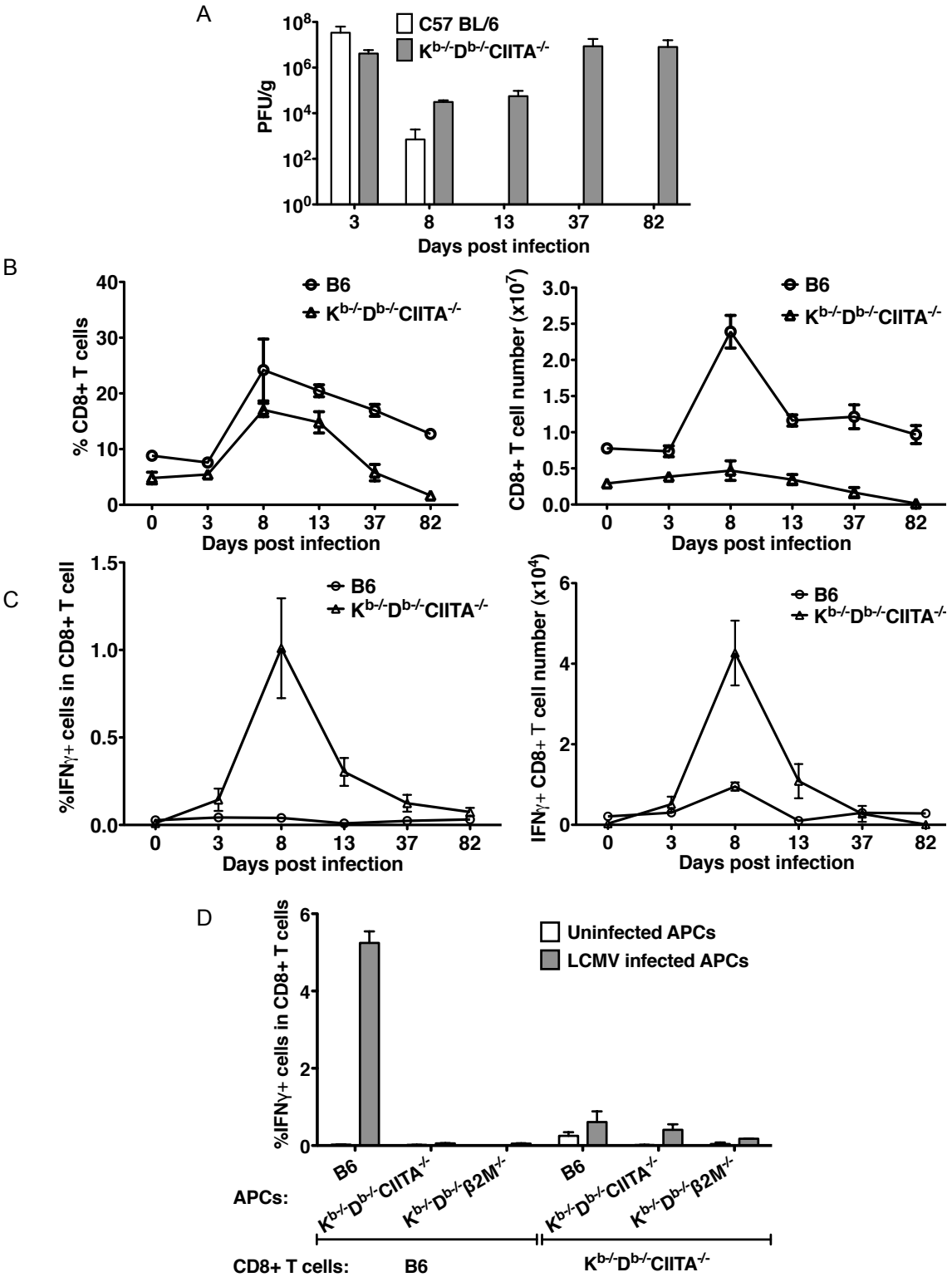
A
C57 BL/6
Kb-/-Db-/-CIITA-/-
PFU/g
Days post infection
B
B6
Kb-/-Db-/-CIITA-/-
% CD8+ T cells
CD8+ T cell number (x10^7)
Days post infection
C
%IFNγ+ cells in CD8+ T cell
IFNγ+ CD8+ T cell number (x10^4)
Days post infection
D
Uninfected APCs
LCMV infected APCs
%IFNγ+ cells in CD8+ T cells
APCs:
B6
Kb-/-Db-/-CIITA-/-
Kb-/-Db-/-β2M-/-
CD8+ T cells:
B6
Kb-/-Db-/-CIITA-/-

$K^{b-/-}D^{b-/-}CIITA^{-/-}$ mice were used in the study. In response to the infection, the CD8+ T cells proliferated, secreted IFNγ and granzyme B *in vivo*. The virus infection was partially but not fully controlled during the first 2 weeks of the infection, and in long-term, the infection became chronic in the MHC class Ia deficient mice. The partial control relied on the CD8+ T cells that in the CD8+ T cell depleted mice, the infection totally lost control. The *in vitro* restimulation assay proved that the $K^{b-/-}D^{b-/-}$ and $K^{b-/-}D^{b-/-}CIITA^{-/-}$ CD8+ T cell anti-LCMV response was dependent on β2m but independent of MHC class Ia molecule K^b or D^b, suggesting the reaction was restricted by β2m-bearing MHC class Ib molecules. The $K^{b-/-}D^{b-/-}CIITA^{-/-}$ mice were not able to fully clear the virus infection. As the infection went on, the CD8+ T cell percentage and number dropped continuously. The CD8+ T cells in the naïve $K^{b-/-}D^{b-/-}CIITA^{-/-}$ mice had proliferated by homeostatic expansion, that they might easily become exhausted upon infection induced activation and proliferation (37, 38); many cells might die as the infection became chronic; the remaining live cells gradually lost their ability to produce IFNγ cytokines as shown by the *in vitro* restimulation assay at later time point postinfection.

MHC class Ib restricted T cell response were found during bacteria infections. The H2-M3 participated in the immune response against *Listeria monocytogenes* and *Mycobacteria tuberculosis* (3, 14, 39-41). $K^{b-/-}D^{b-/-}$ mice could protect the mice from Listeria infection as efficient as the wild type mice, suggesting the MHC class Ib restricted CD8+ T cells were potent to kill the Listeria infected target cells and to restrain the spread of the virus infection (40). Qa-1^b also participated in anti-bacterial response that a group of CTLs specifically react to Salmonella GroEL peptides presented by Qa-1^b (12, 13). There was very few research studying the participation of MHC class Ib

molecules in anti-viral response. $K^{b-/-}D^{b-/-}$ mice control γ-herpes virus 68 infections to the same level as B6 mice, but the restriction element of the CD8+ T cells was not clear (18). The CD8+ T cells expanded and produced cytokines, and the number of unconventional CD8+ T cells in $K^{b-/-}D^{b-/-}$ mice at day 42 postinfection was comparable to the CD8+ T cells number in the B6 mice (18). In our experiment, after the LCMV infection, the unconventional CD8+ T cells expanded and gradually contracted to a level lower than in naïve mice and lost their ability to produce IFNγ cytokine. These suggested that the virus type and infection pattern influenced the unconventional CD8+ T cell response. It could be that unconventional CD8+ T cells were capable to control the herpes virus infection at the acute phase and when the herpes infection became latent, there were very few herpes antigens to stimulate CD8+ T cell response that the CD8+ T cell turnover rate became slow and the cells could survive for long time. While during LCMV-Arm infection, the virus expanded continuously, and in response, the CD8+ T cells in the MHC class Ia deficient mice also expanded cycle after cycle to keep in pace with the virus expansion and tried to clear the virus; eventually, the cells expanded too many cycles that they became exhausted and many of the cells die by apoptosis and even the live cells gradually lost their ability to control virus infection (42). The LCMV virus replication in the MHC class Ia knockout mice might overwhelm the few-numbered CD8+ T cell response that the infection became chronic (36). MHC class Ib restricted anti-viral response was clearly demonstrated in a polyoma virus infection mouse model, in which H2-Q9 was identified as the restriction element for a polyoma virus VP2 peptide (17). Our study on the LCMV virus extended the knowledge on MHC class Ib restricted anti-viral response. Although the MHC class Ia deficient mice were not able to fully clear

the virus, the CD8+ T cells clearly showed MHC class Ib restricted anti-LCMV response. The lack of clearance might be due to the low CD8+ number in the MHC class Ia deficient mice. The CD8+ T cells in these mice had undergone homeostatic expansion, and that might lead to the early exhaustion of the T cells. The well-known individual MHC class Ib molecules, Qa-1, Qa-2, H2-M3, CD1d, MR1, were tested in the *in vitro* restimulation assay. Qa-2 seems to restrict a small part of the CD8+ T cell response, but the response was not fully diminished when the CD8+ T cells were stimulated with Qa-2$^{-/-}$ APCs. The response might be restricted by multiple MHC class Ib elements or restricted by an unknown MHC class Ib.

Acknowledgements

I'd like to thank Jared Fairbanks for his great technical support, Dr. Matthew Williams for critical reagents and helpful discussions, David Cole for maintaining the mice repertoire.

References

1. Harty JT, Tvinnereim AR, White DW. 2000. CD8+ T cell effector mechanisms in resistance to infection. *Annu Rev Immunol* 18: 275-308

2. Williams MA, Bevan MJ. 2007. Effector and memory CTL differentiation. *Annu Rev Immunol* 25: 171-92

3. Seaman MS, Wang CR, Forman J. 2000. MHC class Ib-restricted CTL provide protection against primary and secondary Listeria monocytogenes infection. *J Immunol* 165: 5192-201

4. Shawar SM, Vyas JM, Rodgers JR, Rich RR. 1994. Antigen presentation by major histocompatibility complex class I-B molecules. *Annu Rev Immunol* 12: 839-80

5. Rodgers JR, Cook RG. 2005. MHC class Ib molecules bridge innate and acquired immunity. *Nat Rev Immunol* 5: 459-71

6. Perarnau B, Saron MF, San Martin BR, Bervas N, Ong H, Soloski MJ, Smith AG, Ure JM, Gairin JE, Lemonnier FA. 1999. Single H2Kb, H2Db and double H2KbDb knockout mice: peripheral CD8+ T cell repertoire and anti-lymphocytic choriomeningitis virus cytolytic responses. *Eur J Immunol* 29: 1243-52

7. Das G, Das J, Eynott P, Zhang Y, Bothwell AL, Van Kaer L, Shi Y. 2006. Pivotal roles of CD8+ T cells restricted by MHC class I-like molecules in autoimmune diseases. *J Exp Med* 203: 2603-11

8. Jay DC, Reed-Loisel LM, Jensen PE. 2008. Polyclonal MHC Ib-restricted CD8+ T cells undergo homeostatic expansion in the absence of conventional MHC-restricted T cells. *J Immunol* 180: 2805-14

9. Pamer EG, Wang CR, Flaherty L, Lindahl KF, Bevan MJ. 1992. H-2M3 presents a Listeria monocytogenes peptide to cytotoxic T lymphocytes. *Cell* 70: 215-23

10. Gulden PH, Fischer P, 3rd, Sherman NE, Wang W, Engelhard VH, Shabanowitz J, Hunt DF, Pamer EG. 1996. A Listeria monocytogenes pentapeptide is presented to cytolytic T lymphocytes by the H2-M3 MHC class Ib molecule. *Immunity* 5: 73-9

11. Kerksiek KM, Busch DH, Pilip IM, Allen SE, Pamer EG. 1999. H2-M3-restricted T cells in bacterial infection: rapid primary but diminished memory responses. *J Exp Med* 190: 195-204

12. Lo WF, Ong H, Metcalf ES, Soloski MJ. 1999. T cell responses to Gram-negative intracellular bacterial pathogens: a role for CD8+ T cells in immunity to Salmonella infection and the involvement of MHC class Ib molecules. *J Immunol* 162: 5398-406

13. Lo WF, Woods AS, DeCloux A, Cotter RJ, Metcalf ES, Soloski MJ. 2000. Molecular mimicry mediated by MHC class Ib molecules after infection with gram-negative pathogens. *Nat Med* 6: 215-8

14. Chun T, Serbina NV, Nolt D, Wang B, Chiu NM, Flynn JL, Wang CR. 2001. Induction of M3-restricted cytotoxic T lymphocyte responses by N-formylated peptides derived from Mycobacterium tuberculosis. *J Exp Med* 193: 1213-20

15. Ugrinovic S, Brooks CG, Robson J, Blacklaws BA, Hormaeche CE, Robinson JH. 2005. H2-M3 major histocompatibility complex class Ib-restricted CD8 T cells induced by Salmonella enterica serovar Typhimurium infection recognize proteins released by Salmonella serovar Typhimurium. *Infect Immun* 73: 8002-8

16. Tvinnereim A, Wizel B. 2007. CD8+ T cell protective immunity against Chlamydia pneumoniae includes an H2-M3-restricted response that is largely CD4+ T cell-independent. *J Immunol* 179: 3947-57

17. Swanson PA, 2nd, Pack CD, Hadley A, Wang CR, Stroynowski I, Jensen PE, Lukacher AE. 2008. An MHC class Ib-restricted CD8 T cell response confers antiviral immunity. *J Exp Med* 205: 1647-57

18. Braaten DC, McClellan JS, Messaoudi I, Tibbetts SA, McClellan KB, Nikolich-Zugich J, Virgin HW. 2006. Effective control of chronic gamma-herpesvirus infection by unconventional MHC Class Ia-independent CD8 T cells. *PLoS Pathog* 2: e37

19. Rojek JM, Spiropoulou CF, Campbell KP, Kunz S. 2007. Old World and clade C New World arenaviruses mimic the molecular mechanism of receptor recognition used by alpha-dystroglycan's host-derived ligands. *J Virol* 81: 5685-95

20. Kotturi MF, Peters B, Buendia-Laysa F, Jr., Sidney J, Oseroff C, Botten J, Grey H, Buchmeier MJ, Sette A. 2007. The CD8+ T-cell response to lymphocytic choriomeningitis virus involves the L antigen: uncovering new tricks for an old virus. *J Virol* 81: 4928-40

21. Masopust D, Murali-Krishna K, Ahmed R. 2007. Quantitating the magnitude of the lymphocytic choriomeningitis virus-specific CD8 T-cell response: it is even bigger than we thought. *J Virol* 81: 2002-11

22. Matloubian M, Kolhekar SR, Somasundaram T, Ahmed R. 1993. Molecular determinants of macrophage tropism and viral persistence: importance of single amino acid changes in the polymerase and glycoprotein of lymphocytic choriomeningitis virus. *J Virol* 67: 7340-9

23. Khanolkar A, Fuller MJ, Zajac AJ. 2002. T cell responses to viral infections: lessons from lymphocytic choriomeningitis virus. *Immunol Res* 26: 309-21

24. Sullivan BM, Emonet SF, Welch MJ, Lee AM, Campbell KP, de la Torre JC, Oldstone MB. 2011. Point mutation in the glycoprotein of lymphocytic choriomeningitis virus is necessary for receptor binding, dendritic cell infection, and long-term persistence. *Proc Nat Acad Sci USA* 108: 2969-74

25. Chiu NM, Wang B, Kerksiek KM, Kurlander R, Pamer EG, Wang CR. 1999. The selection of M3-restricted T cells is dependent on M3 expression and presentation of N-formylated peptides in the thymus. *J Exp Med* 190: 1869-78

26. Cho H, Bediako Y, Xu H, Choi HJ, Wang CR. 2011. Positive selecting cell type determines the phenotype of MHC class Ib-restricted CD8+ T cells. *Proc Natl Acad Sci U S A* 108: 13241-6

27. Swanson PA, 2nd, Hofstetter AR, Wilson JJ, Lukacher AE. 2009. Cutting edge: shift in antigen dependence by an antiviral MHC class Ib-restricted CD8 T cell response during persistent viral infection. *J Immunol* 182: 5198-202

28. Ahmed R, Salmi A, Butler LD, Chiller JM, Oldstone MB. 1984. Selection of genetic variants of lymphocytic choriomeningitis virus in spleens of persistently infected mice. Role in suppression of cytotoxic T lymphocyte response and viral persistence. *J Exp Med* 160: 521-40

29. Matloubian M, Concepcion RJ, Ahmed R. 1994. CD4+ T cells are required to sustain CD8+ cytotoxic T-cell responses during chronic viral infection. *J Virol* 68: 8056-63

30. Thomsen AR, Johansen J, Marker O, Christensen JP. 1996. Exhaustion of CTL memory and recrudescence of viremia in lymphocytic choriomeningitis virus-infected MHC class II-deficient mice and B cell-deficient mice. *J Immunol* 157: 3074-80

31. Fung-Leung WP, Kundig TM, Zinkernagel RM, Mak TW. 1991. Immune response against lymphocytic choriomeningitis virus infection in mice without CD8 expression. *J Exp Med* 174: 1425-9

32. Butz EA, Bevan MJ. 1998. Massive expansion of antigen-specific CD8+ T cells during an acute virus infection. *Immunity* 8: 167-75

33. Hobbs JA, Cho S, Roberts TJ, Sriram V, Zhang J, Xu M, Brutkiewicz RR. 2001. Selective loss of natural killer T cells by apoptosis following infection with lymphocytic choriomeningitis virus. *J Virol* 75: 10746-54

34. Lin Y, Roberts TJ, Wang CR, Cho S, Brutkiewicz RR. 2005. Long-term loss of canonical NKT cells following an acute virus infection. *Eur J Immunol* 35: 879-89

35. Liu K, Catalfamo M, Li Y, Henkart PA, Weng NP. 2002. IL-15 mimics T cell receptor crosslinking in the induction of cellular proliferation, gene expression, and cytotoxicity in CD8+ memory T cells. *Proc Nat Acad Sci USA* 99: 6192-7

36. Bergthaler A, Flatz L, Hegazy AN, Johnson S, Horvath E, Lohning M, Pinschewer DD. 2010. Viral replicative capacity is the primary determinant of lymphocytic choriomeningitis virus persistence and immunosuppression. *Proc Nat Acad Sci USA* 107: 21641-6

37. Wherry EJ. 2011. T cell exhaustion. *Nat Immunol* 12: 492-9

38. Wherry EJ, Ha SJ, Kaech SM, Haining WN, Sarkar S, Kalia V, Subramaniam S, Blattman JN, Barber DL, Ahmed R. 2007. Molecular signature of CD8+ T cell exhaustion during chronic viral infection. *Immunity* 27: 670-84

39. Xu H, Chun T, Choi HJ, Wang B, Wang CR. 2006. Impaired response to Listeria in H2-M3-deficient mice reveals a nonredundant role of MHC class Ib-specific T cells in host defense. *J Exp Med* 203: 449-59

40. Lenz LL, Dere B, Bevan MJ. 1996. Identification of an H2-M3-restricted Listeria epitope: implications for antigen presentation by M3. *Immunity* 5: 63-72

41. Doi T, Yamada H, Yajima T, Wajjwalku W, Hara T, Yoshikai Y. 2007. H2-M3-restricted CD8+ T cells induced by peptide-pulsed dendritic cells confer protection against Mycobacterium tuberculosis. *J Immunol* 178: 3806-13

42. Richter K, Brocker T, Oxenius A. 2012. Antigen amount dictates CD8(+) T-cell exhaustion during chronic viral infection irrespective of the type of antigen presenting cell. *European J Immunol* doi: 10.1002/eji.201142275

CHAPTER 3

H2-T11, A FUNCTIONAL PARALOG OF H2-T23

Abstract

H2-T11 is a gene with high similarity to the Qa-1^b encoding gene, H2-T23. Hybrid H2-T11 and H2-T23 expressing H2-D^b α3 domain were used to study the properties of H2-T11. H2-T11 was transcribed in multiple organs in mice and the hybrid molecule could be expressed at comparable level to H2-T23 on Hela and T2 cell surfaces. *In vitro* folding experiments showed that T11 can fold with or without Qdm peptide, and the folded T11 had a typical MHC circular dichroism spectrum. T11 were able to bind Qdm peptides, but the complex was not stable at 37°C. Functional studies showed that T11 does not have the same functions as T23. T11 cannot present an insulin peptide to a T23 (Qa-1b)-restricted T cell hybridoma (6C5) and it does not interact with NK receptors. Peptide elution from molecules isolated from Hela cells expressing hybrid T11 or T23 showed that although Qdm was the dominant peptide bound to T23, there were still many other peptides eluted from T23. Multiple peptides were also eluted from T11, including Qdm, but Qdm was not abundant in the T11 peptide pool.

Introduction

MHC class Ib molecules are nonclassical MHC molecules that share similar structure to the classical MHC class I, but have more restricted tissue distribution and lower expression levels. The majority of MHC class Ib molecules are encoded at the

telomeric end of MHC region. In the mouse, that region is divided into three parts, H2-Q, T, and M (1, 2). There are about 40 MHC class Ib genes encoded in the mouse, and about 20 of them were transcribed (3). Only a few of the MHC class Ib molecules have been studied, and many of them remain to be characterized. The well-studied MHC class Ib molecules have special functions that are distinct from classical MHC. $CD1^d$ molecules present lipid antigens to the TCRs of natural killer cells bearing invariant Vβ chains (4-7). H2-M3 has selective preference for N-formylated peptides that are encoded in the prokaryotic organisms and in mitochondria of eukaryotic cells (8-12). $Qa\text{-}1^b$ predominantly binds Qdm peptides generated from the leader sequence of other MHC class I molecules, and presents them to the CD94/NKG2 receptors of NK cells and NKT cells; the signal initiated by the $Qa\text{-}1^b$/Qdm/NKG2A interaction inhibits the activation of the NK cells and NKT cells; the decoding of $Qa\text{-}1^b$/Qdm/NKG2A interaction provides one of the molecular mechanisms for the NK cell "missing-self" theory (13-18).

$Qa\text{-}1^b$ is encoded by H2-T23 gene in the mouse MHC T region. The gene is ubiquitously transcribed, but the $Qa\text{-}1^b$ protein surface expression level is lower compared to the classical MHC class I molecules, which are also expressed on almost all the nucleated cells (3). In the mouse T region, there are several other genes encoded, which may have derived from gene duplication and mutation. The phylogenetic tree analysis showed that H2-T11 is very close to H2-T23 evolutionarily (19). These genes may have duplicated recently. By alignment of the potential cDNA, the nucleotides are over 95% identical between T11 and T23 in B6 mice; the amino acids of the putative proteins were 91% identical. We hypothesized that H2-T11 might encode proteins with functions similar to $Qa\text{-}1^b$. Because there is no antibody available to recognize H2-T11,

the H2-T11 α3 domain was replaced with an antibody-recognizable H2-D^b α3 domain, and the peptide binding α1 and α2 domain were retained (20). As a control, an H2-T23 hybrid molecule was generated in the same way. The expression, biochemical properties, and peptide binding functions of H2-T11 were studied in this project.

Materials and methods

Mice

C57BL/6 mice were purchased from Jackson Laboratories. Qa-$1^{b-/-}$ mice were gift from Dr. Harvey Cantor (Harvard Medical School) (21). All the mice were maintained in the University of Utah specific pathogen-free animal facility and used according to the Institutional Animal Care and Use Committee policies.

Gene expression analysis

H2-T11 cDNA sequence was provided by Dr. Attila Kumanovics (University of Utah). H2-T23 cDNA sequence was from NCBI database (GI: 111074554). The H2-T11 cDNA sequence was aligned to H2-T23/Qa-1^b by BLAST. The putative T11 protein sequence was translated by ApE application and aligned to Qa-1^b.

The primers used for amplifying H2-T11 and H2-T23 from mouse genome and total RNA were as follows: T11 forward, CGGTATTTCCACACCGTCGTA; T11 reverse, TAGAGATATGCGAGGCTAAGTTG; T23 forward, AGTATTGGGAGCGGGAGACTT; T23 reverse: AGCACCTCAGGGTGACTTCAT (19). The polymerase was Taq (Invitrogen). PCR reaction was done as regular on a TC-4000 machine (Techne).

Murine RNA polymerase 2A (POLR2A) was used as the reference gene for T11 during quantitative-PCR (Q-PCR). The primers for Q-PCR were: T11 forward, TAAACCTGAGGACCCTGCTC; T11 reverse, TAGGCCTCCTGACAATACCC; POLR2A forward, GACAAAACTGGCTCCTCTGC; POLR2A reverse, GCTTGCCCTCTACATTCTGC. The mouse tissues were stored in RNAlater solution (Ambion) for less than a week at 4°C before RNA was extracted. The total RNA was extracted by RNeasy mini kit (Qiagen). The cDNA was synthesized by QuantiTect Reverse Transcription kit (Qiagen). The quantitative-PCR kit was Absolute QPCR SYBR Green Mix (Thermal Scientific) and the Q-PCR was done on Lightcycler 480 system (Roche).

Molecular cloning

The α3 domain of H2-T11 and H2-T23 was replaced with the α3 domain of H2-D^b cDNA, and the hybrid molecules were named as H2-T11D3 and H2-T23D3, respectively. The H2-T11D3 and H2-T23D3 cDNA were synthesized (Biomatik). The synthesized cDNA were sequenced to verify the sequences before being cloned to expression vectors. The cDNAs were cloned into mammalian expression retroviral vector MigR1 (22) and bacteria expression vector pTCF (NIH tetramer core facility), and the cloning products were verified by restriction enzyme digestion and sequencing. All the restriction enzymes were from NEB laboratories. GoTaq (Promega) was used for PCR. The plasmids were purified by Plasmid Mini kit (Qiagen) for general testing and cloning, and by EndoFree Plasmid Maxi kit (Qiagen) for transfection experiments.

Cell culture

Phoenix, Hela and T2 cells were cultured in DMEM complete media supplemented with 10% FBS, 100 U/ml penicillin, 100 mg/ml streptomycin, 292 mg/ml L-glutamine, 100 mM nonessential amino acids, 1 mM sodium pyruvate, and 55 mM 2-mercaptoethanol (Invitrogen). The primary mouse cells were cultured in RPMI-1640 complete media supplemented the same way as DMEM media. All the cells were maintained at 37°C humidified cell culture incubator containing 5% CO_2.

Retroviral transduction

Phoenix-GP cells were added at $4x10^6$ cells/dish to a 6 cm collagen I coated cell culture dish (BD). Eighteen hours later, 10 μg MigR1 vector containing the H2-T11D3 cDNA or H2-T23D3 cDNA was co-transfected with 5 μg Env plasmid to the phoenix cells by calcium-phosphate precipitation. Two days later, the supernatant containing the packaged retrovirus was harvested and passed through 0.45 μl sterile filter for transduction. Half ml of $1x10^6$/ml Hela or T2 cells were mixed with 0.5 ml of the retroviral supernatant in the presence of 5 μg/ml polybrene (sigma), and the cells were distributed evenly on collagen-I coated 6 cm plates (BD). Four hours later, 4 ml fresh media were added. After at least 3 days, the cells were harvested and the target gene expression was examined by flow cytometry. The cells were sorted at least twice by EGFP expression level to get cells stably expressing high levels of target genes.

Expression of recombinant protein

The pTCF vector containing the T11D3 or T23D3 genes were transduced to BL21(DE3) *E.coli* (Invitrogen). Target gene positive clones were tested for producing

recombinant proteins before they were expanded in 2L Luria Broth media. 1mM IPTG was added to the culture when the OD600 reached ~0.6. The bacteria were harvested 4 hours later. The bacteria was pelleted by centrifugation, resuspended in resuspension buffer (50 mM pH 8.0 Tris-HCl, 25% (W/V) sucrose, 1 mM EDTA, 0.1% (w/v) NaAzide, 10 mM DTT) and stored in -80°C. The frozen bacteria were thawed and 1mg/ml lysozyme, 5mM $MgCl_2$, 33 μg/ml DNaseI, 3.3% (V/V) Triton-X, and 10mM DTT were added to the bacteria. The bacteria were stirred and lysed at room temperature for 1 hour before being sonicated. The inclusion body was washed multiple times with wash buffer (50 mM pH8.0 Tris-HCl, 0.5% Triton-X100, 100 mM NaCl, 1 mM EDTA, 0.1% NaAzide, 1mM DTT) until the protein pellet was white and the supernatant was clear. The pellet was washed one more time with the wash buffer without DTT. The recombinant inclusion body was solubilized in 6M guanidine chloride and was aliquoted and stored at -80°C until use.

In vitro MHC class I folding

Soluble T11D3 and T23D3 recombinant proteins were folded *in vitro* as before (23). Briefly, T11D3 or T23D3 heavy chain inclusion body together with 6 mg human β2-microglobulin (β2m) light chain was diluted in 100 mM Tris folding buffer (pH 8.0) containing 400 mM L-arginine, 2 mM EDTA, 0.5 mM oxidized glutathione, 5 mM reduced glutathione, 0.2 mM PMSF in the absence or presence of Qdm peptides. The gram ratio of heavy chain : light chain : peptide was 3 : 1 : 1. The folding reaction was kept in 10°C for 2 days before it was harvested and concentrated by the Amicon ultrafiltration cell (Millipore). The concentrated sample was filtered through 0.45 μm

filter and purified by S300 gel filtration column. The purified folding product was concentrated by Amicon Ultra centrifugal filters (Millipore), buffer exchanged to PBS and stored at -80°C.

Gel electrophoresis

All the DNA products were examined using 1% or 2% agarose gel. The recombinant inclusion body was examined using 12% SDS-polyacrylamide gel. The MHC folding products were examined using 4%-20% gradient Tris–HCl gel (Bio-rad).

Antigen presentation assay

Hela transfectant cells ($5x10^4$) or B6 splenocytes ($1x10^6$) were used as antigen presenting cells, and co-cultured with $1x10^5$ 6C5 T cell hybridoma responding cells (24) overnight in the presence of different doses of bovine insulin (Sigma) in 96-well plates. The supernatant was harvested, and the production of IL-2 was measured by Europium-based immunoassay (25).

Eu-based peptide binding assay

The peptide binding was examined by Europium-based immune assay (25). Briefly, 96-well ELISA plate (greiner Microlon) was coated with 50µl 5µg/ml anti human β2m antibody (clone BB7.7) at 37°C for 2 hours; the plate was blocked by 200µl MTB (5% powdered skim milk, 1% BSA, 0.01% NaAzide in TTBS) for 30 minutes at room temperature; 1µg folded MHC monomers were diluted in 100 µl MTBN and incubated in the antibody coated plate for >2 hours at 4°C; the biotin-labeled peptides were diluted in 0.01% NP-40 substitute (Fluka) in PBS and incubated in the plate overnight at room

temperature; the plate was developed by the Europium reagent and the fluorescence signal was recorded by Victor3V plate reader (Perkin Elmer); the plate was washed extensively by the TTBS buffer (50 mM Tris, 150 mM NaCl, 0.1% Tween-20, pH7.5) before the addition of a new reagent.

Fluorescence polarization assay

Folded MHC monomers were incubated with Alexa Fluro488-labeled Qdm4C peptides in Citrate/PO_4 buffer (200 mM citric acid, 200 mM Na_2HPO_4, pH7). The parallel and perpendicular fluorescence signals (I_{II} and $I_{\perp}$) were recorded at 60 seconds intervals for total 60000 seconds by Infinite F200 microplate reader (Tecan) at 37°C or 25°C. Pure MHC monomer, AF488-labeled peptide, or buffer were also detected independently to record the background signal. After the background signals were subtracted, the anisotropy was calculated according to following formula: $A = \frac{I_{II} - I_{\perp}}{I_{II} + 2I_{\perp}}$ (26).

Circular Dichroism assay

The CD spectrum was measured by AVIV 410 CD instrument (AVIV Biomedical Inc.). The folded MHC monomer concentration was determined by OD280 and was diluted to 250 μg/ml in PBS. The far-UV CD spectrum was recorded in a cuvette with 1mm path-length at 25°C. The sample was scanned from 200 nm to 260 nm with a step of 1nm. The averaging time was 3 seconds and every step was scanned three times. The PBS background data were recorded in the same cuvette and was subtracted from all the sample data.

The thermal stability of the folded MHC was studied by detecting the CD signal at 222 nm. The temperature was increased by a step of 2°C from 25°C to 79°C. At each temperature point, the sample was equilibrated for 30 seconds before collecting the data. The averaging time was 30 seconds.

MHC class I tetramer

MHC tetramer was prepared as described before (27). S300 purified MHC monomer was buffer exchanged to 10 mM Tris buffer (pH8.0) and concentrated to 2 mg/ml. 1 mg of the MHC monomer (8/10 volumes) was mixed with 1/10 volume 10xBiomixA, 1/10 volume of 10xBiomixB and 5 μg BirA enzyme (GeneCopoeia). The reaction was kept at room temperature overnight. The product was further purified by MonoQ anion exchange column. The biotinylated MHC monomer was tetramerized by gradually adding 1/10 of the total required APC-labeled streptavidin to the sample and incubating at room temperature for 10 minutes after each addition, so that each streptavidin was saturated and the final ratio of biontinylated MHC to streptavidin was 4:1. The biotinylated MHC was snap-frozen and stored at -80°C. The tetramer was stored at 4°C and used within 6 months.

Abs and flow cytometry

FITC labeled anti-mouse CD3ε, PerCP-Cy5.5 labeled anti-mouse B220, PE labeled anti-mouse NKp46, PE-Cy7 labeled anti-mouse NK1.1 antibodies were purchased from eBioscience and Biolegend. The staining was done in a buffer composed of PBS, 0.5% BSA, and 2 mM EDTA. The suspended cells were incubated with the antibodies and the tetramer for 20 minutes at 4°C. The stained cells were washed twice

with the buffer and fixed with 1% paraformaldehyde. The fluorescence was detected on a FACS Canto II machine (BD Biosciences). The data was analyzed by Flowjo application (Tree Star).

Peptide elution and identification

The T11D3 and T23D3 bound peptides were eluted as described before (28). Hela-MigR1, Hela-T11D3 and Hela-T23D3 cells were cultured in T150 cell culture flasks. Each cell type was cultured in 20~25 flasks and harvested when they were 80% to 90% confluent so that the total cell collected for each cell type was more than $1x10^9$. The cells were spin down, washed twice with cold DPBS, and the pellet was stored in -80°C for less than 2 months until the next step. The cells were lysed by NP-40 buffer (0.5% nonidet P-40, 500 mM pH8.0 Tris-HCl, 150 mM NaCl and protease inhibitors). The lysate was centrifuged several times, and the supernatant was passed through a Tris-blocked Sepharose column to pre-clear the lysate. The hybrid MHC was immunoprecipitated by protein A beads cross-linked with 28-14-8s antibody. The beads then were washed with four different buffers in sequence: (1) 0.005% Nonidet P-40, 50 mM Tris-HCl (pH 8.0), 150 mM NaCl, 5 mM EDTA; (2) 50 mM Tris-HCl (pH 8.0), 150 mM NaCl; (3) 50 mM Tris-HCl (pH 8.0), 450 mM NaCl; (4) 50 mM Tris-HCl (pH 8.0). The MHC-peptide complexes were eluted from the beads by 10% acetic acid, lyophilized, resuspended in 100 μl DMSO, loaded to HPLC and fractionated by HPLC (Beckman Coulter) to 27 fractions. Each fraction was concentrated to ~10 μl before mass spectrometry. The sequences of the eluted peptides were gained by LC-tandem mass spectrometry.

Results

Transcription of T11 gene in B6 and Qa-$1^{b-/-}$ mice

H2-T11 and H2-T23 sequences are highly homologous to each other and they might be recently duplicated genes (19). Over 95% of the cDNA nucleotides of H2-T11 match the ones of H2-T23, and 91% amino acids of the putative proteins are identical to each other (Figure 3.1A and B). Despite their high similarity, primers were designed to distinguish them. The sequence of the T11 primers were: CGGTATTTCCACACCGTCGTA and TAGAGATATGCGAGGCTAAGTTG; T23 primers were: AGTATTGGGAGCGGGAGACTT and AGCACCTCAGGGTGACTTCAT (19). Genomic DNA analysis showed both T11 and T23 gene were detected in wild type mice, while only T11 was detected in T23 knockout mice (Qa-$1^{b-/-}$) (Figure 3.2A). Reverse-transcriptional PCR showed that T11 is transcribed in the two major lympohoid organs, spleen and thymus. The T23 transcript was also detected in spleen and thymus as expected (Figure 3.2B). The amplified cDNA sequences were 415 bp for T11 and 438 bp for T23, and were sequenced to confirm that they were truly T11 and T23 transcripts.

Quantitative-PCR was performed to study the tissue-specific expression of T11. Because of the high similarity of T23 and T11, it was hard to design short quantitative-PCR primers specifically recognizing T11. The three pairs of Q-PCR primers designed to distinguish T11 and T23 failed to amplify any DNA in the preliminary tests (data not shown). To circumvent this problem, T11 expression level was studied using Qa-$1^{b-/-}$ mouse tissue RNA instead of wild type mouse RNA. The T23 exon 1, 2 and 3 are deleted in Qa-$1^{b-/-}$ mice (21). Primers targeting T11 exon 1, 2 and 3 were designed; after

A

```
H2-T23   1   MLLFAHLLQLLVSATVPTQSSPHSLRYFTTAVSRPGLGEPRFIIVGYVDDTQFVRFDSDA 60
             MLLFAHLLQLLVSATVPTQSS HSLRYF T VSRPGLGEPRFIIVGYVDDTQFVRFDSD+
H2-T11   1   MLLFAHLLQLLVSATVPTQSSSHSLRYFHTVVSRPGLGEPRFIIVGYVDDTQFVRFDSDS 60

H2-T23   61  ENPRMEPRARWIEQEGPEYWERETWKARDMGRNFRVNLRTLLGYYNQSNDESHTLQWMYG 120
             ENPRMEPRARWIEQEGPEYWERET KARDMGRNFRVNLRTLLGYYNQS DESHTLQWMYG
H2-T11   61  ENPRMEPRARWIEQEGPEYWERETRKARDMGRNFRVNLRTLLGYYNQSKDESHTLQWMYG 120

H2-T23   121 CDVGPDGRLLRGYCQEAYDGQDYISLNEDLRSWTANDIASQISKHKSEAVDEAHQQRAYL 180
             CDVGPDGRLLRGYCQEAYDGQDYISLNEDLRSWTA ++AS ISK KSEAVDEAHQQRAYL
H2-T11   121 CDVGPDGRLLRGYCQEAYDGQDYISLNEDLRSWTATNLASHISKCKSEAVDEAHQQRAYL 180

H2-T23   181 QGPCVEWLHRYLRLGNETLQRSDPPKAHVTHHPRSEDEVTLRCWALGFYPADITLTWQLN 240
             QGPCVEWLH YL+LG+ETL RSDPPKAHVT HPR E +VTLRCWALGFYPADITLTWQLN
H2-T11   181 QGPCVEWLHTYLQLGSETLLRSDPPKAHVTRHPRPEGDVTLRCWALGFYPADITLTWQLN 240

H2-T23   241 GEELTQDMELVETRPAGDGTFQKWAAVVVPLGKEQYYTCHVYHEGLPEPLTLRWEPPPST 300
             GEELTQDME VETRPAGDGTFQKWA+VVVPLGKEQ YTCHVYHEGLPEPLTLRWEPPPST
H2-T11   241 GEELTQDMEFVETRPAGDGTFQKWASVVVPLGKEQNYTCHVYHEGLPEPLTLRWEPPPST 300

H2-T23   301 VSNMVIIAVLVVLGAVIILGAVVAFVMKRRR-HIGVKGCYAHVLGSKSFQTSDWPQKA 357
             VSNMVIIAVLVVLGAVI++ AVVAFVMKRR+  +GVKGCYAHVLGSKSFQTSDWPQKA
H2-T11   301 VSNMVIIAVLVVLGAVIVIVAVVAFVMKRRKTQVGVKGCYAHVLGSKSFQTSDWPQKA 358
```

B

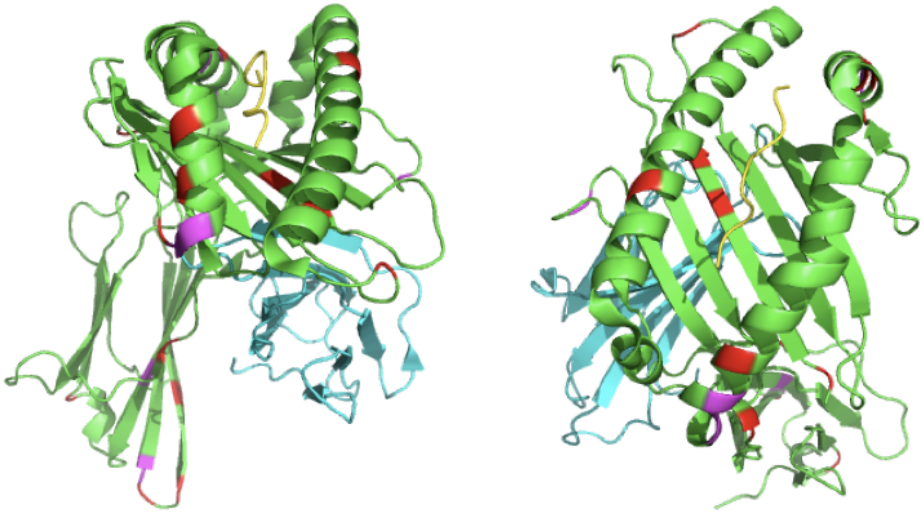

Figure 3.1 Alignment of H2-T11 putative protein sequence to H2-T23/Qa-1^{b} sequence. (A) Blast of H2-T11 sequence to H2-T23 sequence. "+" indicates conserved substitutions. (B) Alignment of H2-T11 to the structure of Qa-1^{b}/Qdm. Green color is MHC heavy chain; cyan colar is β2m; yellow color is the peptide. Megenta color indicates conserved substitutions; red color indicates nonconserved substituions.

preliminary testing, a pair of primers flanking T11 exon 2 and 3 was used in the quantitative-PCR assay. The T11 amplicon size was 127 bp. Murine RNA polymerase 2A (POLR2A) was used as the reference gene (29). The Q-PCR result showed that T11 was expressed at relatively high level in spleen, thymus and intestine, but at low level at kidney, heart and pancreas. The highest T11 expression level was detected in the thymus (Figure 3.2C).

Expression of H2-T11 protein on surface of $TAP^{+/+}$ and $TAP^{-/-}$ cells

Hybrid T11D3 and T23D3 were transduced into Hela and T2 cells using the MigR1 retroviral system, which has a EGFP gene connected by IRES to the target gene (22). The cells express intrinsic human β2m to form MHC structure with the transduced heavy chain. Clone 6A8 (mouse IgG1, κ) and 28-14-8s (mouse IgG2a, κ) were used to detect the surface expression of the transduced genes. 6A8 recognizes the α2 domain of Qa-1^b, and 28-14-8s targets the hybrid H2-D^b α3 domain (Figure 3.3A). The T23D3 was recognized by both 6A8 and 28-14-8s antibodies, proving their surface-localized expression (Figure 3.3B). Although 6A8 was generated against Qa-1^b, it might also recognize T11D3, suggesting a 6A8 epitope shared by T11 and T23. The recognition of T11 by 6A8 antibody was much weaker than T23. Qa-1^b has a wide tissue distribution that it is expressed in most nucleated cells similar to MHC class Ia molecules, but unlike Ia molecules which requires the TAP complex for the cell surface expression, Qa-1^b cell surface expression occurs in the absence of TAP (17). The T23D3 hybrid molecule was detected on the surface of T2 cells, which are TAP deficient. T11D3 was also expressed on the T2 cell surface at levels similar to T23D3, as shown by 28-14-8s staining,

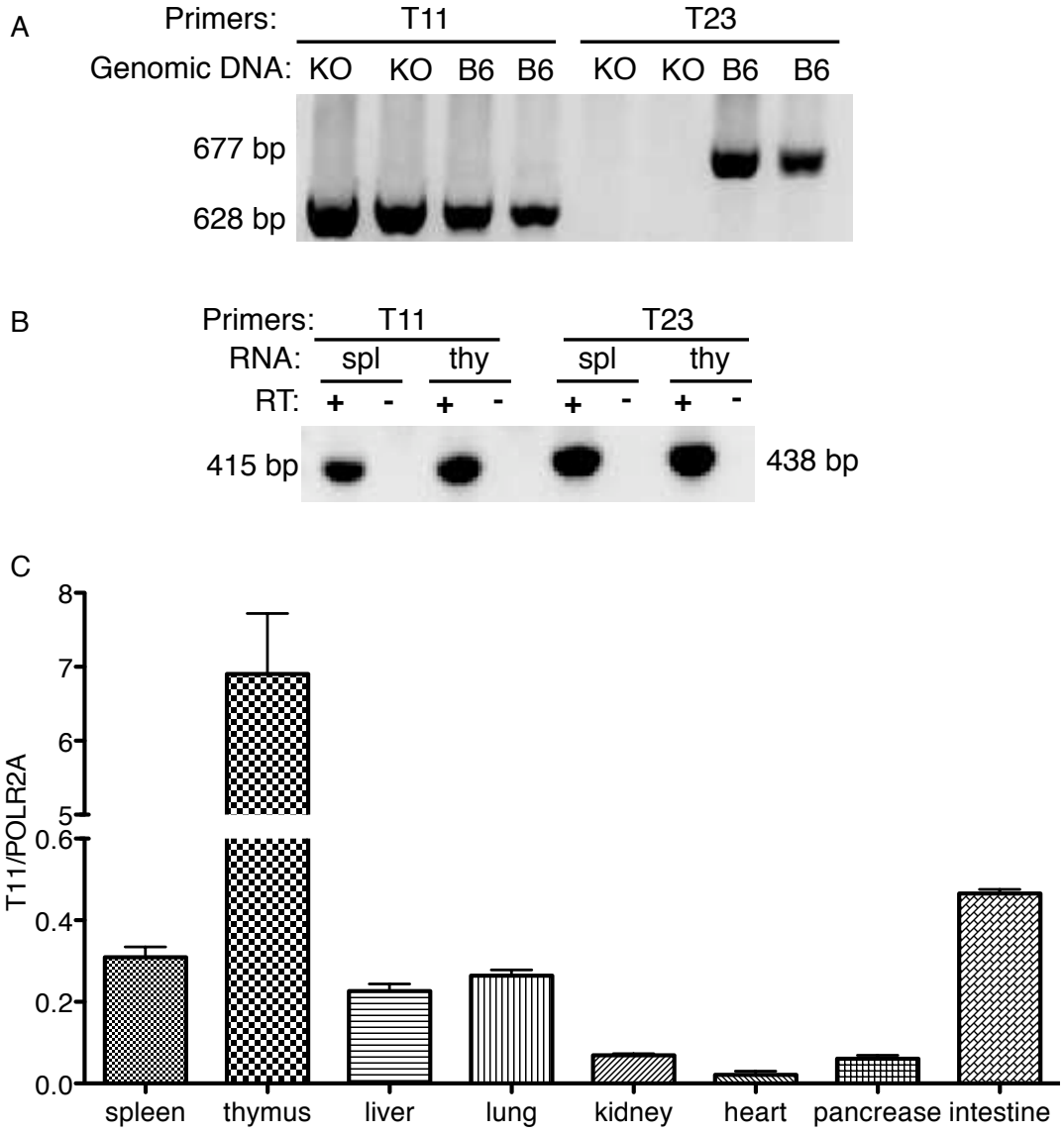

Figure 3.2 Transcription of T11 genes. (A) PCR amplification of T11 and T23 genes from the wild type C57BL/6 (B6) mouse and Qa-1$^{b-/-}$ (KO) genomic DNA. The T11 amplicon size was 628bp and the T23 amplicon size was 677bp. (B) Reverse-transcriptional PCR amplification of T11 and T23 transcripts from the B6 mouse spleen (spl) and thymus (thy). The amplicon sizes are 415 bp and 438 bp for T11 and T23 respectively. RT: reverse transcriptase. (C) Quantitative-PCR to determine the T11 transcription level in different tissues. The total RNA was extracted from Qa-1$^{b-/-}$ mice. The reference gene was RNA polymerase 2A (POLR2A). The ratio of T11 to POLR2A was calculated according to the Pfaffl method.

suggesting that TAP was also dispensable for T11 surface expression (Figure 3.3B).

Antigen presentation function

Our lab found that a small subset of CD8+ T cells responding to insulin was selected by Qa-1^b in the mouse (24, 30). The CD8+ T cell hybridoma, 6C5, can respond to Qa-1^b presented bovine insulin by producing IL-2 in a dose-dependent way. T11D3, T23D3 transduced Hela cells were examined for their ability to present insulin to 6C5 cells. Empty vector transduced Hela-MigR1 cells were used as a negative control, and B6 splenocytes, which containing Qa-1^b expressing antigen presenting cells, were used as positive control (Figure 3.3C). The antigen presenting cells were co-cultured with the 6C5 hybridoma in the presence of different doses of bovine insulin. The Eu-based assay showed that Hela-T23D3 cells had the best capacity to present insulin to 6C5. Much higher IL-2 levels were detected in the supernatant of Hela-T23D3/6C5 cultures than in splenocytes/6C5 cultures. By contrast, there was no IL-2 detected in the Hela-T11D3/6C5 cultures, suggesting that either T11 could not present insulin or insulin presented by T11 could not be recognized by the Vα3.2-Vβ5.1/5.2 TCR on 6C5 T cells.

Folding of T11 with or without Qdm peptide *in vitro*

Qdm has the ideal sequence for binding to Qa-1^b, and it can form a stable complex with Qa-1^b at 4°C (23). To test whether Qdm can bind to T11, recombinant T11D3 and T23D3 were folded with human β2m at 10°C in the presence or absence of Qdm peptide, and the folding products were passed through S300 size-exclusion column to purify the folded MHC monomer. The elution profile showed that T23D3 requires

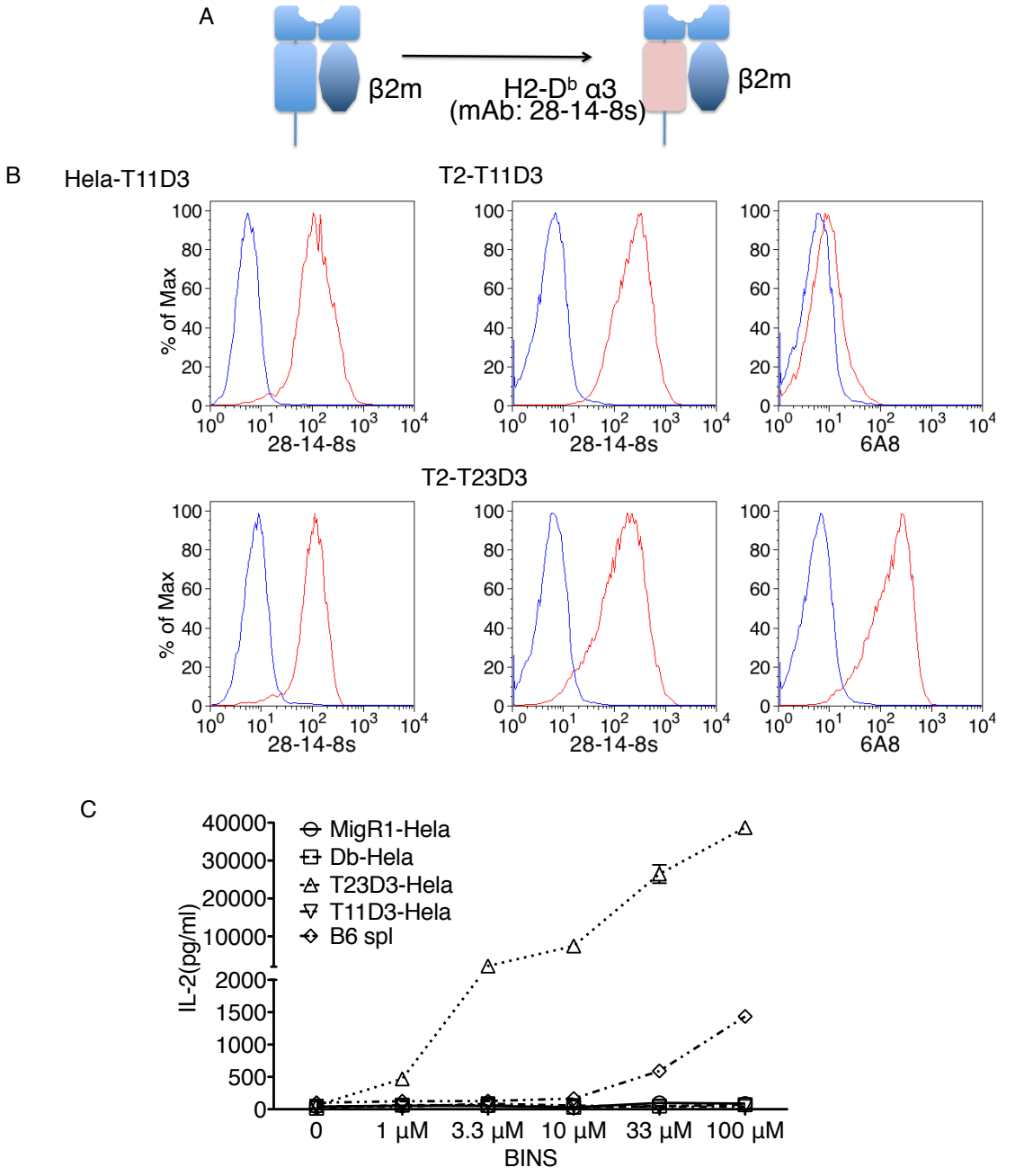

Figure 3.3 Expression of hybrid T11 and T23 molecules and the functional test of hybrid molecule expressing cells. (A) Strategy for making the hybrid MHC molecule. The T11 and T23 α3 domain was replaced with the H2-D^b α3 domain, which could be recognized by the 28-14-8s antibody. (B) Expression of hybrid T11 and T23 on the surface of Hela and T2 cells. Hela cells were stained with 28-14-8s antibody and T2 cells were stained with 28-14-8s antibody and 6A8.6F10.1A6 antibody. (C) Antigen presentation assay to test the hybrid molecule-expressing cells' capability to present insulin to 6C5 hybridoma. (BINS: bovine insulin)

Qdm peptides for folding. In the absence of Qdm, no folding peak was detected (Figure 3.4A). In contrast, an apparent folding peak was detected when T11D3 folded with β2m in the absence of exogenous peptide ligand, but the peak was consistently higher when Qdm was included in the folding reaction (Figure 3.4A). The peaks representing the correct folding products were concentrated and examined by SDS-PAGE. Both heavy chain and light chain were detected, indicating correct folding (Figure 3.4B). The product was also examined by Europium-based fluorescence immunoassay where the folding product was captured by anti-β2m antibody (BB7.7) and detected by the 28-14-8s or 6A8 antibody. The result showed that folded T11 and T23 products could be recognized by both 28-14-8s and 6A8 antibodies, but 6A8 recognized T23 better than T11 (Figure 3.4C). The signal for T11D3-β2m was lower than T11D3-β2m-Qdm even though the same amount of folding products were added, suggesting that there might be a structure change that influenced antibody recognition, or T11D3-β2m was less stable than T11D3-β2m-Qdm.

To confirm that T11D3 and T23D3 did form MHC structures with β2m, circular dichroism was used to study secondary structure. The results showed that T11D3-β2m, T11D3-β2m-Qdm, T23D3-β2m-Qdm all had typical MHC wavelength spectrums as reported in previous studies (Figure 3.5A) (31-34). This included a single peak signal at ~220nm, which was in conformity with MHC β-sheet dominated structure. Thermal stability experiments showed that the folded T11 product had reduced stability compared to T23. MHC proteins lose their regular secondary structure and form random coils at increasing temperature, such that molar elipticity gradually approaches zero (31, 32, 35). When the temperature was increased, T11 denatured as shown by the increased molar

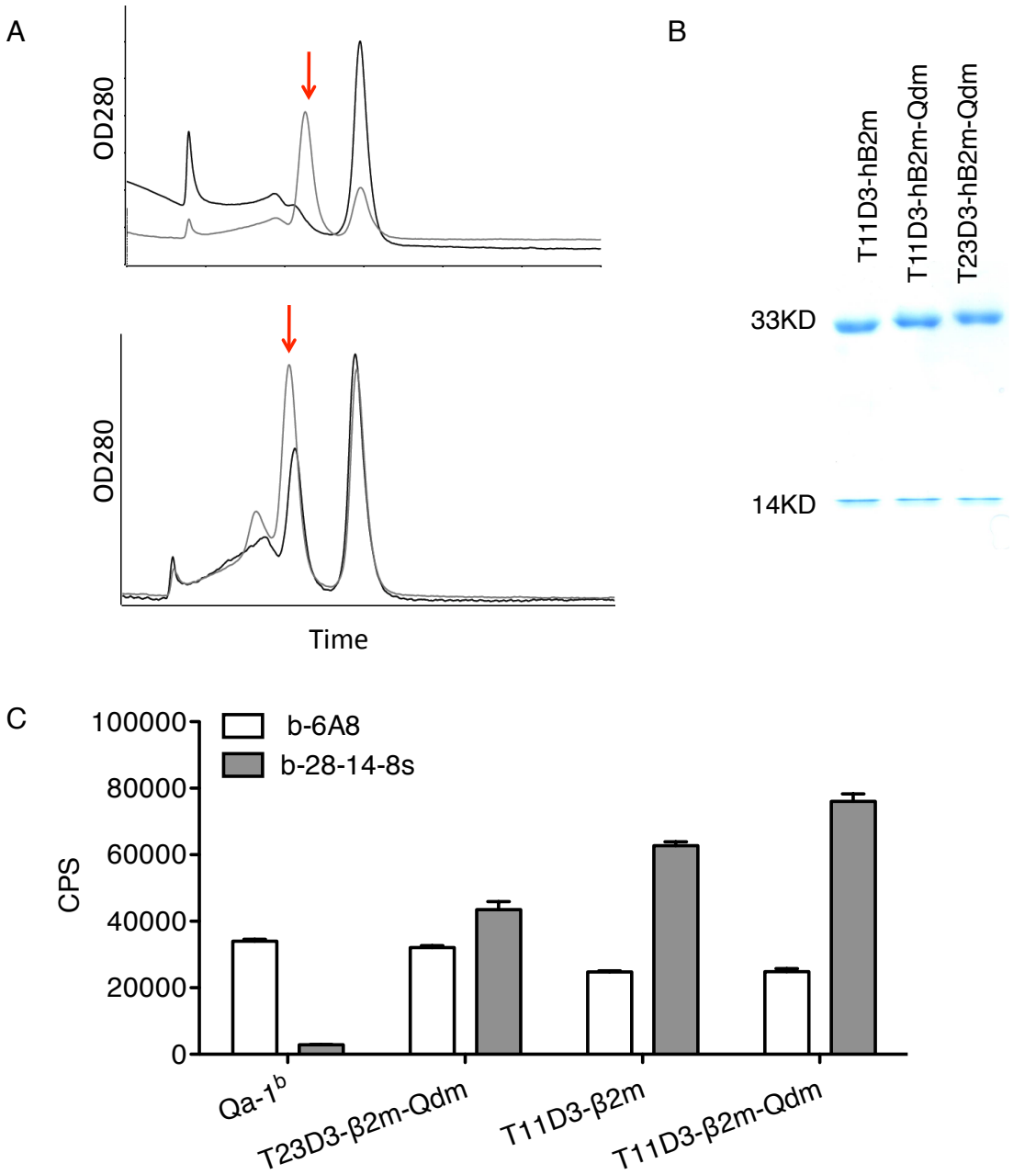

Figure 3.4 *In vitro* folding of the hybrid T11 and T23 molecules. (A) S300 spectrum of the folding products. Arrows indicate the correct folding product peak. Top panel: black line, T23D3-β2m folding, gray line, T23D3-β2m-Qdm folding; bottom panel: T11D3-β2m folding, gray line, T11D3-β2m-Qdm folding. (B) SDS-PAGE of the purified folding products. The MHC heavy chain is ~33kD and the light chain is ~14kD. (C) Eu-based immunoassay to examine the folding products. Folding MHC monomer was captured by the anti-β2m antibody and detected by the 28-14-8s and 6A8 antibody.

elipticity, but the denaturation was not complete. It looked like T11 had a transient stable structure such that the molar elipticity remained at a level between zero and the value characteristic of folded MHC (Figure 3.5B).

The capacity of T11 to bind Qdm peptide

The peptide binding capability of the folded MHC proteins were tested by using Eu-based immunoassay. The folded hybrid T23 monomer was observed to bind labeled Qdm peptide, as expected, but it did not bind the K^b-specific SIINFEKL peptide. Folded T11 monomer can also bind Qdm peptide, but only if when Qdm was present in the folding reaction; the "empty" T11 monomer was not able to bind Qdm (Figure 3.6A). Direct peptide elution from the T11D3-β2m-Qdm folding monomers showed that about half of the monomers were folded with the Qdm peptides (data not shown). Exogenous addition of Qdm peptide to the folding reaction might help the T11 monomer to form a Qdm adaptable structure. The peptide binding was also examined using a fluorescence polarization assay. Alexfluor488 labeled Qdm peptide was incubated with the folded MHC monomer and the binding signal was detected in real-time. The result showed that Qdm binds to T23D3 and Qa-1^b monomers with similar association kinetics. However, T11 monomer appears to be unstable at 37°C (Figure 3.6B). It had a very fast initial Qdm binding kinetics followed by a rapid decay at 37°C. Qdm binding was more stable at 25°C such that both the binding and the signal decay were slower (Figure 3.6C).

T11-Qdm tetramers do not bind NK receptors

Qa-1^b /Qdm complexes specifically interact with CD94/NKG2 receptors on NK

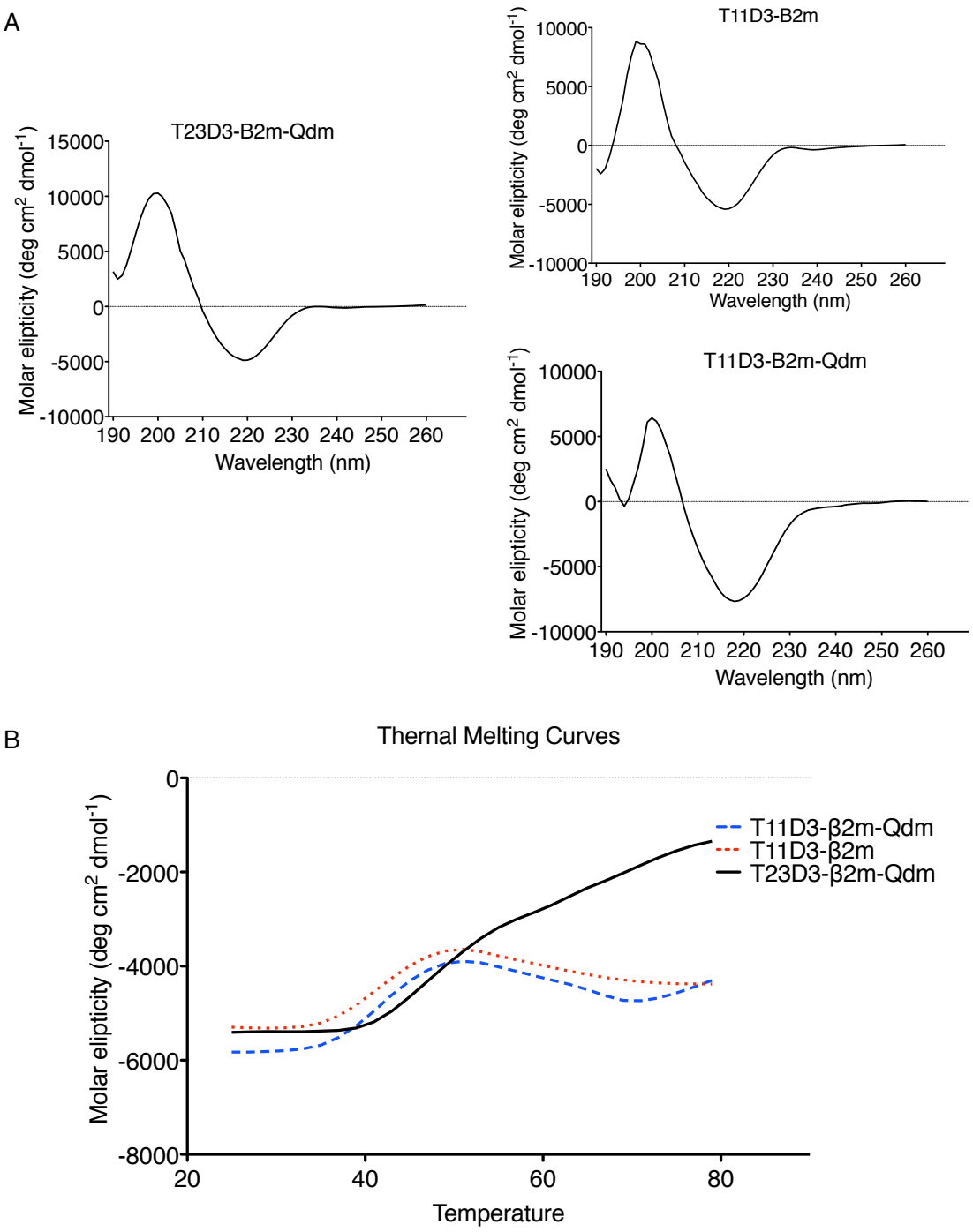

Figure 3.5 Circular dichroism studies of the *in vitro* folded MHC monomers. (A) Far-UV circular dichroism spectrum of folded MHC. Each figure was the average of three scans, and represented one of three independent experiments. (B) Thermal denaturation curves were CD signals recorded at 222nm and the temperature was increased at 2°C interval from 25°C to 79°C. Each curve was the average of three independent experiments.

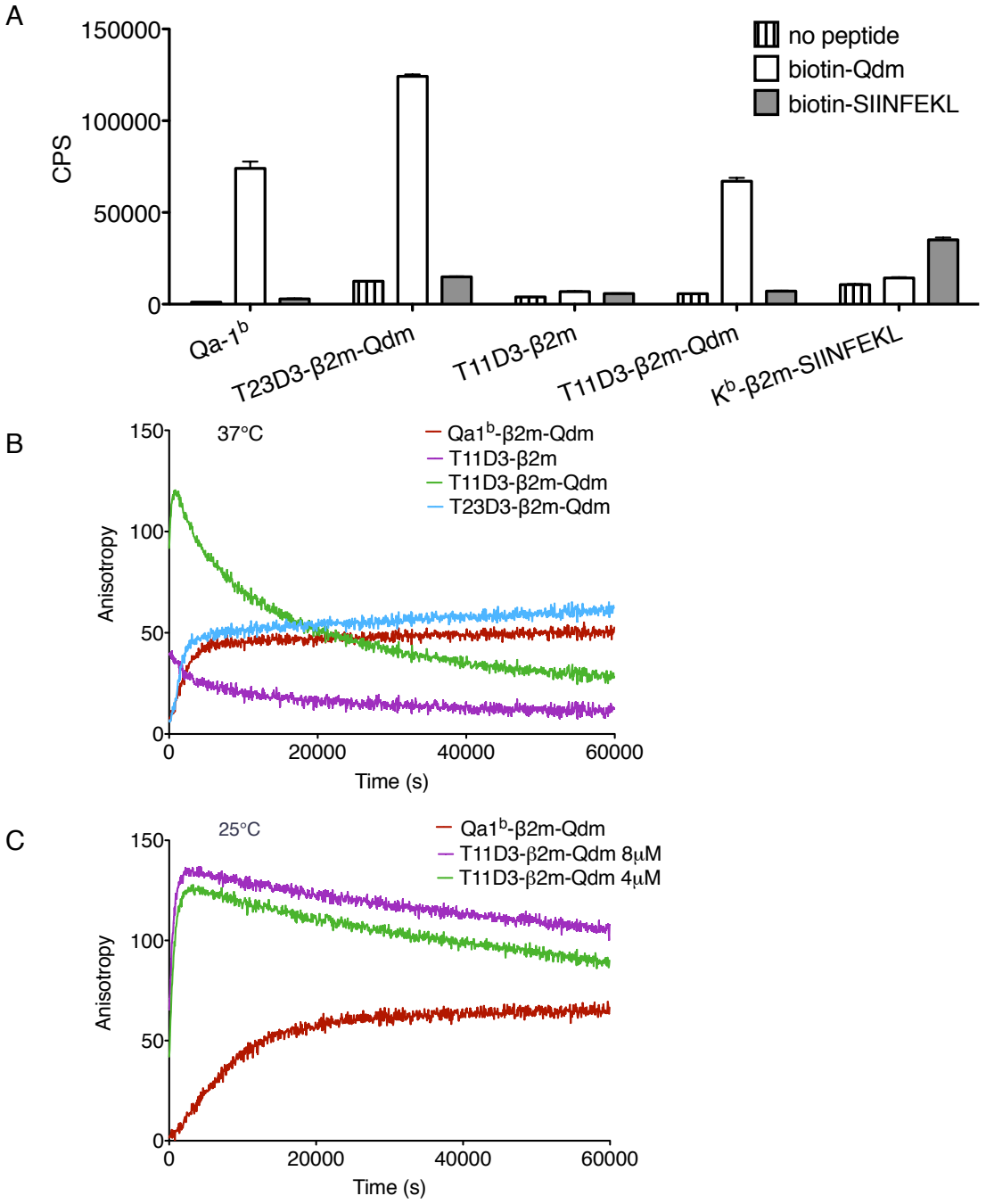

Figure 3.6 Qdm-binding capability of T11. (A) Eu-based immunoassay to test the ability of folded T11 and T23 monomers to bind Qdm peptide. Folded MHC monomers were captured on plate and incubated with the biotin-labeled peptides at room temperature overnight. (B) and (C) Fluorescence polarization (FP) assay. Folded MHC monomers were incubated with Alexfluro488 labeled Qdm peptides and the FP signal was recorded at 37°C (B) and 25°C (C) at every 60 seconds.

cells and NKT cells (15, 16, 36). About half of NK1.1+ cells in mice express CD94/NKG2 receptors and these cells can be identified by the Qa-1^b/Qdm tetramers (14). To determine if T11 can also function as a CD94/NKG2 ligand, MHC tetramers were generated by biotinylating folded T11D3-β2m-Qdm and T23D3-β2m-Qdm monomers, following by tetramerization with APC labeled streptavidin (Figure 3.7A). C57BL/6 spleen and liver lymphocytes were stained with the tetramer. About half of the natural killer cells (CD3-NKp46+) stained positive for T23 tetramer (Figure 3.7B). 24% of the CD3+ liver lymphocytes were T23 tetramer positive, representing the natural killer T cells, which are abundant in livers (37). Unlike T23 tetramer staining, no cells stained significantly positive with T11 tetramer (Figure 3.7B). Lymphocytes from thymus, iLN, mLN, payer's patches and bone marrow were also examined and no T11 tetramer positive population was detected. This suggests that T11 is not a ligand for NK receptors. It is also possible that Qdm is not the natural peptide ligand for T11, and that a receptor may exist that recognizes T11 bound with a yet to be determined peptide.

Peptide elution from Hela cells expressing T11 and T23 hybrid molecules

T11 and T23 bound peptides were eluted from Hela-T11D3 and Hela-T23D3 cells respectively (Table 3.1 and 3.2). The background peptides from Hela-MigR1 were subtracted from the eluted peptide pool. Forty-one unique peptides with length of 8 to 12 amino acids were eluted from T23D3, and 23 unique peptides with length of eight to ten amino acids were eluted from T11D3. For all the unique peptides, 30/41 and 19/23 eluted from T23D3 and T11D3 were 9mers, respectively (Figure 3.8A). More than half of the 9mers were shared between T11D3 and T23D3. T11D3 eluted peptide sequences show

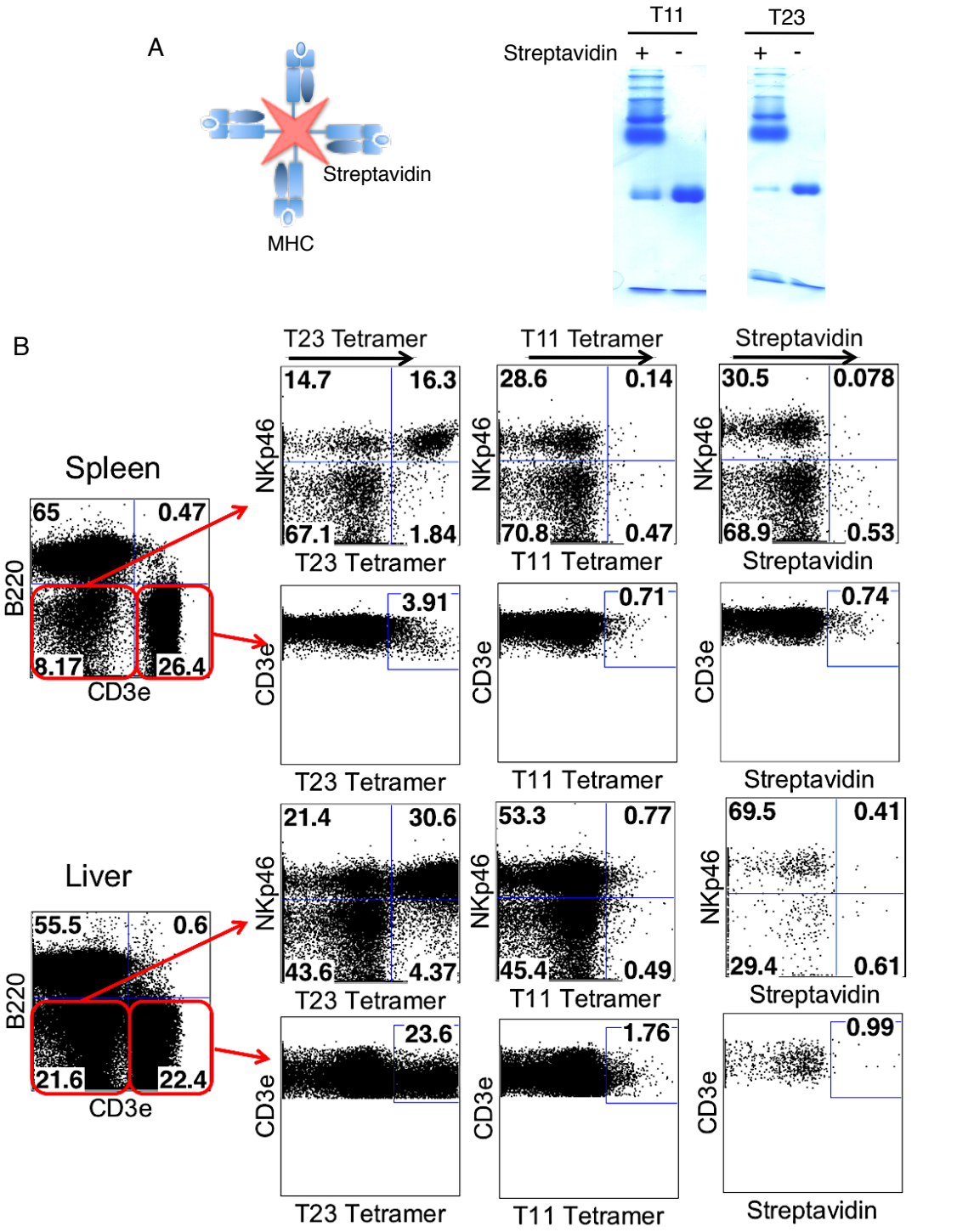

Figure 3.7 MHC tetramer staining. (A) Streptavidin binding of biotinylated MHC monomers. Biotinylated MHC was incubated with or without over-dosed streptavidin for 1 hour at room temperature, and the samples were examined by SDS-PAGE. (B) B6 spleen and liver lymphocytes were stained with B cell, T cell, NK cell markers and the hybrid T23 and T11 tetramers. APC labeled streptavidin was used as a negative control.

that Ala is dominant at P2, and the major amino acids in the P9 position are Leu, Val and Tyr (Figure 3.8B). Qdm was found in both the T23D3 and T11D3 eluted peptide pools, but it was only showed up once in the T11D3 pool, not more frequent than the other peptides, whereas Qdm was detected up nine times in the T23D3 pool (data not shown), consistent with previous reports that Qdm is the dominant peptide that associates with T23 in cells. The peptide elution data suggest that T11 molecules can bind multiple peptides including Qdm, with binding motif that overlaps with T23, but that T11 does not have the same optimized structure for binding Qdm as does T23.

Discussion

The H2-T11, an MHC class Ib gene from the mouse MHC H2-T region, encodes an MHC protein. Despite the high homology of H2-T11 to H2-T23, unlike the ubiquitously expressed T23 gene (3), T11 is transcribed in relatively high level in spleen, thymus, intestine, but transcribed at very low level in kidney, heart and pancreas, suggesting that after the gene duplication, T11 and T23 evolved independently, and mutations might accumulate in their expression regulatory elements after their duplication, leading to tissue specific expression patterns (38, 39). T11 was expressed at very high levels in thymus, suggesting it might participate in the T cell maturation and that T11-restricted T cells might be selected in the thymus. Future investigation will be informed by analysis of the expression of T11 in specific cell subpopulations in the thymus.

Although Qa-1^b does not require TAP for surface expression, the binding of Qdm to Qa-1^b is TAP-dependent (40). In TAP deficient cells, in the absence of the high affinity Qdm peptide, the Qa-1^b binding groove was reported to be occupied by various

Table 3.1 Peptides eluted from Hela-T11D3 cells

MHC	Sequence	Peptide Length	Peptide Origination
T11	NIFRNVEV	8	Ras-related GTP-binding protein A
	AAFDKIQQL	9	Cleavage and polyadenylation specificity factor subunit 2
	AAFLKAIGY	9	Splicing factor 3B subunit 1
	AAMPRPVSY	9	Kelch-like protein 24
	AASSIQRVL	9	Alpha-1,2-glucosyltransferase ALG10-A
	AQRMTTQLL	9	Folate receptor alpha precursor
	DVIYPMAVV	9	mRNA export factor
	EDDNISVTI	9	SAFB-like transcription modulator
	EIFADPRTV	9	Phosphomannomutase 1
	GAFGKPSSL	9	Uncharacterized protein C19orf21
	GKAPLNVQF	9	Filamin-B
	ISTPVIRTF	9	UPF0318 protein FAM120A
	MTPEIIQKL	9	Pre-mRNA-processing factor 19
	RQADFVQVL	9	Conserved oligomeric Golgi complex component 6
	SAIDRIFTL	9	SET domain-containing protein 3
	SAKTPGFSV	9	Protein AATF
	SAVPFKILY	9	Receptor-type tyrosine-protein phosphatase F precursor
	TASPLVKSV	9	Rho GTPase-activating protein 11A
	VAAPQVQQV	9	Sterol regulatory element-binding protein 2
	VMAPRTLVL	9	HLA class I histocompatibility antigen, A-2 alpha chain precursor
	ALIEFIRSEY	10	Threonyl-tRNA synthetase, cytoplasmic
	ETFNTPAMYV	10	ANKRD26-like family C member 1A
	QAVAKCAQLL	10	Coiled-coil domain-containing protein 108

Table 3.2 Peptides eluted from Hela-T23D3 cells.

MHC	Sequence	Peptide Length	Peptide Origination
T23	HDLIRVVY	8	Protein FAM126B
	LPMFIIVV	8	Sodium/myo-inositol cotransporter
	NIFRNVEV	8	Ras-related GTP-binding protein A
	SLINEFKL	8	Taste receptor type 2 member 3
	AAFAYTVKY	9	Ubiquitin-conjugating enzyme E2 J2
	AAFDKIQQL	9	Cleavage and polyadenylation specificity factor subunit 2
	AAFHEEFVV	9	Fragile X mental retardation syndrome-related protein 1
	AAFLKAIGY	9	Splicing factor 3B subunit 1
	AAMPRPVSY	9	Kelch-like protein 24
	AKYPEIKSL	9	Sphingolipid delta(4)-desaturase DES1
	AQLPEKVEY	9	Probable global transcription activator SNF2L4
	DVIYPMAVV	9	mRNA export factor
	EDDNISVTI	9	SAFB-like transcription modulator
	EIFADPRTV	9	Phosphomannomutase 1
	ETYPDAVKI	9	Non-structural maintenance of chromosomes element 1 homolog
	FAYPAIRYL	9	Mitochondrial 28S ribosomal protein S29
	FGFHKPKMY	9	Protein FAM60A
	FVPAEKIVI	9	Interleukin-20 receptor alpha chain precursor
	GKAPLNVQF	9	Filamin-B
	GQLPGLHEY	9	Nuclear protein localization protein 4 homolog
	HSAEILAEI	9	Anamorsin
	HTANIQTLI	9	Protein CASC5

Table 3.2 continued

MHC	Sequence	Peptide Length	Peptide Origination
T23	ISTPVIRTF	9	UPF0318 protein FAM120A
	KLFGSTSSF	9	Complement decay-accelerating factor precursor
	LAAQILAVL	9	Transmembrane protein 101
	MTPEIIQKL	9	Pre-mRNA-processing factor 19
	RQADFVQVL	9	Conserved oligomeric Golgi complex component 6
	SAIDRIFTL	9	SET domain-containing protein 3
	SAIPHPLIM	9	COP9 signalosome complex subunit 2
	SAKTPGFSV	9	Protein AATF
	SAVPFKILY	9	Receptor-type tyrosine-protein phosphatase F precursor
	TASPLVKSV	9	Rho GTPase-activating protein 11A
	VMAPRTLIL	9	HLA class I histocompatibility antigen, Cw-3 alpha chain precursor
	VMAPRTLVL	9	HLA class I histocompatibility antigen, A-2 alpha chain precursor
	ALIEFIRSEY	10	Threonyl-tRNA synthetase, cytoplasmic
	ETFNTPAMYV	10	ANKRD26-like family C member 1A
	VFGPILASLL	10	Small G protein signaling modulator
	YAYDGKDYIA	10	HLA class I histocompatibility antigen, A-2 alpha chain precursor
	RAFDQGADAIY	11	Cytochrome b-c1 complex subunit 9
	RKLEAAEDIAY	11	Prohibitin
	SKLPIGDVATQY	12	T-complex protein 1 subunit eta

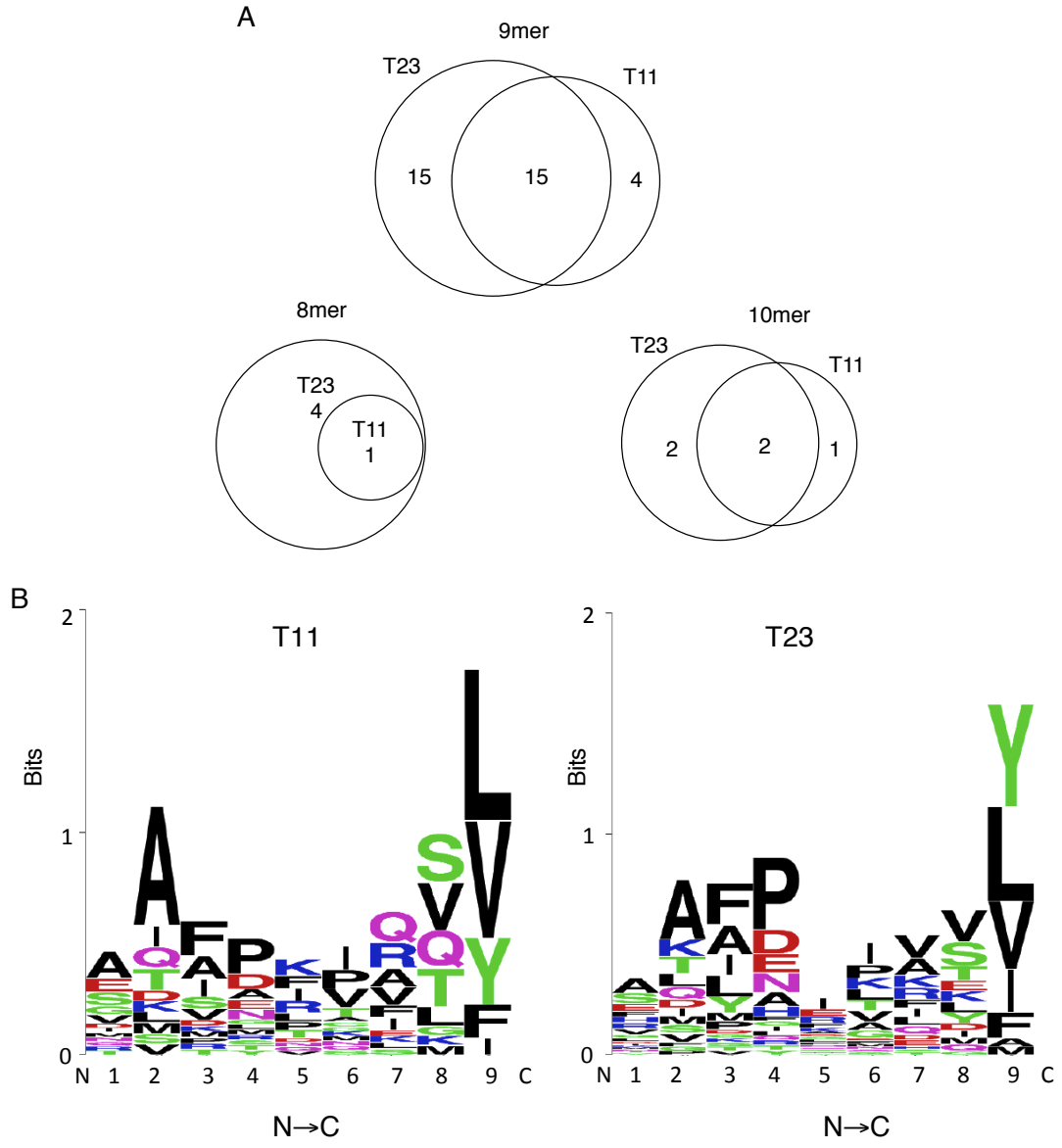

Figure 3.8 Peptide elution from Hela-T11D3 and Hela-T23D3 cells. (A) Length distribution of the eluted peptides. The unique peptides from the T23 eluted and T11 eluted peptide pool were analyzed. Number of 8mer, 9mer and 10mer peptides were shown in the Venn diagram. (B) Sequence logo of the total eluted unique peptides from T23 and T11. Each column represents one amino acid position in the peptide. Amino acids with different properties were labeled with different colors.

peptides from endogenous protein that could select CTLs responding to antigen processing deficient cells (41). The hybrid T23 on Hela cells predominantly binds the human version of Qdm, the peptide generated from HLA-A2 expressed in Hela, as shown by the peptide elution assay. In contrast, Qdm peptide was eluted from Hela-T11D3 not more frequently than other peptides. Qdm was found only once in the T11 eluted peptide pool and it was the only MHC-originated peptide found in the T11 peptide pool. It seems likely that the expression of T11D3 on Hela cell surface is stabilized by diverse peptides generated from human proteins other than MHC. Although Hela cells are TAP+/+, it is still not known whether those eluted peptides require TAP for their presentation. The TAP deficient T2 cells also express T11D3 on their surface at comparable level to Hela. The T11 on T2 cells may bind the same peptides as the ones on Hela. It is also possible that on T2 cells, some of the T11 binding grooves are empty, since T11D3 can fold with β2m in the absence of exogenous peptides in the *in vitro* folding assay. Another possibility is that T11 binds various self-originated peptides like Qa-1^b does in the TAP deficient cells (41), providing a mechanism for the immune system to recognize TAP deficient cells based on the expression of a set of peptides that are not expressed in normal cells.

Classical MHC requires binding of peptides for their stable expression. The peptide binding groove in MHC class II molecules is occupied by CLIP before the loading of antigenic peptides through peptide exchange mechanisms (42). MHC class Ia molecules have very fast recycling rates on the cell surface in the absence of bound peptides, unless the cells are incubated with the MHC class I specific peptides (43). One special property of MHC class Ib molecules is that some of them can exit without any

peptide bound, such as thymic leukemia antigen encoded by T18d (34, 44). The two alpha helices of TL positioned close to each other such that the binding groove is closed (45). T23D3 did not fold with β2m in the absence of peptides. T11D3 folded with β2m without the addition of peptides. Protein sequence alignment of T11 and T23 showed that there were seven amino acid mutations at the alpha helix motifs, which formed the peptide-binding groove. Those mutations may change the conformation of the T11 groove, makes it slightly stable without bound peptide. This difference in conformation might also be responsible for the inability of T11 to present insulin to 6C5 T cells. This could be a consequence of changes in the TCR interaction surface or alterations on the conformation of bound peptide.

T23D3 tetramers recognize half of the natural killer cells, which is in consistent with previous findings that ~50% of the natural killer cells express CD94/NKG2 (13-18). T11 tetramer made by the folded T11D3-β2m-Qdm could not recognize any receptor on C57BL/6 NK cells or any other cell types in the organs examined. This again suggests that T11 is functionally different from T23, and that it cannot serve as a ligand for inhibitory receptors in NK cells. From the peptide elution experiments, Qdm was detected on T11 with no greater frequency than other peptides. Unlike T23, Qdm does not appear to be the dominant peptide presented by T11 molecules.

Peptide elution showed that T11 bound fewer peptides than T23, suggesting that the structure of T11 might be less flexible than that of T23. Although Qdm was eluted from both T11 and T23 transduced Hela cells, it was more frequently found in the T23 peptide pool, suggesting that Qdm is the dominant peptides bind to T23, but the case might not be the same for T11. There were fewer peptides eluted from T11 than T23. It

might be that empty T11 is more stable than T23, that some of the hybrid T11 molecules were transported to Hela cell surface without peptides bound.

Although T11 does not seem to be a ligand for the NK receptors, various peptides were eluted from the Hela-T11D3 cells, suggesting T11 has antigen presentation function. T11 is transcribed in major lymphoid organs, spleen and thymus. The expression level was high in the thymus, suggesting that T11 may function as a restriction element for T cell development. TLA and MR1 restrict T lymphocytes with innate characteristics in the intestinal mucosa (46, 47). T11 is also transcribed at relatively high level in intestine, suggesting T11 may have some function in the intestine that T cells selected in the thymus by T11 may migrate to intestine for their further functions. An *E.coli* derived peptide was eluted from the T11 *in vitro* folding product (SMEALKPIL) (data not shown). The peptide was conserved in multiple bacteria, such as *Salmonella enterica*, *Citrobacter freundii* and *Yersinia enterocolitica*, suggesting that T11 has the capability to bind bacteria peptides and may restrict T cell anti-bacterial responses. Further studies are needed to investigate the functions of T11.

Acknowledgements

We thank Xiaomin Wang and Hu Dai for great technique support, Matthew Weinstock for the help with the circular dichroism study, and Dr. Julio Delgado, Eduardo Reyes-Vargas, Brant Rudd and Hernando Escobar for the peptide elution experiment.

References

1. Shawar SM, Vyas JM, Rodgers JR, Rich RR. 1994. Antigen presentation by major histocompatibility complex class I-B molecules. *Annu Rev Immunol* 12: 839-80

2. Kumanovics A, Takada T, Lindahl KF. 2003. Genomic organization of the mammalian MHC. *Annu Rev Immunol* 21: 629-57

3. Howcroft TK, Singer DS. 2003. Expression of nonclassical MHC class Ib genes: comparison of regulatory elements. *Immunol Res* 27: 1-30

4. Chen YH, Chiu NM, Mandal M, Wang N, Wang CR. 1997. Impaired NK1+ T cell development and early IL-4 production in CD1-deficient mice. *Immunity* 6: 459-67

5. Moody DB, Reinhold BB, Guy MR, Beckman EM, Frederique DE, Furlong ST, Ye S, Reinhold VN, Sieling PA, Modlin RL, Besra GS, Porcelli SA. 1997. Structural requirements for glycolipid antigen recognition by CD1b-restricted T cells. *Science* 278: 283-6

6. Silk JD, Salio M, Brown J, Jones EY, Cerundolo V. 2008. Structural and functional aspects of lipid binding by CD1 molecules. *Annu Rev Cell Dev Biol* 24: 369-95

7. Pellicci DG, Patel O, Kjer-Nielsen L, Pang SS, Sullivan LC, Kyparissoudis K, Brooks AG, Reid HH, Gras S, Lucet IS, Koh R, Smyth MJ, Mallevaey T, Matsuda JL, Gapin L, McCluskey J, Godfrey DI, Rossjohn J. 2009. Differential recognition of CD1d-alpha-galactosyl ceramide by the V beta 8.2 and V beta 7 semi-invariant NKT T cell receptors. *Immunity* 31: 47-59

8. Gulden PH, Fischer P, 3rd, Sherman NE, Wang W, Engelhard VH, Shabanowitz J, Hunt DF, Pamer EG. 1996. A Listeria monocytogenes pentapeptide is presented to cytolytic T lymphocytes by the H2-M3 MHC class Ib molecule. *Immunity* 5: 73-9

9. Lenz LL, Dere B, Bevan MJ. 1996. Identification of an H2-M3-restricted Listeria epitope: implications for antigen presentation by M3. *Immunity* 5: 63-72

10. Chiu NM, Chun T, Fay M, Mandal M, Wang C-R. 1999. The majority of H2-M3 is retained intracellularly in a peptide-receptive state and traffics to the cell surface in the presence of N-formylated peptides. *J Exp Med* 190: 423-34

11. Xu H, Chun T, Choi HJ, Wang B, Wang CR. 2006. Impaired response to Listeria in H2-M3-deficient mice reveals a nonredundant role of MHC class Ib-specific T cells in host defense. *J Exp Med* 203: 449-59

12. Cho H, Choi HJ, Xu H, Felio K, Wang CR. 2011. Nonconventional CD8+ T cell responses to Listeria infection in mice lacking MHC class Ia and H2-M3. *J Immunol* 186: 489-98

13. Aldrich CJ, Rodgers JR, Rich RR. 1988. Regulation of Qa-1 expression and determinant modification by an H-2D-linked gene, Qdm. *Immunogenetics* 28: 334-44

14. Salcedo M, Bousso P, Ljunggren HG, Kourilsky P, Abastado JP. 1998. The Qa-1b molecule binds to a large subpopulation of murine NK cells. *Eur J Immunol* 28: 4356-61

15. Vance RE, Kraft JR, Altman JD, Jensen PE, Raulet DH. 1998. Mouse CD94/NKG2A is a natural killer cell receptor for the nonclassical major histocompatibility complex (MHC) class I molecule Qa-1(b). *J Exp Med* 188: 1841-8

16. Vance RE, Jamieson AM, Raulet DH. 1999. Recognition of the class Ib molecule Qa-1(b) by putative activating receptors CD94/NKG2C and CD94/NKG2E on mouse natural killer cells. *J Exp Med* 190: 1801-12

17. Jensen PE, Sullivan BA, Reed-Loisel LM, Weber DA. 2004. Qa-1, a nonclassical class I histocompatibility molecule with roles in innate and adaptive immunity. *Immunol Res* 29: 81-92

18. Natarajan K, Dimasi N, Wang J, Mariuzza RA, Margulies DH. 2002. Structure and function of natural killer cell receptors: multiple molecular solutions to self, nonself discrimination. *Annu Rev Immunol* 20: 853-85

19. Ohtsuka M, Inoko H, Kulski JK, Yoshimura S. 2008. Major histocompatibility complex (Mhc) class Ib gene duplications, organization and expression patterns in mouse strain C57BL/6. *BMC Genomics* 9: 178

20. Oliveira CC, van Veelen PA, Querido B, de Ru A, Sluijter M, Laban S, Drijfhout JW, van der Burg SH, Offringa R, van Hall T. 2010. The nonpolymorphic MHC Qa-1b mediates CD8+ T cell surveillance of antigen-processing defects. *J Exp Med* 207: 207-21

21. Hu D, Ikizawa K, Lu L, Sanchirico ME, Shinohara ML, Cantor H. 2004. Analysis of regulatory CD8 T cells in Qa-1-deficient mice. *Nat Immunol* 5: 516-23

22. Pear WS, Miller JP, Xu L, Pui JC, Soffer B, Quackenbush RC, Pendergast AM, Bronson R, Aster JC, Scott ML, Baltimore D. 1998. Efficient and rapid induction of a chronic myelogenous leukemia-like myeloproliferative disease in mice receiving P210 bcr/abl-transduced bone marrow. *Blood* 92: 3780-92

23. Kambayashi T, Kraft-Leavy JR, Dauner JG, Sullivan BA, Laur O, Jensen PE. 2004. The nonclassical MHC class I molecule Qa-1 forms unstable peptide complexes. *J Immunol* 172: 1661-9

24. Sullivan BA, Kraj P, Weber DA, Ignatowicz L, Jensen PE. 2002. Positive selection of a Qa-1-restricted T cell receptor with specificity for insulin. *Immunity* 17: 95-105

25. Jensen PE, Moore JC, Lukacher AE. 1998. A europium fluoroimmunoassay for measuring peptide binding to MHC class I molecules. *J Immunol Methods* 215: 71-80

26. Rossi AM, Taylor CW. 2011. Analysis of protein-ligand interactions by fluorescence polarization. *Nat Protoc* 6: 365-87

27. Altman JD, Moss PA, Goulder PJ, Barouch DH, McHeyzer-Williams MG, Bell JI, McMichael AJ, Davis MM. 1996. Phenotypic analysis of antigen-specific T lymphocytes. *Science* 274: 94-6

28. Escobar H, Crockett DK, Reyes-Vargas E, Baena A, Rockwood AL, Jensen PE, Delgado JC. 2008. Large scale mass spectrometric profiling of peptides eluted from HLA molecules reveals N-terminal-extended peptide motifs. *J Immunol* 181: 4874-82

29. Liu G, Gramling S, Munoz D, Cheng D, Azad AK, Mirshams M, Chen Z, Xu W, Roberts H, Shepherd FA, Tsao MS, Reisman D. 2011. Two novel BRM insertion promoter sequence variants are associated with loss of BRM expression and lung cancer risk. *Oncogene* 30: 3295-304

30. Tompkins SM, Kraft JR, Dao CT, Soloski MJ, Jensen PE. 1998. Transporters associated with antigen processing (TAP)-independent presentation of soluble insulin to alpha/beta T cells by the class Ib gene product, Qa-1(b). *J Exp Med* 188: 961-71

31. Fahnestock ML, Tamir I, Narhi L, Bjorkman PJ. 1992. Thermal stability comparison of purified empty and peptide-filled forms of a class I MHC molecule. *Science* 258: 1658-62

32. Bouvier M, Wiley DC. 1994. Importance of peptide amino and carboxyl termini to the stability of MHC class I molecules. *Science* 265: 398-402

33. Crowley MP, Reich Z, Mavaddat N, Altman JD, Chien Y. 1997. The recognition of the nonclassical major histocompatibility complex (MHC) class I molecule, T10, by the gammadelta T cell, G8. *J Exp Med* 185: 1223-30

34. Weber DA, Attinger A, Kemball CC, Wigal JL, Pohl J, Xiong Y, Reinherz EL, Cheroutre H, Kronenberg M, Jensen PE. 2002. Peptide-independent folding and CD8 alpha alpha binding by the nonclassical class I molecule, thymic leukemia antigen. *J Immunol* 169: 5708-14

35. Dedier S, Reinelt S, Reitinger T, Folkers G, Rognan D. 2000. Thermodynamic stability of HLA-B*2705. Peptide complexes. Effect of peptide and major histocompatibility complex protein mutations. *J Biol Chem* 275: 27055-61

36. Lanier LL. 1997. Natural killer cells: from no receptors to too many. *Immunity* 6: 371-8

37. Godfrey DI, MacDonald HR, Kronenberg M, Smyth MJ, Van Kaer L. 2004. NKT cells: what's in a name? *Nat Rev Immunol* 4: 231-7

38. van den Elsen PJ, Holling TM, Kuipers HF, van der Stoep N. 2004. Transcriptional regulation of antigen presentation. *Curr Opin Immunol* 16: 67-75

39. Gobin SJ, van den Elsen PJ. 2000. Transcriptional regulation of the MHC class Ib genes HLA-E, HLA-F, and HLA-G. *Hum Immunol* 61: 1102-7

40. Aldrich CJ, DeCloux A, Woods AS, Cotter R, Soloski MJ, Forman J. 1994. Identification of a Tap-dependent leader peptide recognized by alloreactive T cells specific for a class Ib antigen. *Cell* 79: 649-58

41. Oliveira CC, van Veelen PA, Querido B, de Ru A, Sluijter M, Laban S, van der Burg SH, Offringa R, van Hall T. 2010. The nonpolymorphic MHC Qa-1b mediates CD8+ T cell surveillance of antigen-processing defects. *J Exp Med* 207: 207-21, S1-2

42. Jensen PE, Weber DA, Thayer WP, Chen X, Dao CT. 1999. HLA-DM and the MHC class II antigen presentation pathway. *Immunol Res* 20: 195-205

43. Ploegh HL. 2007. The peptide cargo of class I molecules: not just passive passengers. *J Immunol* 179: 4299-300

44. Holcombe HR, Castano AR, Cheroutre H, Teitell M, Maher JK, Peterson PA, Kronenberg M. 1995. Nonclassical behavior of the thymus leukemia antigen: peptide transporter-independent expression of a nonclassical class I molecule. *J Exp Med* 181: 1433-43

45. Liu Y, Xiong Y, Naidenko OV, Liu JH, Zhang R, Joachimiak A, Kronenberg M, Cheroutre H, Reinherz EL, Wang JH. 2003. The crystal structure of a TL/CD8alphaalpha complex at 2.1 A resolution: implications for modulation of T cell activation and memory. *Immunity* 18: 205-15

46. Le Bourhis L, Martin E, Peguillet I, Guihot A, Froux N, Core M, Levy E, Dusseaux M, Meyssonnier V, Premel V, Ngo C, Riteau B, Duban L, Robert D, Huang S, Rottman M, Soudais C, Lantz O. 2010. Antimicrobial activity of mucosal-associated invariant T cells. *Nat Immunol* 11: 701-8

47. Leishman AJ, Naidenko OV, Attinger A, Koning F, Lena CJ, Xiong Y, Chang HC, Reinherz E, Kronenberg M, Cheroutre H. 2001. T cell responses modulated through interaction between CD8alphaalpha and the nonclassical MHC class I molecule, TL. *Science* 294: 1936-9

CHAPTER 4

DISCUSSION

Summary of findings

This thesis is focused on the study of nonclassical major histocompatibility complex molecules (MHC class Ib). MHC class Ib molecules are expressed at relatively low levels compared to MHC class Ia molecules and most of them also have a restrained expression pattern. Yet there are so many types of MHC class Ib molecules that they still make important contribution to the immune system.

Chapter 2 of the thesis was focused on the CD8+ T cell anti-LCMV responses in MHC class Ia deficient mice. The CD8+ T cells in Ia deficient mice expanded *in vivo* after acute viral infection and produced cytokines and cytotoxic factors. The virus infection was partially controlled at the early phase in a β2-microglobulin dependent and CD8+ T cell dependent manner. The CD8+ T cell response was restricted by yet to be identified MHC class Ib molecules. The mice lacking MHC class Ia were not able to completely clear the virus infection and the infection became chronic, accompanied by exhaustion and death of the CD8+ T cells.

Chapter 3 focused on an MHC class Ib gene, H2-T11, which has high similarity to the Qa-1^b encoding gene, H2-T23. T11 was transcribed at high levels in the major immune organs including spleen and thymus, and the hybrid T11 was detected on the cell surface at similar level to hybrid Qa-1^b, indicating the likelihood that T11 is a

protein-encoding gene and not a pseudogene. T11 could fold *in vitro* with or without Qdm peptide, and Qdm could bind to the folded T11 molecules as long as Qdm was included during the folding process. Folded T11 had a typical MHC class I secondary structure based on circular dichroism spectra. T23/Qdm tetramers could recognize NK and NKT cells as expected, but T11/Qdm tetramer failed to recognize any examined cell types. Peptide elution showed T11 and T23 shared many peptides, including Qdm, but Qdm was more commonly found in T23 elution products than T11.

MHC class Ib restricted anti-LCMV response

CD8+ T cell mediated immune responses play critical role in the defense against intracellular pathogen infections. The majority of the CD8+ T cells in wild type animals are selected by MHC class Ia molecules in the thymus. The MHC class Ib molecules usually have low expression level and limited tissue distribution, but there are so many types of MHC class Ib molecules, that in theory, a number of CD8+ T cells are restricted by the various MHC class Ib molecules. It's impossible to determine how many cells are restricted by MHC class Ib molecules in the wild type animals. The $K^{b-/-}D^{b-/-}$ mice do not express MHC class Ia. When $K^{b-/-}D^{b-/-}$ CD8+ T cells were transferred to lymphopenic B6, $K^{b-/-}D^{b-/-}$ or $\beta2m^{-/-}$ mice, they undergo homeostatic expansion only in B6 and $K^{b-/-}D^{b-/-}$ mice, but not in $\beta2m^{-/-}$ mice, suggesting that many of the CD8+ T cells in $K^{b-/-}D^{b-/-}$ mice have specificity for β2m-bearing MHC class Ib molecules (1). In $K^{b-/-}D^{b-/-}$ mice, the MHC class Ib restricted T cells represent less than 1% of the total lymphocyte population in mouse spleen and inguinal lymph nodes (1). But when the CD4+ T cells are also deficient, the CD8+ T cell population grows up to 15% in the iLN and to 5% in the

spleen due to homeostatic expansion (1). The CD8+ T cells in the $K^{b-/-}D^{b-/-}$ and $K^{b-/-}D^{b-/-}$ $CIITA^{-/-}$ mice show activated phenotypes (1).

LCMV-Arm infection usually induces acute infection in mice, followed by dramatic expansion of CD8+ T cells within a week post infection (2-6). The virus is cleared in 1 to 2 weeks after the infection; the majority of the effector CD8+ T cells die by apoptosis and a small fraction becomes memory cells (7). The majority of the effector CD8+ T cells are restricted by H2-D^b and H2-K^b with the dominant peptides generated from LCMV glycoprotein (GP) and nucleoprotein (NP) (8). Our study showed that MHC class Ib molecules could also restrict a CD8+ T cell response against LCMV virus, together with studies from other groups, suggesting a general role MHC class Ib molecules participating in the anti-viral immune response. The MHC class Ib restricted CD8+ T cells were few in number, probably due to the limited availability of the Ib molecules for their selection in the thymus and for their homeostatic maintenance in the peripheral (9, 10). Upon acute viral infection, the few MHC class Ib restricted CD8+ T cells responded more vigorously than the Ia restricted CD8+ T cells such that each cell produced more granzyme B. The cells continuously produced IFNγ until late time points after infection. It looks like that the few Ib restricted CD8+ T cells reacted as much as they could to compensate for the scarcity of cell number. But still, the total response was not strong enough to fully inhibit viral replication, such that in the MHC class Ia deficient mice, the CD8+ T cells gradually lose their ability to expand and to produce IFNγ, showing the typical phenotype of exhaustion (11-13), and the infection was never fully controlled.

H2-M3 selects a subset of CD8+ T cells specifically recognizing *Listeria monocytogene* peptide f-MIGWIIA (14). These CD8+ T cells responded earlier than the classical CD8+ T cells; in addition to that, H2-M3 restricted cells did not show enhanced expansion upon secondary challenge, indicating the lack of memory responses (15, 16). The CD8+ T cells in LCMV infected $K^{b-/-}D^{b-/-}CIITA^{-/-}$ mice also show early production of IFNγ and granzyme B, suggesting that MHC class Ib restricted T cells may function between the innate and adaptive responses.

MHC class Ia deficient $K^{b-/-}D^{b-/-}$ mice were reported to control the chronic γ-herpes 68 virus (γHV68) infection to the same extent as the wild type mice, and better than the $CD8^{-/-}$, $\beta2m^{-/-}$, and $K^{b-/-}D^{b-/-}\beta2m^{-/-}$ mice, indicating the importance of MHC class Ib-restricted CD8+ T cell response during γHV68 infection (17). The nonclassical CD8+ T cells expanded to similar numbers as those in B6 mice after 6 weeks of infection, and the T cells had a TCR usage skewed toward Vβ4. More than 60% of CD8+ T cells in $K^{b-/-}D^{b-/-}$ mice expressed Vβ4 after 6 weeks of infection (17). The Vβ usage analysis in LCMV-Arm infected $K^{b-/-}D^{b-/-}CIITA^{-/-}$ mice showed that CD8+ T cells have multiple Vβ usage with slight skewing toward Vβ8.1/Vβ8.2, Vβ10 and Vβ13. This indicates that class Ib restricted CD8+ T cells may have more diversified response to LCMV than to γHV68.

A population of Q9 restricted CD8+ T cells was identified in polyoma virus (PyV) infected $K^{b-/-}D^{b-/-}$ mice (18). The CD8+ T cells specifically recognize a peptide from the virus VP2 protein. The VP2 specific, Q9-restricted CD8+ T cells were dominant in the $K^{b-/-}D^{b-/-}$ mice, but in contrast to the large proportion of PyV specific, MHC class Ia restricted CD8+ T cells, Q9-restricted CD8+ T cells represented only a very small fraction of the total T cell response in the PyV-infected B6 mice. Class Ia restricted T

cells might compete with the Ib restricted T cells for proliferation and survival factors. Low expression levels of Ib molecules in the wild type mice may also limit the expansion of the Ib restricted T cells.

Notably, both γHV68 and PyV viruses induce chronic infections even in wild type animals. Class Ib restricted CD8+ T cells have the ability to control these virus infections to a low level, but they were not able to clear the infections, neither do the Ia restricted CD8+ T cells. MHC class Ib restricted CD8+ T cells may also play roles in other chronic viral infections. It seems that class Ib restricted T cells behave differently when combatting acute viral infections rather than chronic infection. During our study, in which LCMV-Arm was used as the model pathogen, class Ia deficient mice were able to partially control the acute viral infection at the early phase, but failed to clear the virus infection in long-term, indicating that rapid viral replication might overwhelm the Ib-restricted CD8+ T cell response.

MHC class Ib restricted CD8+ T cells may participate in various infections as do Ia restricted CD8+ T cells. It is hard to determine their importance in the anti-microbial response without knowing the exact restricting MHC class Ib molecules and the ligands they bind. In only one case has the specificity of class Ib-restricted anti-viral CD8+ T cells been defined (Q9/VP2 in mouse polyoma virus infection). There are about 40 MHC class Ib genes in the mouse and 20 genes in human. Most of them have not been studied and some of them may have interesting functions (19). To figure out which MHC class Ib molecule/molecules might restrict the anti-LCMV response, T cells from LCMV-infected $K^{b-/-}D^{b-/-}CIITA^{-/-}$ mice were restimulated by MHC class Ib knockout APCs or APCs blocked by MHC class Ib antibodies; no significant T cell response reduction was

observed. A reduction was observed when the T cells were stimulated with Qa-2$^{-/-}$ APCs, suggesting that Qa-2 might restrict partial K$^{b-/-}$D$^{b-/-}$CIITA$^{-/-}$ T cell response against LCMV. Multiple Ib molecules might be involved in the anti-LCMV response. It is also possible that the response might be restricted by some yet-to-be studied MHC class Ib molecule/molecules.

Class Ia knockout mice provide us with a useful tool to study the functions of Ib molecules (20). Class Ib restricted T cell responses were examined by directly inoculating the Ia knockout mice with pathogens (17, 18, 21). Most if not all the studies, including this one, showed that MHC class Ib molecules could restrict T cell responses, and these T cells responded by producing cytokines and cytotoxic factors earlier than the Ia-restricted T cells and lacked memory response (15, 16, 21-25). Although the Ib restricted CD8+ T cells may only compose a very small fraction of the total CD8+ T cell repertoire in wild type mice, they have the capacity to expand to large population upon microbial infections. The class Ib restricted T cells may bridge the innate and adaptive immune responses (25).

T11 as a functional paralog of T23

There are over 40 MHC class Ib genes in the mouse, most of which are encoded in the mouse MHC region telomeric end and are not characterized. Genetic studies suggest that these genes originated from gene duplication; as mutations gathered during evolution, they gradually diverged from each other after the duplication, such that some of them have lost their original functions and some of them have gained new functions (26-33). The genes duplicated recently may not have enough mutations and still retain original functions. H2-T11 might have duplicated from H2-T23 as they share high

similarity in gene sequence such that the putative proteins that they encode also retain high identity in amino acid sequence. T23 encodes the Qa-1^b protein, which binds Qdm peptides and presents them to the CD94/NKG2A inhibitory receptors on NK and NKT cells. T11 hybrid molecules were expressed efficiently on Hela and T2 cell surfaces at levels comparable to T23, suggesting that expression of T11 on cell surface is independent of TAP machinery. The 6A8 antibody made to detect the Qa-1^b α2 domain, also weakly recognized T11, suggesting T11 shares the same or a similar 6A8 recognized epitope within T23. The hybrid T11 recombinant protein could fold *in vitro* with or without Qdm peptide, and the folding efficiency was better with the addition of Qdm peptide to the folding reaction, suggesting the Qdm peptides helped to stabilize the MHC structure. But to our surprise, the T11/Qdm tetramer, although made with Qdm peptides, did not bind to CD94/NKG2 receptors on NK or NKT cells. This suggested that T11 does not have the same function as T23 to regulate NK cell function. This could be because of the amino acid change at the contact interface of MHC/NK receptor, poor binding of Qdm peptide, or indirect conformational changes compared to T23/Qdm that affect NK receptor binding. Estimated from the HLA-E/CD94/NKG2A co-crystal structure, the change at T11 position 85 from tryptophan to arginine might interfere the interaction between T11 and CD94/NKG2A.

We identified peptides eluted from class Ib molecules purified from Hela cells expressing T23 or T11 hybrid molecules. This result provides strong evidence that T11 has the capacity to bind peptide ligands (unlike TLA), and it suggests that it can bind diverse peptide sequences. Qdm was found in both T23 and T11 elution products, but was much more abundant in the T23 elution repertoire than in the T11 repertoire, which

is consistent with previous studies demonstrating that Qdm is the dominant peptide binding to T23 (34, 35). The Qa-1^b /Qdm crystal structure reveals the features of the peptide binding groove that allow Qa-1^b to preferentially bind Qdm peptides (36). The alignment of T11 protein to the Qa-1^b protein shows that all the amino acids that form van der Waals and hydrogen bonds with Qdm peptides are conserved. The majority of the peptides eluted from T11 could be found in the T23 elution products, indicating significant conservation between T11 and T23 in peptide binding specificity. There are two amino acid changes at the bottom of the peptide-binding groove, T9H and A11V. The change of threonine to histidine may interfere with the interaction between T11 and Qdm, favoring the formation of a salt bridge between T11 and bound peptide. In fact, an *E.coli* derived peptide with a glutamic acid at peptide position 3 was eluted from the T11 *in vitro* folding product (SMEALKPIL), and the glutamic acid was in a potentially good position to interact with the T11 histidine. Whether this peptide can really bind T11 is under investigation. There are also several amino acid changes in the α-helixes of the peptide-binding groove, which may also slightly alter the T11 conformation and change the peptide-binding pattern.

A similar strategy was used to express a Qa-1^b hybrid molecule in TAP deficient mouse cell line EC7.1 and peptides were eluted from the hybrid Qa-1^b molecules (37). The hybrid molecule expressed the H2-D^b α3 domain and antibody against this domain was used to precipitate the MHC. The peptides eluted had a motif with dominant asparagine at position 5 and the motif pattern was very close to the motif pattern of H2-D^b binding peptides (38), which make us suspect that the peptides were actually derived from D^b molecules but not from the hybrid Qa-1^b. Although EC7.1 cell is TAP deficient

and D^b molecules are not detectable on the cell surface by flow cytometry, D^b molecules are still synthesized and assembled inside EC7.1 cells and D^b molecules may be present in these cell bearing self-originated peptides present inside the ER.

Although T11 does not seem to have the same function as T23, it is transcribed at high level in thymus, suggesting the possibility that it may participate in the T cell maturation process. Qa-1^b/H2-T23 select a subset of T cells specific for insulin in the thymus (39). T11 may also act as a restriction element to select T cells. T11 is also transcribed at relatively high level in spleen and intestine, suggesting it may present antigens to the T cells in the peripheral. The relatively high T11 expression level in the intestine provides the possibility that T11 might interact with the innate CD8αα+ T cells or γδ+ T cells in the intestine, like MR1 and TLA do.

Mouse Qa-1^b molecule shares 73% amino acid identity with human HLA-E, and they have similar functions in presentation of Qdm or Qdm-like peptides to specifically interact with CD94/NKG2 receptors, this regulating the activation of NK and NKT cells (40-42). The amino acid identity between T11 and HLA-E is 71% identical. T11 and HLA-E might have evolved independently, like T23 and HLA-E (43). But T11 seems to have evolved in different directions from T23 and HLA-E, such that T11 does not retain this dominant function in regulating NK cell activation.

Although the hypothesis that T11 may have similar functions to Qa-1^b/H2-T23 was proved not true, the peptides eluted from Hela-T11D3 cells will be useful to further study T11 function. The synthesized peptides may be used to immunize MHC class Ia deficient mice to see whether they can induce T11-restricted T cell response. The immunized mice T cells may be re-stimulated *in vitro* with the T11 expressing cell line in

the existence of the peptides. Tetramers can also be made by the recombinant T11 folded with the synthesized peptides; the new tetramer may be used to stain mouse cells to find the potential receptors.

Studies on MHC class Ib molecules indicated that some of them have unique properties and important functions. H2-T23 deficient mice had much higher virus burden than wild type mice when infected with mouse poxvirus, indicating the essential role for H2-T23 during the virus infection (44). Besides immune functions, some nonclassical MHC class I molecules have special functions other than presenting antigens. Neonatal Fc receptor (FcRn) can bind and release IgG antibodies in pH dependent manner and help the transportation of IgG from the mother to the fetus, providing passive immunity to the fetus (45). Another nonclassical MHC class I molecule, HFE, binds transferrin receptor 1, and mutation of HFE is associated with hereditary hemochromatosis (46). Both FcRn and HFE fold with β2m but do not bind peptides. Some MHC-like molecules even do not bind β2m, such as Zn-α2-glycoprotein (ZAG) (47). There are many MHC class Ib molecules that remain to be studied. Our research on T11 provides more information on these nonclassical MHC molecules and may be used as a template to study other Ib molecules.

Conclusions

This thesis focused on MHC class Ib molecules and the CD8+ T cell responses restricted by them. It proved that the MHC class Ib restricted CD8+ T cells were able to respond to viral infections by proliferating and secreting effective factors just like classical CD8+ T cells do; but the virus could only be partially cleared during the early phase of the infection in MHC class Ia deficient mice; MHC class Ib restricted CD8+ T

cells continually respond to the uncleared viral infection and eventually lost function. The study of a specified MHC, H2-T11, proved that although H2-T11 has very similar sequence to H2-T23, and shares many binding peptides with T23, it has different functions from T23. T11/insulin does not activate Qa-1^b/insulin specific T cell hybridoma. Neither does T11/Qdm recognize NK or NKT cells.

References

1. Jay DC, Reed-Loisel LM, Jensen PE. 2008. Polyclonal MHC Ib-restricted CD8+ T cells undergo homeostatic expansion in the absence of conventional MHC-restricted T cells. *J Immunol* 180: 2805-14

2. Anderson J, Byrne JA, Schreiber R, Patterson S, Oldstone MB. 1985. Biology of cloned cytotoxic T lymphocytes specific for lymphocytic choriomeningitis virus: clearance of virus and in vitro properties. *J Virol* 53: 552-60

3. Byrne JA, Oldstone MB. 1984. Biology of cloned cytotoxic T lymphocytes specific for lymphocytic choriomeningitis virus: clearance of virus in vivo. *J Virol* 51: 682-6

4. Byrne JA, Ahmed R, Oldstone MB. 1984. Biology of cloned cytotoxic T lymphocytes specific for lymphocytic choriomeningitis virus. I. Generation and recognition of virus strains and H-2b mutants. *J Immunol* 133: 433-9

5. Riviere Y, Southern PJ, Ahmed R, Oldstone MB. 1986. Biology of cloned cytotoxic T lymphocytes specific for lymphocytic choriomeningitis virus. V. Recognition is restricted to gene products encoded by the viral S RNA segment. *J Immunol* 136: 304-7

6. Byrne JA, Oldstone MB. 1986. Biology of cloned cytotoxic T lymphocytes specific for lymphocytic choriomeningitis virus. VI. Migration and activity in vivo in acute and persistent infection. *J Immunol* 136: 698-704

7. Khanolkar A, Fuller MJ, Zajac AJ. 2002. T cell responses to viral infections: lessons from lymphocytic choriomeningitis virus. *Immunol Res* 26: 309-21

8. Gairin JE, Mazarguil H, Hudrisier D, Oldstone MB. 1995. Optimal lymphocytic choriomeningitis virus sequences restricted by H-2Db major histocompatibility complex class I molecules and presented to cytotoxic T lymphocytes. *J Virol* 69: 2297-305

9. Takada K, Jameson SC. 2009. Naive T cell homeostasis: from awareness of space to a sense of place. *Nat Rev Immunol* 9: 823-32

10. Sprent J, Surh CD. 2011. Normal T cell homeostasis: the conversion of naive cells into memory-phenotype cells. *Nat Immunol* 12: 478-84

11. Nolz JC, Harty JT. 2011. Protective capacity of memory CD8+ T cells is dictated by antigen exposure history and nature of the infection. *Immunity* 34: 781-93

12. Wherry EJ. 2011. T cell exhaustion. *Nat Immunol* 12: 492-9

13. Williams MA, Bevan MJ. 2007. Effector and memory CTL differentiation. *Annu Rev Immunol* 25: 171-92

14. Chiu NM, Wang B, Kerksiek KM, Kurlander R, Pamer EG, Wang C-R. 1999. The selection of M3-restricted T cells is dependent on M3 expression and presentation of N-formylated peptides in the thymus. *J Exp Med* 190: 1869-78

15. Kerksiek KM, Busch DH, Pilip IM, Allen SE, Pamer EG. 1999. H2-M3-restricted T cells in bacterial infection: rapid primary but diminished memory responses. *J Exp Med* 190: 195-204

16. Seaman MS, Wang C-R, Forman J. 2000. MHC class Ib-restricted CTL provide protection against primary and secondary Listeria monocytogenes infection. *J Immunol* 165: 5192-201

17. Braaten DC, McClellan JS, Messaoudi I, Tibbetts SA, McClellan KB, Nikolich-Zugich J, Virgin HW. 2006. Effective control of chronic gamma-herpesvirus infection by unconventional MHC Class Ia-independent CD8 T cells. *PLoS Pathog* 2: e37

18. Swanson PA, Pack CD, Hadley A, Wang C-R, Stroynowski I, Jensen PE, Lukacher AE. 2008. An MHC class Ib-restricted CD8 T cell response confers antiviral immunity. *J Exp Med* 205: 1647-57

19. Howcroft TK, Singer DS. 2003. Expression of nonclassical MHC class Ib genes: comparison of regulatory elements. *Immunol Res* 27: 1-30

20. Pérarnau B, Saron MF, San Martin BR, Bervas N, Ong H, Soloski MJ, Smith AG, Ure JM, Gairin JE, Lemonnier FA. 1999. Single H2Kb, H2Db and double H2KbDb knockout mice: peripheral CD8+ T cell repertoire and anti-lymphocytic choriomeningitis virus cytolytic responses. *Eur J Immunol* 29: 1243-52

21. Seaman MS, Pérarnau B, Lindahl KF, Lemonnier FA, Forman J. 1999. Response to Listeria monocytogenes in mice lacking MHC class Ia molecules. *J Immunol* 162: 5429-36

22. Cho H, Choi HJ, Xu H, Felio K, Wang CR. 2011. Nonconventional CD8+ T cell responses to Listeria infection in mice lacking MHC class Ia and H2-M3. *J Immunol* 186: 489-98

23. Xu H, Chun T, Choi H-J, Wang B, Wang C-R. 2006. Impaired response to Listeria in H2-M3-deficient mice reveals a nonredundant role of MHC class Ib-specific T cells in host defense. *J Exp Med* 203: 449-59

24. Chiang EY, Stroynowski I. 2006. The role of structurally conserved class I MHC in tumor rejection: contribution of the Q8 locus. *J Immunol* 177: 2123-30

25. Rodgers JR, Cook RG. 2005. MHC class Ib molecules bridge innate and acquired immunity. *Nat Rev Immunol* 5: 459-71

26. Obata Y, Satta Y, Moriwaki K, Shiroishi T, Hasegawa H, Takahashi T, Takahata N. 1994. Structure, function, and evolution of mouse TL genes, nonclassical class I genes of the major histocompatibility complex. *Proc Natl Acad Sci USA* 91: 6589-93

27. Stroynowski I, Tabaczewski P. 1996. Multiple products of class Ib Qa-2 genes which ones are functional? *Res Immunol* 147: 290-301

28. Apanius V, Penn D, Slev PR, Ruff LR, Potts WK. 1997. The nature of selection on the major histocompatibility complex. *Crit Rev Immunol* 17: 179-224

29. Yamaguchi H, Hirai M, Kurosawa Y, Hashimoto K. 1997. A highly conserved major histocompatibility complex class I-related gene in mammals. *Biochem Biophys Res Commun* 238: 697-702

30. Riegert P, Wanner V, Bahram S. 1998. Genomics, isoforms, expression, and phylogeny of the MHC class I-related MR1 gene. *J Immunol* 161: 4066-77

31. Jeffery KJ, Bangham CR. 2000. Do infectious diseases drive MHC diversity? *Microbes Infect* 2: 1335-41

32. Horton R, Wilming L, Rand V, Lovering RC, Bruford EA, Khodiyar VK, Lush MJ, Povey S, Talbot CC, Wright MW, Wain HM, Trowsdale J, Ziegler A, Beck S. 2004. Gene map of the extended human MHC. *Nat Rev Genet* 5: 889-99

33. Ohtsuka M, Inoko H, Kulski JK, Yoshimura S. 2008. Major histocompatibility complex (Mhc) class Ib gene duplications, organization and expression patterns in mouse strain C57BL/6. *BMC Genomics* 9: 178

34. Kurepa Z, Forman J. 1997. Peptide binding to the class Ib molecule, Qa-1b. *J Immunol* 158: 3244-51

35. Kraft JR, Vance RE, Pohl J, Martin AM, Raulet DH, Jensen PE. 2000. Analysis of Qa-1(b) peptide binding specificity and the capacity of CD94/NKG2A to discriminate between Qa-1-peptide complexes. *J Exp Med* 192: 613-24

36. Zeng L, Sullivan LC, Vivian JP, Walpole NG, Harpur CM, Rossjohn J, Clements CS, Brooks AG. 2012. A Structural Basis for Antigen Presentation by the MHC Class Ib Molecule, Qa-1. *J Immunol* 188: 302-10

37. Oliveira CC, van Veelen PA, Querido B, de Ru A, Sluijter M, Laban S, van der Burg SH, Offringa R, van Hall T. 2010. The nonpolymorphic MHC Qa-1b mediates CD8+ T cell surveillance of antigen-processing defects. *J Exp Med* 207: 207-21, S1-2

38. Delgado JC, Escobar H, Crockett DK, Reyes-Vargas E, Jensen PE. 2009. Identification of naturally processed ligands in the C57BL/6 mouse using large-scale mass spectrometric peptide sequencing and bioinformatics prediction. *Immunogenetics* 61: 241-6

39. Sullivan BA, Kraj P, Weber DA, Ignatowicz L, Jensen PE. 2002. Positive selection of a Qa-1-restricted T cell receptor with specificity for insulin. *Immunity* 17: 95-105

40. Braud VM, Allan DS, O'Callaghan CA, Soderstrom K, D'Andrea A, Ogg GS, Lazetic S, Young NT, Bell JI, Phillips JH, Lanier LL, McMichael AJ. 1998. HLA-E binds to natural killer cell receptors CD94/NKG2A, B and C. *Nature* 391: 795-9

41. Vance RE, Kraft JR, Altman JD, Jensen PE, Raulet DH. 1998. Mouse CD94/NKG2A is a natural killer cell receptor for the nonclassical major histocompatibility complex (MHC) class I molecule Qa-1(b). *J Exp Med* 188: 1841-8

42. Salcedo M, Bousso P, Ljunggren HG, Kourilsky P, Abastado JP. 1998. The Qa-1b molecule binds to a large subpopulation of murine NK cells. *Eur J Immunol* 28: 4356-61

43. Sullivan LC, Hoare HL, McCluskey J, Rossjohn J, Brooks AG. 2006. A structural perspective on MHC class Ib molecules in adaptive immunity. *Trends Immunol* 27: 413-20

44. Fang M, Orr MT, Spee P, Egebjerg T, Lanier LL, Sigal LJ. 2011. CD94 is essential for NK cell-mediated resistance to a lethal viral disease. *Immunity* 34: 579-89

45. Roopenian DC, Akilesh S. 2007. FcRn: the neonatal Fc receptor comes of age. *Nat Rev Immunol* 7: 715-25

46. Alexander J, Kowdley KV. 2009. HFE-associated hereditary hemochromatosis. *Genet Med* 11: 307-13

47. Sanchez LM, Chirino AJ, Bjorkman P. 1999. Crystal structure of human ZAG, a fat-depleting factor related to MHC molecules. *Science* 283: 1914-9